UNIVERSIDAD AUTONOMA METROPOLITANA

Contribución al estudio de la hidrodinámica y transferencia simultánea de masa en biorreactores airlift de tres fases: producción de un consorcio microbiano degradador de petróleo

TESIS

Que para obtener el grado de Doctor en Biotecnología

PRESENTA

Manuel Alejandro Lizardi Jiménez

DIRECTOR

Dr. Mariano Gutiérrez Rojas

Junio de 2011

El Doctorado en Biotecnología de la Universidad Autónoma Metropolitana está incluido en el Programa Nacional de Posgrados de Calidad (PNPC) del CONACYT, con la referencia 001466

Iztapalapa, D.F. a 8 de Junio de 2011

El jurado designado por la división de Ciencias Biológicas y de la Salud aprobó la tesis

Contribución al estudio de la hidrodinámica y transferencia simultánea de masa en biorreactores airlift de tres fases: Producción de un cosorcio microbiano degradador de petróleo

Que presentó

Manuel Alejandro Lizardi Jiménez

Comité tutorial:

Director: Dr. Mariano Gutiérrez Rojas Universidad Autónoma Metropolitana
Asesor: Dr. Gerardo Saucedo Castañeda Universidad Autónoma Metropolitana
Asesor: Dr. Frédéric Thalasso Siret Centro de Investigación y Estudios Avanzados

Jurado:

Dr. Gerardo Saucedo Castañeda Universidad Autónoma Metropolitana

Dr. Sergio Huerta Ochoa Universidad Autónoma Metropolitana

Dr. Alejandro Medina Moreno Universidad Politécnica de Pachuca

Dr. Alejandro Coreño Alonso Universidad de Guanajuato

"La única lucha que se pierde es la que se abandona"

Ernesto “Che” Guevara

AGRADECIMIENTOS

A la Universidad Autónoma Metropolitana por ser mí casa. Al consejo Nacional de Ciencia y Tecnología por la beca otorgada. Al Dr. Mariano Gutiérrez por dirigir esta tesis e incursionar conmigo en el interesante campo de las ideas que representa este trabajo y, por supuesto, por brindarme su amistad. A mis asesores: Dr. Gerardo Saucedo y Dr. Fred Thalasso. A los doctores Sergio Huerta, Alejandro Medina y Alejandro Coreño por enriquecer con su conocimiento y experiencia este trabajo. Al Dr. Jaime Vernon por ser mi "asesor no oficial".

A mis compañeros del grupo de investigación de residuos sólidos por hacer inmejorable mi estancia en el laboratorio.

A Gaby por quererme tanto.

A mi familia, especialmente a Lidia por enseñarme que ningún obstáculo resiste a la constancia y a Vania por ser mi más exigente crítica. A las dos por todo el amor.

A mis tíos José de Jesús y Mario Jiménez Galván por pagar con su vida mi derecho a pensar distinto. A ellos dedico esta tesis.

Índice

Capítulo **Página**

Índice de Figuras

Índice de Tablas

Nomenclatura

a	Area específica de transferencia de masa	$L^2 L^{-3}$
BAL	Biorreactor airlift	
C	Concentración	$M L^{-3}$
C*	Concentración de saturación	$M L^{-3}$
D	Diámetro del BAL	L
d_{32}	Diámetro promedio Sauter	L
HTR	Tasa de transferencia de hexadecano (hexadecane transfer rate)	$M L^{-3}T^{-1}$
HXD	Hexadecano	
K	Coeficiente de fricción	adimensional
k_L	Coeficiente de transferencia de masa	$L T^{-1}$
k_La	Coeficiente volumétrico de transferencia de masa	T^{-1}
L	A ltura de operación del BAL	L
OTR	Tasa de transferencia de oxígeno (Oxygen transfer rate)	$M L^{-3}T^{-1}$
q	Tasa de consumo	$M L^{-3}T^{-1}$
Re	Número de Reynolds	adimensional
SS	Concentración de sólidos suspendidos	$M L^{-3}$
TTH	Tasa de transferencia de hexadecano	$M L^{-3}T^{-1}$
TTO	Tasa de transferencia de oxígeno	$M L^{-3}T^{-1}$
Ug	Velocidad superficial de la fase gaseosa	$L T^{-1}$
V	Velocidad de la fase líquida	$L T^{-1}$
Letras griegas		
ε	Coeficiente de retención	adimensional
μ	Viscosidad	$M L^{-1}T^{-1}$
ρ	densidad	$M L^{-3}$
ϕ	Fracción de fase dispersa	adimensional
σ	Tensión superficial	$M T^{-2}$

Subindices

aq	Fase acuosa
g	Fase gaseosa
HXD	Fase HXD
oil	Fase HXD en el artículo publicado en la RMIQ
r	Zona de ascenso (riser)
d	Zona de descenso (downcomer)

1. Resumen/Abstract

Resumen

Los biorreactores multifásicos son sistemas en los cuales una fase orgánica es adicionada a la fase acuosa (por ejemplo agua contaminada con petróleo). Estos sistemas son relativamente recientes y todavía poco estudiados. En este trabajo, se estudió la hidrodinámica en biorreactores de 10 L tipo airlift (BAL) de tres fases, lo que permitió: (i) seleccionar la configuración geométrica del BAL que generó los mejores números de Reynolds de la fase acuosa (Re_{aq}); (ii) proponer un Re representativo del BAL, que relacionó la hidrodinámica con la transferencia de masa de la fase orgánica (constituida por hexadecano (HXD)) a la fase acuosa; éste se definió como la diferencia entre el Re de la fase HXD (Re_{HXD}) y Re_{aq}, ($Re_{aq\text{-}HXD}$); (iii) caracterizar las zonas de operación del BAL usando $Re_{aq\text{-}HXD}$ como criterio. La configuración geométrica con la relación de diámetros (tubo concéntrico/BAL) que generó los mejores Re_{aq} fue 0.65 y la de alturas fue 0.77. El $Re_{aq\text{-}HXD}$ fue el mismo en la zona de ascenso y descenso para Ug mayores de 0.6 cm s^{-1} (alrededor de 3000).

Con la configuración geométrica seleccionada y con el $Re_{aq\text{-}HXD}$ como criterio característico de las zonas de estudio en los BAL se estudió la transferencia de masa en biorreactores de 10 L, lo que permitió: (i) desarrollar una nueva técnica analítica para la determinación dinámica de la tasa de transferencia de HXD (TTH); (ii) proponer el cociente entre las tasas de transferencia de HXD y oxígeno TTH/TTO como el criterio de ingeniería que considera la tasa con la que se transfieren los dos sustratos involucrados en un proceso biotecnológico de degradación aerobia de HXD y (iii) asociar el criterio TTH/TTO con las velocidades de la fase gaseosa y facilitar su aplicación práctica. TTH/TTO fue menor a 0.03 a lo largo de los 14 días de cultivo mostrando que no hubo limitaciones por oxígeno.

Se aplicó el criterio del cociente TTH/TTO a un proceso biotecnológico, lo que permitió: (i) incrementar la eficiencia (rendimiento y productividad) de la producción del consorcio

microbiano y (ii) el escalamiento descendente (BAL de 0.5 y 10 L, factor de escala 20) de la producción del consorcio microbiano. La mayor productividad del consorcio (1.02 ± 0.03 g SS $(L\ h)^{-1}$) fue alcanzada usando una estrategia de Ug variable, que considera el cociente TTH/TTO y requiere un menor gasto de energía. Una de las aportaciones principales de este trabajo es el estudio de un bioproceso con transferencia de masa y reacción (degradación de HXD y crecimiento microbiano) simultánea. El uso del cociente TTH/TTO permitió mejorar la productividad del consorcio microbiano degradador de petróleo, que puede ser utilizado como inóculo para la remediación de agua y suelos (al menos en el horizonte A, que es la capa de suelo superficial) contaminados.

Abstract

Multiphasic bioreactors are systems in wich an organic phase is added to the aqueous phase (i.e. oil-contaminated water). The development of these reactors are relatively recent and they are still poorly understood. In this work, The hydrodynamic in 10 L three-phase airlift bioreactors (ALB) was studied. Our results allowed: (i) to select the geometrical configuration for that ALB with better aqueous-phase Reynolds numbers (Re_{aq}); (ii) to propose a representative Re for ALB able to associate hydrodynamics with the organic phase (constituted by hexadecane (HXD)) mass transfer to the aqueous phase as the difference between the HXD phase Re (Re_{HXD}) and Re_{aq}, ($Re_{aq\text{-}HXD}$) and, (iii) to characterize the ALB operation zones using $Re_{aq\text{-}HXD}$. The diameters relation (draft tube/ALB) that generated the highest Re_{aq} was 0.65 andthe de height relation was 0.77. $Re_{aq\text{-}HXD}$ was the same for riser and downcomer at Ug higher than 0.6 cm s^{-1} (around 3000).

Mass transfer studies in three phases 10-L airlift type bioreactors, allowed us: (i) to develop a new dynamic technique for determining the rate of transfer of HXD (HTR) and (ii) to propose the ratio transfer rates between oxygen and HXD HTR/OTR as the engineering criterion that considers the rate at which the two of the substrates involved in a biotechnological process of aerobic degradation of HXD are transferred into the aqueous phase to be consumed. HTR/OTR was lower than 0.03 along 14-days culture showing no oxygen limitations.

The ratio HTR/OTR was applied to a biotechnological process, which allowed: (i) to increase efficiency (performance and productivity) of the microbial consortium production and (ii) scaling down (scaling factor 20) the production of microbial consortium. The largest consortium productivity (1.02 ± 0.03 g SS $(L\ h)^{-1}$) was reached using a variable Ug strategy, by considering HTR/OTR ratio at lower total energy consumption. One of the main contributions of this work is the study of a bioprocess with simultaneous mass transfer and reaction (HXD degradation and microbial growth) considerations. The use ratio HTR/OTR simultaneous mass transfer) allows to enhance the oil-degrading consortium, able to remediate soil and water oil-contaminated, productivity.

2. Introducción

En el presente documento se aborda, como tema principal, la evaluación experimental del cociente de las tasas de transferencia de hidrocarburo entre la tasa de transferencia de oxígeno TTH/TTO. Se estudia también su aplicación para la producción eficiente de un consorcio microbiano degradador de petróleo en biorreactores airlift (BAL). El consorcio producido puede ser utilizado como un inóculo capaz de remediar suelos (al menos en el horizonte A que es el suelo superficial en donde ocurren la mayoría de los procesos de biodegradación) qy aguas contaminadas con petróleo.

Este trabajo está dividido en nueve capítulos. Los capítulos uno y dos se refieren al resumen y la introducción al trabajo. En el capítulo tres se presenta la revisión bibliográfica acerca del tema que se desarrolla, exponiéndose que, para alcanzar una producción eficiente de los consorcios microbianos es necesario considerar el modelo de biorreactor trifásico y no sólo el modelo bifásico tradicionalmente estudiado. En el capítulo cuatro, se define el problema, su originalidad y los alcances. En el capítulo cinco, se plantea la hipótesis y los objetivos del trabajo. En el capítulo seis, se plantea la estrategia de trabajo experimental, se hace énfasis en la publicación de tres artículos producto del trabajo experimental de este proyecto. En el capítulo siete, se presentan los materiales utilizados y los métodos seguidos en el trabajo experimental intentando, en la medida de lo posible, no repetir los que se detallan en los artículos mencionados y que constituyen el eje central del capítulo ocho, que tiene una gran importancia pues muestra los resultados experimentales obtenidos así como una valoración crítica en la determinación de parámetros hidrodinámicos (Artículo publicado en Revista Mexicana de Ingeniería Química, RMIQ) tales como el número de Reynolds (Re) de la fase acuosa (Re_{aq}) y de la fase orgánica constituida por hexadecano (HXD) (Re_{HXD}), hidrocarburo utilizado como modelo experimental. Con base en la hidrodinámica y los parámetros resultantes, tales como Re_{aq}, Re_{HXD} y el coeficiente de retención de la fase gaseosa (εg) se realizó la selección de una configuración geométrica del biorreactor. A continuación, se caracterizó la emulsión (tamaño de gota del HXD emulsificado) y se estudió la transferencia

de masa del oxígeno y del HXD mediante el cálculo de las tasas de transferencia de oxígeno (TTO) y HXD (TTH) respectivamente. TTH y TTO están definidas en unidades de concentración de sustrato transferido por unidad de tiempo. La determinación de la TTH supuso un reto analítico que al resolverse mediante la estimación del coeficiente de transferencia de HXD (k_{LHXD}) y del área específica del HXD libre (a_{HXD}) así como de la constante de saturación del HXD (C_{HXD}*) se consideró pertinente publicar los resultados (Artículo publicado en International Journal of Chemical Reactor Engineering, IJCRE). En la tercera publicación (Artículo enviado a Chemical Engineering Journal, CEJ) se usa el cociente TTH/TTO como criterio de operación para la producción de un consorcio microbiano degradador de petróleo. En esta publicación se propone que el cociente TTH/TTO debe mantenerse debajo del cociente de consumo estequiométrico teórico, es decir, en la zona de no limitación por oxígeno y se desarrolla una estrategia de velocidad de la fase gaseosa (Ug) variable que disminuya el gasto total de energía obteniendo los mismos niveles de producción que con la estrategia que usa la mayor Ug constante. La estrategia de Ug variable también se utilizó para el escalamiento descendente del BAL (factor de escalamiento 20) obteniéndose valores similares de productividad (gramos de sólidos suspendidos, SS, que incluyen al consorcio microbiano por litro por día), y rendimiento (gramos de SS producidos por gramo de HXD consumido) final en ambas escalas. En el capítulo nueve se exponen las principales conclusiones del trabajo. Los artículos completos y en su formato original se incluyen al final de la tesis como anexos. Con el objetivo de evitar repeticiones las referencias bibliográficas de los tres artículos se incorporan al final en la tesis. Las tablas y figuras de la tesis se numeraron de acuerdo al capítulo, respetando la numeración original en el caso de las tablas y figuras de los artículos. En el caso del artículo enviado al CEJ se cambio el formato de citas con el objetivo de homogenizarlo con respecto al de la tesis, sin embargo, en el Anexo 3 se respeta el formato original.

3. Revisión bibliográfica

3.1. Contaminación de suelos y agua por derrames de petróleo

Debido a la necesidad energética global el sector petrolero ha crecido de manera acelerada en la producción de energéticos (González, 2009). En México se reconoce la presencia de ductos de petróleo y tuberías de gas, entre otros, que atraviesan por toda la República mexicana (Orozco, 2010); con frecuencia estos ductos están deteriorados y se producen derrames (Schmidt-Etkin, 2010). El deterioro que resulta en agua y suelos ha llegado a ser evidente en los años recientes, la explotación de pozos petroleros, derrames no controlados y procedimientos inadecuados de disposición final de hidrocarburos de petróleo, son algunas causas frecuentes de este deterioro (Saval, 2000). El petróleo derramado en agua y suelo es susceptible a los procesos microbianos de degradación (Lizardi-Jiménez y col., 2009) generando un gran interés industrial y de investigación por el desarrollo de tecnologías capaces de recuperar agua y suelos contaminados con petróleo tales como la excavación y confinamiento, extracción con vapor, estabilización y solidificación, lavado de suelos, precipitación química, vitrificación, incineración, entre otras (Skladany y Metting, 1993). Muchos de estos tratamientos no destruyen a los hidrocarburos contaminantes sino que los transfieren de un lugar a otro, además de que algunos de estos métodos son costosos y generan subproductos en ocasiones más tóxicos que requieren tratamientos posteriores. La alternativa biotecnológica presentada en este trabajo se refiere al uso de consorcios microbianos degradadores de petróleo, alternativa que no tiene estas desventajas.

3.2. Consorcios microbianos para remediar sitios contaminados con petróleo

Para algunas de las opciones biotecnológicas relacionadas con la biorremediación de aguas y suelos contaminados por petróleo, la alternativa se basa en el uso de microorganismos. Trabajos recientes encontraron que el contacto directo con los contaminantes del petróleo funciona como una presión selectiva que selecciona a los consorcios con mayor capacidad

degradadora dentro de una comunidad microbiana nativa (Röling y col., 2002) mejorando la eficiencia de remoción del petróleo en suelos (Lu y col., 2009) y la limpieza y descontaminación de efluentes acuosos (Gargouri y col., 2011). Los consorcios microbianos degradadores de hidrocarburos pueden ser aislados de las raíces de algunas plantas que crecen de manera natural en sitios contaminados con petróleo, ya que el microambiente que se desarrolla en la rizósfera de estas plantas promueve el crecimiento de poblaciones microbianas que han demostrado ser eficaces degradadoras (Díaz-Ramírez y col., 2003). Trabajos recientes (Tzintzun-Camacho y col., 2011), cultivando un consorcio constituido por: *Xanthomonas sp*, *Acinetobacter bouvetii*, *Shewanella sp y Defluvibacter lusatiensis* enfatizan que la dinámica de poblaciones y la interrelación entre las cepas constituyentes confieren a los consorcios una cierta capacidad especial para degradar hidrocarburos, en su caso hexadecano (HXD), una de las cepas al poseer el gene que codifica para la síntesis de la enzima alcano monooxigenasa, alk-B (*Xanthomonas sp*), degradó el 46 % del HXD inicial y otra de las cepas del consorcio (*Acinetobacter bouvetii*) produjo un bioemulsificante (posiblemente emulsan) que favoreció el consumo de HXD (72 %). El HXD es un sustrato de baja solubilidad en agua ($\sim 10^{-7}$ mg L^{-1}) que puede presentarse en formas libres (gotas macroscópicas y soluble) y/o en formas emulsificadas (microgotas) (Mehrnia y col., 2005), siempre y cuando se encuentre en presencia de agentes emulsificantes, con lo que aumenta su concentración en la fase acuosa (62 mg L^{-1}) (Quijano y col., 2010) y con esto su biodisponibilidad. Una vez biodisponible, el HXD es una fuente de carbono y energía para muchos microorganismos tanto en cultivos puros (Pepi y col., 2005) como en cultivos mixtos como los consorcios microbianos (Medina-Moreno y col., 2005). La biodegradación de HXD usualmente requiere la cooperación de varias especies microbianas, con diferentes capacidades metabólicas, dado que el uso de consorcios microbianos produce un aumento en la tasa de consumo de los hidrocarburos (Ghazali y col., 2004). En los consorcios, algunas cepas poseerían el genotipo para degradar hidrocarburos y otras la capacidad de producir biosurfactantes (Saravanan y col., 2009). En el presente trabajo, se utilizó al HXD como molécula modelo de fácil seguimiento en el laboratorio. Este hidrocarburo alifático posee un peso molecular de 226 g mol^{-1}, un punto de ebullición 151 ^{o}C y una densidad relativa de 0.773. En un trabajo previo (Lizardi-Jiménez y col., 2007) ensayando con un consorcio constituido por cinco cepas bacterianas:

Achromobacter (Alcaligenes) xylosoxidans, Bacillus cereus, Bacillus subtilis, Brevibacterium luteum y *Pseudomonas pseudoalcaligenes* se utilizó hexadecano (HXD) como única fuente de carbono, para la producción de biomasa microbiana degradadora de petróleo en un biorreactor de columna de burbujas; sin embargo, aunque los niveles de producción (medidos como gramos de consorcio por litro de reactor) fueron mejorados con respecto a trabajos precedentes (Medina-Moreno y col., 2005) el rendimiento y la productividad se vieron disminuidas aun con un pequeño cambio de escala del biorreactor (de 0.5 a 10 L), es decir, la producción con fines industriales de los consorcios microbianos degradadores de petróleo se ve limitada en este tipo de biorreactores neumáticos. Es posible que otro biorreactor del tipo neumático *i.e.* airlift (BAL), con distintas características hidrodinámicas y de transferencia de masa corrija estas deficiencias.

3.3. Biorreactores airlift

Un biorreactor airlift (BAL) es un equipo agitado neumáticamente que se caracteriza por que el suministro de energía para mantener homogeneidad en su interior tiene lugar mediante la expansión isotérmica de la fase gaseosa introducida (Chisti, 1989). En los BAL se observan importantes ventajas sobre otro tipo de biorreactores. En bioprocesos, la principal ventaja de los BAL sobre los biorreactores de columna de burbujas y los tanques agitados es que producen un menor daño celular, aceptan mayores tasas de aireación y menores costos energéticos (Chisti y Jáuregui-Haza, 2002). En los BAL, la fluidización de sólidos no es una consecuencia directa del burbujeo del gas sino que es, más bien, debida a la circulación del líquido dentro del biorreactor. Debido a lo anterior, estos equipos ofrecen la posibilidad de una fluidización de sólidos muy simple, de alta eficiencia y permiten establecer ambientes internos con esfuerzos de corte aproximadamente constantes en todo el contenido del biorreactor. Esto es debido a que la distribución de la energía suministrada para agitación y mezclado se realiza por expansión del gas inyectado y no se transfiere mediante la energía cinética de una propela en movimiento; por lo tanto, se evitan cambios morfológicos y metabólicos en las células de cultivo y por esa razón los BAL son ampliamente usados en bioprocesos (Chisti y Jáuregui-Haza, 2002). Las ventajas principales de los BAL con respecto a las columnas de burbujas,

son: mayores capacidades de transferencia de masa, mayores velocidades superficiales de líquido y gas, y los patrones de flujo bien definidos que se obtienen en ellos; con respecto a los tanques agitados las ventajas de los BAL son que su construcción es simple debido a que no tienen partes mecánicas móviles para agitar (Chisti, 1989), se abaten los costos por suministro de energía, ya que el aire cumple con la doble función de airear y agitar (Chisti y Jáuregui-Haza, 2002). Los BAL se han utilizado ampliamente para la producción en escala industrial de proteína unicelular desde hace casi tres décadas (Smith, 1980) y de levaduras desde hace más de una (Ichii y col., 1993). El número de aplicaciones de los BAL en tecnologías de biorremediación ambiental se ha incrementado, generando un nicho en bioprocesos que requieren alta transferencia de oxígeno, bajos consumos de potencia y agitación no mecánica (Kilonzo y col., 2006). Dada las ventajas de este tipo de biorreactores es necesario profundizar en el estudio de sus características hidrodinámicas y de transferencia de masa. La hidrodinámica y la transferencia de masa de un BAL dependen fuertemente de su configuración geométrica.

Existen dos configuraciones básicas de los BAL (Chisti, 1989): circulación externa y circulación interna (Figura 3.1). El BAL con circulación externa presenta al menos un "*loop*" o brazo de descenso con un diámetro generalmente menor que el del cuerpo principal del biorreactor, por otro lado el de circulación interna posee un tubo concéntrico que separa el cuerpo principal del biorreactor. En los dos casos, circulación externa e interna se distinguen cuatro zonas que permiten la recirculación del líquido en el biorreactor. La primera zona, en la que el gas se suministra, se conoce como la zona de ascenso que exhibe los coeficientes de retención de la fase gaseosa (εg) más altos en el biorreactor; en esta zona ocurre la mayor parte de la transferencia de oxígeno desde la fase gaseosa a la fase líquida. El líquido que circula en el BAL entra en una zona de liberación de los gases que funciona como un separador gas-líquido. El líquido libre de gas fluye entonces hacia la zona de descenso y viaja hacia el fondo de la columna, en donde completa el ciclo y reingresa a la zona de ascenso. Esta circulación se deriva de un efecto causado por la diferencia entre los εg de la zona de ascenso y descenso y está determinada, entre otras cosas, por las relaciones geométricas en el diseño del BAL.

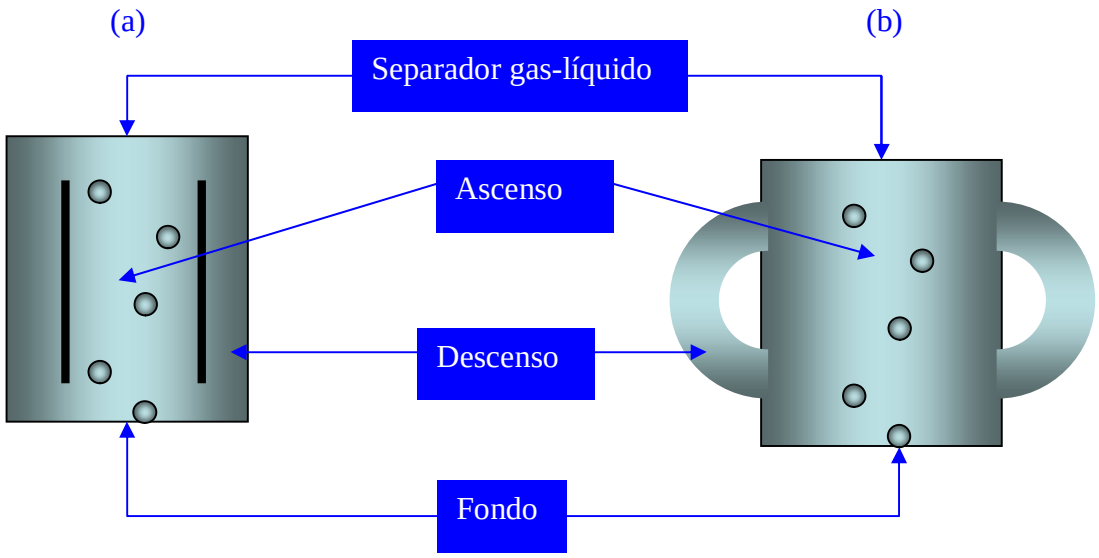

Figura 3.1 Configuraciones de BAL: circulación interna (a) y externa (b).

En la Figura 3.2 se muestran las relaciones geométricas que son consideradas como fundamentales en el diseño de un BAL con recirculación interna: altura del tubo concéntrico (L2), altura de operación (L1) (Chisti y Jáuregui-Haza, 2002), diámetro del tubo concéntrico (D2), diámetro del BAL (D1) (Sánchez-Mirón y col., 2004), distancia de la base del BAL al tubo concéntrico (fondo) y distancia del tubo concéntrico a la altura de operación del BAL (separador gas-líquido) (Kilonzo y col., 2006).

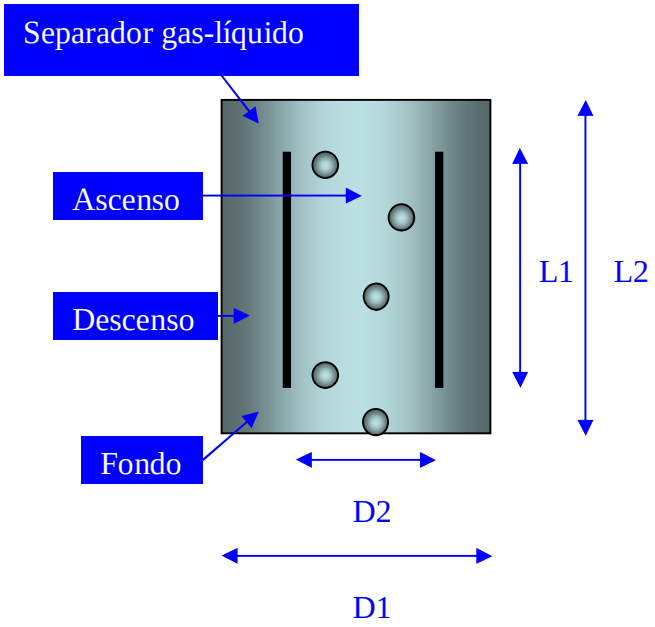

Figura 3.2 Biorreactor tipo airlift con circulación interna. L2 altura del tubo concéntrico, L1 altura de operación del líquido, D2 diámetro del tubo concéntrico, D1 diámetro del BAL.

Los autores en general coinciden (ver Tabla 3.1) en que la relación L2/L1 debe fluctuar entre 0.6 y 0.9, D2/D1 entre 0.61 y 0.74, Fondo/L1 entre 0.04 y 0.09 y Separador gas líquido/L1 entre 0.06 y 0.22. Las relaciones geométricas que se establecen en el BAL determinan en buena medida las características hidrodinámicas (tipo y patrones de flujo) en el biorreactor y por lo tanto tienen influencia sobre los fenómenos de transferencia de masa que limitan los bioprocesos.

Tabla 3.1. Relaciones geométricas para BAL con recirculación interna.

Referencia	L2/L1	D2/D1	Fondo/L1	Separador/L1	Fase líquida
Quintero, 1990	0.6-0.9	0.7-0.74			Biótica
Chisti y Jáuregui-Haza, 2002	0.83	0.66	0.08	0.07	Celulosa/agua
Sánchez-Mirón y col., 2004	0.81	0.74	0.04	0.14	Agua
Cheng-Shing y Shyh-Jye, 2004	0.78	0.66	0.07	0.14	Tolueno/agua
Mehrnia y col., 2005	0.9	0.67		0.06	Derivados del petróleo/agua
Kilonzo y col., 2006			0.05	0.17	CMC/agua
Shariati y col., 2007	0.74	0.71	0.04	0.22	Derivados del petróleo/agua
Cerri y col., 2010a	0.80	0.61	0.09	0.10	Glicerol/agua Xantano/agua
Luo y Al-Dahhan, 2011	0.70	0.69			Agua

3.3.1. Hidrodinámica y transferencia de masa en biorreactores airlift

La hidrodinámica de la o las fases líquidas presentes en el BAL depende de diversos factores: (i) las relaciones geométricas con las que se diseñó el biorreactor, (ii) la velocidad superficial de la fase gaseosa (Ug) con la que se alimenta, y (iii) de las propiedades físicas de la fases,

tales como densidad (ρ), viscosidad (μ) y tensión superficial (σ). Estas variables inciden en el diámetro de burbuja de la fase gaseosa, lo cual es clave para el movimiento de las fases líquidas, dado que burbujas de aire grandes implican menor tiempo de residencia en el reactor y por lo tanto menor εg en la zona de ascenso, dando como consecuencia menores velocidades de circulación. Por otro lado, burbujas de aire pequeñas generan mayores velocidades de la fase líquida (Nielsen y col., 2003). Los fenómenos de transferencia de masa dependen fuertemente de las velocidades de la fase líquida ya que velocidades altas generan números de Reynolds (Re) caracteristicos del flujo turbulento (mayores a 4000) que generan un espesor interfacial reducido de capa límite (Lobo, 1997).

La evaluación de la hidrodinámica en un BAL implica la determinación de la velocidad a la que la fase líquida se mueve debido a la diferencia en el coeficiente de retención de la fase gaseosa (εg) entre la zona de ascenso y la zona de descenso. Estudios recientes en BAL (Mehrnia y col., 2005; Shariati y col., 2007) destacan el papel del coeficiente volumétrico de transferencia de oxígeno de la fase gaseosa a la líquida (k_La_{O2}) como criterio de diseño y operación. El k_La_{O2} es una medida de la capacidad del BAL basada en su diseño para la transferencia de oxígeno. Por otro lado, el mezclado es un proceso que consume energía, y en el caso del BAL ésta es provista por la agitación que proporciona la aireación (Nielsen y col., 2003). En general, a medida que la magnitud del Re aumenta, mayor será la fuerza y energía utilizadas para mover al fluido, y con esto el nivel de turbulencia provocado también será mayor, conduciendo a su vez a un mejor mezclado favoreciendo la transferencia de masa. Trabajos en otros bioreactores neumáticos con sustratos insolubles en agua (Quijano, 2006) destacan el papel del Re, que reduce el diámetro de gota del HXD que para ese proceso representaba la fuente de carbono. El k_La_{O2} y el Re, a su vez están fuertemente correlacionados. Esta correlación, es debida al efecto directo que tiene el Re sobre el espesor de la capa límite entre las fases que intercambian masa, de aquí que las tasas de transferencia de masa resulten importantes parámetros a considerar ya que incluyen no sólo a los coeficientes k_La_{O2} sino también la concentración del sustrato (o sustratos) no soluble(s). Un ejemplo es el estudio de Liu y col., (2006) en donde se diseñó un BAL de 5 m^3 para producir ácido láctico con *Rhizopus sp*, usando la tasa de transferencia de oxígeno (TTO) como criterio

de operación, otro trabajo (Quijano, 2006) reportó que la tasa de transferencia de hexadecano (TTH) es la etapa limitante en la producción de consorcios microbianos degradadores de HXD. De tal manera que resulta pertinente evaluar la TTO en sistemas bifásicos (aire y agua) y adicionalmente la TTH en sistemas trifásicos (aire, agua y HXD) como criterios de operación de un BAL. Generalmente, los biorreactores trifásicos se evaluan como si fueran bifásicos, estudiando únicamente la hidrodinámica de la fase acuosa (Shariati y col., 2007) o la transferencia del oxígeno (Medina-Moreno y col., 2005), sin embargo hay diferencias entre éstos que se destacan a continuación.

El BAL bifásico

Tradicionalmente los BAL han sido estudiados desde la perspectiva del modelo bifásico, en donde una fase líquida continua (generalmente agua) y una fase gaseosa discontinua (generalmente aire) son las únicas presentes. En el modelo bifásico el único fenómeno de transferencia de masa que se considera usualmente es el del oxígeno desde la burbuja de aire hasta el seno de la fase líquida, dado que el oxígeno tiene una solubilidad en agua (~6.6 mg L^{-1}) mucho menor que la de los otros sustratos hidrosolubles (por ejemplo glucosa, 910 g L^{-1} a 25 ^{o}C). Sin embargo, cuando el bioproceso de interés incluye una fase líquida con baja solubilidad en agua (~10^{-7} mg L^{-1}) como en el caso de la biodesulfuración del petróleo (Shariati y col., 2007), o en la producción de consorcios degradadores de petróleo (Medina-Moreno y col., 2005) o para el tratamiento de aguas con nanocontaminantes (Tang y col., 2004) el modelo bifásico no es suficiente para considerar la doble transferencia de masa, de HXD y de oxígeno, para lo cuál se recurre al modelo trifásico.

El BAL trifásico

Los biorreactores con medios líquidos utilizados para estudiar la degradación aerobia de hidrocarburos del petróleo son sistemas trifásicos gas-líquido-líquido, con una fase gaseosa que generalmente es aire y dos fases líquidas: una acuosa, donde se lleva a cabo la reacción, y una orgánica compuesta por el hidrocarburo o una mezcla de hidrocarburos, en este trabajo se

identifica como fase HXD y constituye la única fuente de carbono y energía para los microorganismos que se cultivan. El HXD puede ser degradado via el consumo de las formas emulsificadas (formación de gotas microscópicas) o por contacto directo con el HXD libre (gotas macroscópicas) y el HXD soluble (Figura 3.3). Si se considera que el consumo de hidrocarburos se lleva a cabo principalmente por la vía de la emulsificación del HXD libre se pueden distinguir entonces tres etapas críticas: (i) el transporte de los hidrocarburos de la fase orgánica a la fase acuosa, (ii) el transporte de oxígeno de la fase gaseosa a la fase acuosa y (iii) el consumo de los hidrocarburos y oxígeno por parte de los microorganismos que, en su mayoría, residen en la fase acuosa. Por lo tanto, las tasas de transferencia de masa y de consumo son parámetros fundamentales que determinan el diseño y la operación exitosa del biorreactor que será utilizado en procesos aerobios de biodegradación de hidrocarburos (Quijano, 2006). Si por otra parte, se considera que el consumo de los hidrocarburos puede llevarse a cabo por contacto directo con las gotas macroscópicas de HXD y de la pequeña fracción del HXD soluble, la consideración de este fenómeno no implica una limitación en la transferencia de masa, es decir el contacto directo no impone otra limitación adicional a la que supone el proceso de emulsificación (proceso en donde un líquido se dispersa en otro en forma de pequeñas gotas). Para los dos casos, contacto directo y emulsificación, es siempre el área de las gotas macroscópicas la que se considera para estimar las tasas de transferencia de HXD. A partir de estos conceptos surge el área específica de transferencia de HXD (a_{HXD}), definida como el cociente de la suma del área de todas las gotas macroscópicas de HXD entre el volumen del BAL (Torres-Martínez y col., 2009). En nuestro trabajo, el a_{HXD} disminuye con el tiempo de cultivo dado que el HXD disperso en el medio se va consumiendo por los microorganismos. La dispersión del HXD en la emulsión se puede caracterizar midiendo el díametro de las gotas microscópicas hacía donde se transfiere el HXD desde las gotas macroscópicas. Para los BAL de tres fases (acuosa, orgánica y gaseosa) con consorcios microbianos hay poca información acerca de la transferencia de HXD de la fase orgánica a la acuosa, es decir, tradicionalmente se ha ignorado la limitación que impone la transferencia del hidrocarburo. Con la evaluación de los coeficientes volumétricos de transferencia de masa, de oxígeno, pero también de hidrocarburo, además de las concentraciones de saturación se pueden determinar las tasas de transferencia de masa y mediante una estrategia de aireación

adecuada se puede intentar controlar el cociente de las tasas de transporte TTH/TTO, mismo que considera las dos posibles limitaciones de transferencia de masa, la del oxígeno y la del HXD.

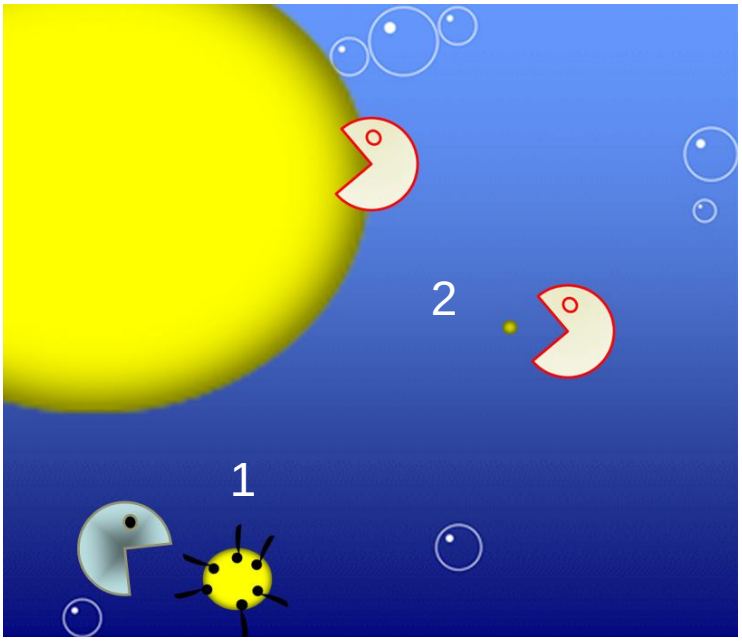

Figura 3.3 El consumo de HXD puede llevarse a cabo por: 1) consumo de las formas emulsificadas (gotas microscópicas) y 2) cosumo por contacto directo de las formas libres (gotas macroscópicas) y el HXD soluble. En amarillo las gotas de HXD.

4. Planteamiento del problema

En México cada año se derraman 7,200 toneladas de petróleo en suelo (PEMEX, 2009). El problema en agua es mucho mayor, por ejemplo el derrame en el golfo de México en 2010 provocado por trabajos de perforación profunda por la empresa British Petroleum. Por lo tanto existe un interés industrial y de investigación por recuperar ambientes contaminados con petróleo. La opción biotecnológica puede utilizar consorcios microbianos para este fin. La producción de consorcios biodegradadores de petróleo es por lo tanto de la mayor importancia, para inocular los diferentes procesos de biodegradación. La producción de esos consorcios debe realizarse en presencia de hidrocarburos para asegurarse que el consorcio microbiano no pierda capacidad degradadora durante su producción. Por tal razón, la producción de consorcios microbianos en presencia de una fase orgánica inmiscible en agua es de la mayor relevancia biotecnológica. En biorreactores airlift pueden cultivarse estos consorcios. La degradación del petróleo por un consorcio microbiano es un sistema complejo ya que es el resultado de la interacción de procesos físicos y biológicos. La tasa de consumo del petróleo no depende solamente de la capacidad metabólica de los microorganismos sino que también depende tanto de las tasas de transferencia de oxígeno y de hidrocarburos a la fase acuosa como de la solubilidad de los sustratos en la fase en que se desarrollan las biotransformaciones. La determinación del cociente de las tasas de transferencia de HXD (TTH) y oxígeno (TTO) y su relación con la velocidad superficial de la fase gaseosa (Ug) resulta indispensable y constituye la parte central de este trabajo. El HXD fue utilizado como molécula modelo de fácil seguimiento. La evaluación del cociente TTH/TTO como un criterio de operación que incluye la hidrodinámica y la transferencia de masa permitirá proponer estrategias de aireación que consideren la doble limitación de transferencia de masa (HXD y oxígeno) en sistemas de tres fases como una aportación al entendimiento y mejoramiento de los procesos que involucran la producción de consorcios microbianos degradadores de petróleo que pueden ser utilizados como inóculo para la remediación de suelo y agua.

5. Hipótesis y objetivos

Hipótesis. El uso de un criterio de operación que considere la hidrodinámica y la transferencia de masa hace eficiente la producción de un consorcio microbiano degradador de petróleo en biorreactores airlift.

Objetivo general. Diseñar un criterio de operación que considere la hidrodinámica y la transferencia de masa en biorreactores airlift de tres fases para la producción eficiente (productividad y rendimiento) de un consorcio microbiano degradador de petróleo.

Objetivos particulares

1. Caracterizar la hidrodinámica de un reactor airlift trifásico mediante la determinación de los números de Reynolds de la fase orgánica (Re_{HXD}) y de la fase acuosa (Re_{aq}).

2. Caracterizar la transferencia de masa de un reactor airlift trifásico mediante la determinación de las tasas de transferencia de HXD (TTH) y oxígeno (TTO).

3. Usar el cociente entre TTH y TTO (TTH/TTO) como criterio de operación para la producción de un consorcio microbiano degradador de petróleo.

6. Estrategia del trabajo experimental

Para caracterizar la hidrodinámica de un reactor airlift trifásico se procedió a la determinación de los números de Reynolds de la fase orgánica (Re_{HXD}) y de la fase acuosa (Re_{aq}) en un biorreactor airlift (BAL) de tres fases, para lo cuál se desarrollaron las siguientes actividades: (i) se seleccionó la configuración geométrica del BAL con mayores Re_{aq}, evaluando el efecto de las relaciones geométricas del tubo concéntrico sobre el Re_{aq} en la zona de ascenso y descenso del BAL e identificando la zona limitante del BAL como aquella con menores Re_{aq} , (ii) se propuso un Re representativo del BAL, que relacionó la hidrodinámica con la transferencia de masa de la fase HXD a la fase acuosa, como la diferencia entre el Re_{HXD} y Re_{aq} y se caracterizaron las zonas de operación del BAL, de ascenso y descenso, usando $Re_{aq-HXD.}$ Algunos de estos resultados se publicaron en la Revista Mexicana de Ingeniería Química (RMIQ) como una aportación al estudio de sistemas trifásicos que involucren dos fases líquidas y una fase gaseosa.

Una vez seleccionada la configuración geométrica del BAL se evaluó el cociente entre las tasas de transferencia de HXD (TTH) y oxígeno (TTO), para lo cuál se realizaron las siguientes actividades: (i) se desarrolló una nueva técnica dinámica para la determinación de la tasa de transferencia de HXD (TTH), preparando un medio modelo abiótico con la misma concentración de saturación de HXD en la fase acuosa (C_{HXD}*) de un medio biótico en donde crece el consorcio microbiano y midiendo el área especifica de transferencia de HXD (a_{HXD}) adicionalmente al coeficiente de transferencia de HXD (k_{LHXD}). Algunos de estos resultados se publicaron en el International Journal of Chemical Reactor Engineering (IJCRE) aportando una novedosa técnica que permitirá no sólo la evaluación de la transferencia de oxígeno sino adicionalmente la de un sustrato insoluble en agua, (ii) se propuso el cociente entre las tasas de transferencia de HXD y oxígeno TTH/TTO como el criterio de ingeniería que considera la tasa con la que se transfieren simultáneamente los dos sustratos involucrados en un proceso biotecnológico de degradación aerobia de HXD, (iii) se determinó el cociente estequiométrico entre el consumo de HXD y oxígeno como el marco de referencia para discutir los resultados

de las evaluaciones del cociente TTH/TTO para distintas Ug constantes a lo largo de los cultivos.

Finalmente, se usó el cociente TTH/TTO como criterio de operación para la producción de un consorcio microbiano degradador de petróleo, para lo cuál se realizaron las siguientes actividades: (i) se evaluó el consumo de HXD y la formación de sólidos suspendidos (SS) para distintas Ug constantes a lo largo del cultivo, (ii) se evaluó el consumo de HXD y la formación de SS usando una estrategia de Ug variable, comparando la productividad y el rendimiento con las estrategias de Ug constante, (iii) se escaló descendentemente (Factor de escala 20) la producción del consorcio microbiano usando la estrategia de Ug variable. Algunos de estos resultados se enviaron para su publicación al Chemical Engineering Journal (CEJ) como una aportación al estudio de bioprocesos con transferencia de masa y reacción (degradación de HXD y crecimiento) simultánea. Un diagrama de bloques que resume la estrategia experimental se presenta en la Figura 6.1.

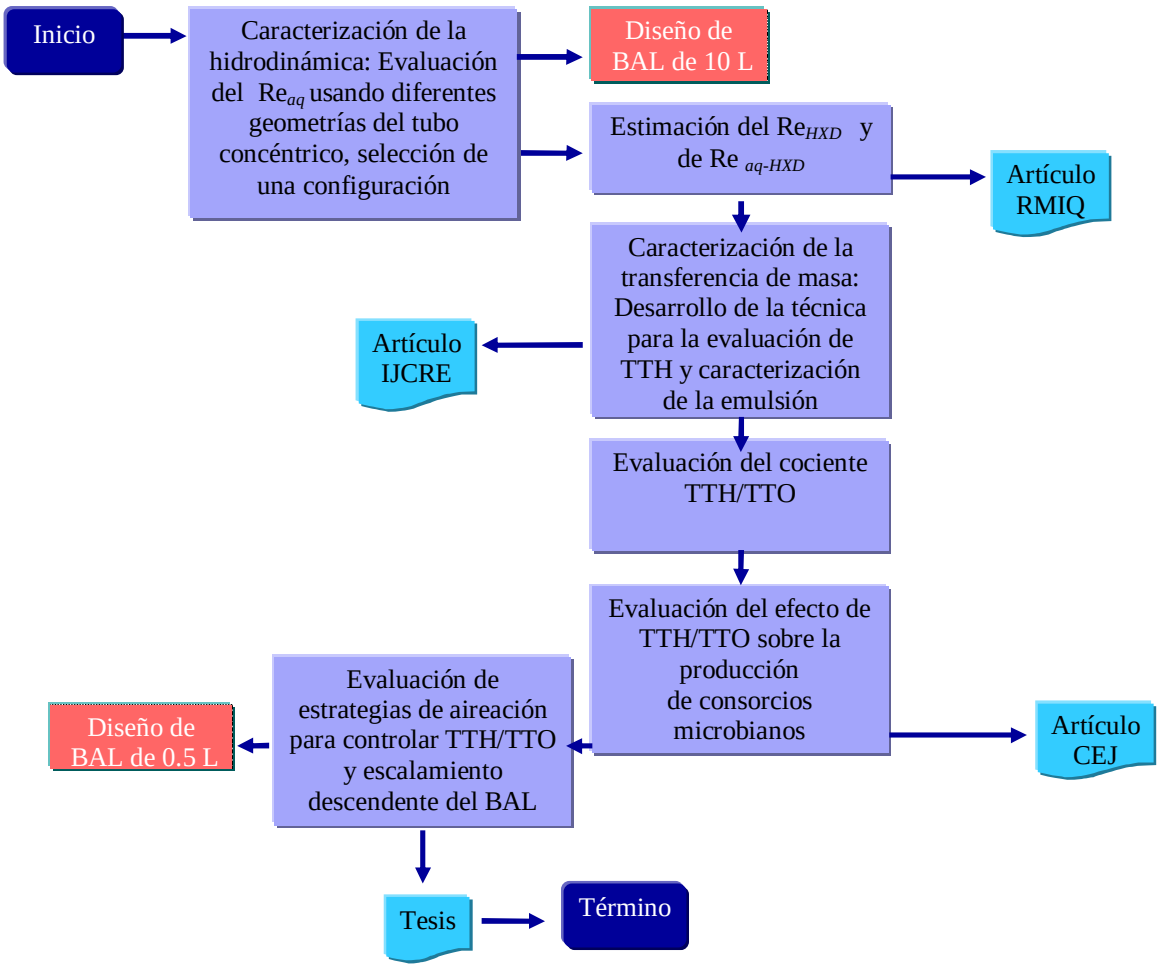

Figura 6.1. Síntesis de la estrategia experimental empleada en el presente trabajo.

7. Materiales y Métodos

7.1. Materiales

7.1.1. Consorcio microbiano

El consorcio microbiano degradador de petróleo fue aislado de la rizósfera de *Cyperus laxus*, planta nativa de pantanos del sureste mexicano, capaz de crecer en suelos contaminados con petróleo (Díaz-Ramírez y col., 2003). La identificación del consorcio se llevó a cabo mediante el análisis y amplificación del gene ribosomal 16s (Tzintzun-Camacho y col., 2011). El consorcio microbiano degradador de petróleo estuvo constituido por cuatro cepas bacterianas: *Xanthomonas sp, Acinetobacter bouvetii, Shewanella sp* y *Defluvibacter lusatiensis.*

7.1.2. Biorreactores

Se utilizaron dos biorreactores airlift (BAL) de vidrio, de 0.5 y 10 L de volumen de operación, con diversas relaciones geométricas, para la selección de la configuración del tubo concéntrico que fue utilizada para los experimentos de transferencia de masa y producción de biomasa. Los biorreactores fueron equipados con: un sensor de oxígeno disuelto (Applikon, Holanda), un termómetro (Steren, México), un potenciómetro (Oakton, Malasia) y un rotámetro (Cole-parmer, E.U.) . Los biorreactores fueron operados a 28 ^{o}C, con Ug variable (entre 0.15 y 1.54 cm s^{-1}) en lotes secuenciales (Medina-Moreno y col., 2005) de 14 días, inoculados con 0.8 g L^{-1} (p/p) del consorcio microbiano. En la Figura 7.1 se muestra el arreglo de los biorreactores utilizados.

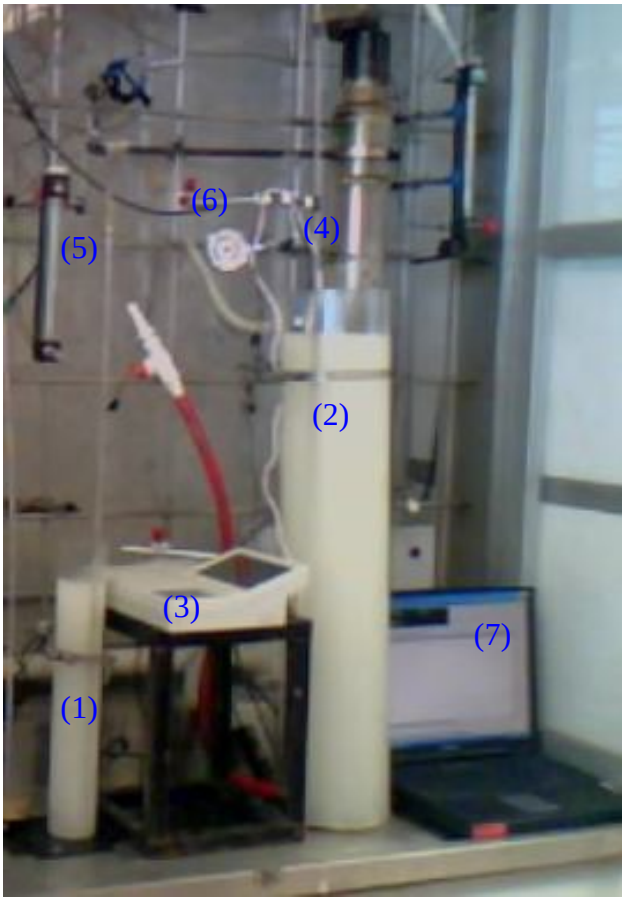

(1) BAL de 0.5 L
(2) BAL de 10 L
(3) Potenciómetro
(4) Sensor de oxígeno disuelto
(5) Rotámetro
(6) Termómetro
(7) Sistema de adquisición de datos

Figura 7.1 Biorreactores y equipamiento.

7.1.3. Medio modelo

El medio modelo fue diseñado igualando sus propiedades físicas, tensión superficial (σ) viscosidad (μ) y densidad (ρ) y la concentración de saturación del HXD (C_{HXD}*) con las del medio biótico en donde crece un consorcio microbiano degradador de petróleo (Medina-Moreno y col., 2005), para lograr lo anterior se adicionó entre 0 y 1.5 mL de Tween 20 (Aldrich Co. Ltd) a un litro de medio mineral.

7.2. Métodos

7.2.1. Influencia de la geometría sobre Re

Se determinaron las relaciones geométricas D/L, diámetro del tubo concéntrico, altura del tubo concéntrico, ensayando su influencia sobre el número de Reynolds (Re) calculando la velocidad de la fase acuosa utilizando esferas de poliacrilato de sodio y la velocidad del hexadecano utilizando esferas de oligosiloxanos. Para estimar las velocidades se utilizó una videocámara (Olympus, USA) y un cronómetro digital (Sony, USA). La evaluación de los Re se publicó en la RMIQ.

7.2.2. Caracterización de la emulsión

Con el objetivo de caracterizar la emulsión se realizaron los siguientes experimentos en ausencia de microorganismos (abióticos): en matraces de 125 mL provistos con mamparas se agregó 20 mL del siguiente medio mineral (en gL^{-1}): 6.75, $NaNO_3$ (J. T. Baker, 99. 9%); 2.15, K_2 HPO_4 (J. T. Baker, 99.3%); 1.13, KCl (J. T. Baker, 99.9%) y 0.54, $MgSO_4 \cdot 5$ H_2O (J. T. Baker, 100.1 %). El pH fue ajustado a 6.5 con HCl 1.0N. Se adicionó HXD a concentraciones menores o iguales a la de saturación (C_{HXD}*) de 62, 45, 30, 15 y 5 mg HXD L^{-1} usando Tween 20 como surfactante. Los matraces se incubaron con agitación a 150 rpm y 28 °C. Para los experimentos bióticos, se preparó otra serie de matraces a las mismas C_{HXD}* que en las pruebas abióticas y se inocularon con 0.8 g L^{-1} del un consorcio microbiano, se ensayó también una concentración de 13 000 mg HXD L^{-1}. Se tomó 2 mL de cada matraz y se analizó con un medidor de tamaño de partícula (Zetasizer, Nano-ZS, Malvern, R.U.). Las determinaciones analíticas se hicieron por triplicado, para cada C_{HXD}*, en matraces fueron retirados a las 2, 4, 10, 24 y 48 h.

7.2.3. Evaluación del consumo de HXD en sus diferentes formas

El HXD residual se determinó con los mismos matraces preparados para las pruebas bióticas de caracterización de la emulsión, es decir, por extracción líquido-líquido seguido de cromatografía de gases (Modelo 3900, Varian, USA) empleando un detector FID a 300 ^oC,

columna DB-Petro narrow bore, J & W Scientific de 30 m x 0.25 mm y helio como gas acarreador. La temperatura del inyector y detector permanecieron constantes a 290^{o} y 300 ^{o}C, respectivamente. El programa de temperatura fue diseñado como sigue: 120 (1 min), 10 ^{o}C min^{-1} hasta 150 ^{o}C (2 min), 15 ^{o}C min^{-1} hasta 170 ^{o}C (1.5 min).

7.2.4. Coeficiente volumétrico y tasa de transferencia de oxígeno

Para la evaluación del k_La_{O2} se utilizó la técnica dinámica acoplada a un electrodo de oxígeno disuelto (Aplissens, USA). La TTO fue calculada como el producto de k_La_{O2} por el gradiente de concentraciones de oxígeno entre la interfase gas-líquido y el seno de la fase líquida.

7.2.5. Coeficiente volumétrico y tasa de transferencia de HXD

Para la determinación del coeficiente de transferencia de HXD (k_{LHXD}) se utilizó una cápsula de acero inoxidable contenedora de hexadecano, la cápsula fue sumergida en el BAL con medio modelo a Ug variable. El BAL se muestreó a partir del momento en que la aireación se estabilizaba, se midió la concentración de HXD por extracción líquido-líquido y cromatografía de gases con respecto al tiempo. Se obtuvo un coeficiente volumétrico de transferencia de HXD (k_La_{HXD}) de la cápsula. Con el área específica conocida (a) de la cápsula se calculó el coeficiente convectivo de transferencia de HXD (k_{LHXD}). Para el cálculo del a de las gotas de HXD (a_{HXD}) se usó una cámara digital y un analizador de imágenes (Image pro plus 4.1, Medya cybernetics, USA) y la Ecuación 1.

$$a_{HXD} = \frac{6}{d_{32HXD}}\phi \qquad (1)$$

En donde d_{32HXD} es el diámetro promedio Sauter de las gotas macroscópicas de HXD (cm) y ϕ es la fracción dispersa de la fase HXD (adimensional). Para poder distinguir al HXD se utilizó una tinción específica con carotenoides de Rodofila (Bioquimex, Mex). El k_La_{HXD} del BAL se obtuvo como un producto del k_{LHXD} por a_{HXD} y TTH como el producto del k_La_{HXD} por

el gradiente de concentraciones (concentración de saturación menos la concentración en el seno de la fase líquida). La técnica para la evaluación del k_La_{HXD} y TTH se publicó en el IJCRE.

7.2.6. Sólidos suspendidos

La determinación de sólidos suspendidos (SS), que contienen al consorcio microbiano degradador de petróleo y el hexadecano (HXD) residual se realizó por gravimetría.

8. Resultados y Discusión

8.1. Selección de la configuración geométrica del BAL

En el diseño y operación de los BAL la configuración geométrica es muy importante ya que de ella depende la hidrodinámica dentro del biorreactor. Con el objetivo de seleccionar la configuración geométrica del BAL y dado que la hidrodinámica local en el BAL depende de la geometría del tubo concéntrico se evaluó el efecto de las relaciones geométricas del tubo concéntrico sobre el Re de la fase acuosa (Re_{aq}) en las zonas de ascenso y descenso. Se ensayaron nueve configuraciones de tubo concéntrico, combinando: tres relaciones de diámetro del tubo/diámetro del BAL (0.55, 0.58 y 0.65) y tres relaciones de altura del tubo/altura del BAL (0.60, 0.77 y 0.90). Con estos experimentos fue posible identificar la zona con limitación hidrodinámica, esto es la zona con el Re_{aq} más bajo, como se detalla a continuación.

Efecto de las relaciones geométricas sobre Re_{aq}

En esta sección se evaluó el efecto de las relaciones geométricas (altura y diámetro) del tubo concéntrico sobre el parámetro hidrodinámico Re_{aq}. En la Figura 8.1 se muestran las variaciones de Re_{aq} en función de la velocidad superficial de la fase gaseosa (Ug) y de la tensión superficial (σ), tanto para la zona de ascenso (a) como el descenso (b) cuando la relación L2/L1 se mantuvo en 0.60 y la relación D2/D1 fue variable, 0.55 (1), 0.58 (2) y 0.65 (3). La Ug fue ensayada en el rango de 0.15 a 0.76 cm s^{-1}. La σ fue ajustada a 65 y 50.5 dinas cm^{-1} para incluir la σ que presenta el medio biótico. Fueron incluidos experimentos independientes usando agua destilada como medio coalescente (72.6 dinas cm^{-1}). El aumento en el diámetro del tubo concéntrico (Figura 8.1) implicó un aumento en el Re_{aq} de la zona de descenso, de 1800 a 2200, y una disminución de esté en la zona de ascenso, de 6500 a 5000. La zona de ascenso exhibió flujo acuoso turbulento (Re_{aq} mayores a 4000), mientras que la zona de descenso presentó valores de Re_{aq} más bajos (Re_{aq} menores a 2100). Por otro lado la

disminución en σ provocó un ligero aumento en Re_{aq} tanto en la zona de ascenso como en el descenso. El incremento del Re_{aq} en la zona de descenso al aumentar la relación D2/D1 se puede explicar vía el principio de Bernoulli ya que el BAL está operando como dos tubos, con diámetros distintos, conectados en serie a través de los cuales fluye una fase acuosa (Chisti, 1989). El aumento en Re_{aq} al disminuir σ es posiblemente debido a la disminución en el díametro de las burbujas de aire, lo cuál genera tiempos de residencia más largos en la zona de ascenso del BAL, mayor coeficiente de retención de la fase gaseosa (εg) (Lizardi-Jimenéz, 2007) y por lo tanto mayores velocidades de circulación de la fase acuosa (Chisti, 1989).

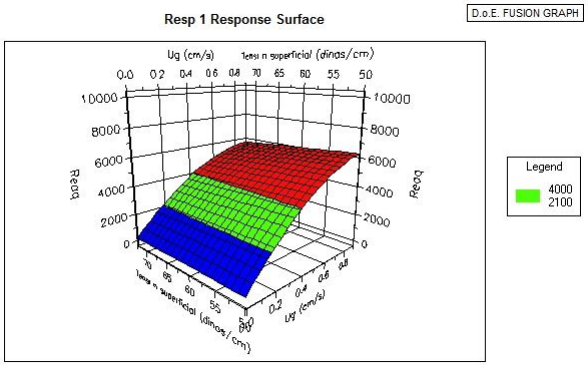

1 (a)

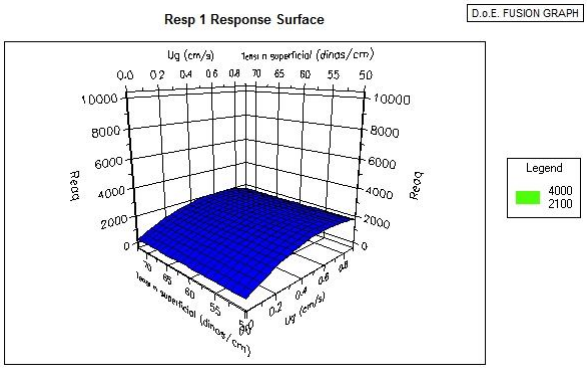

1 (b)

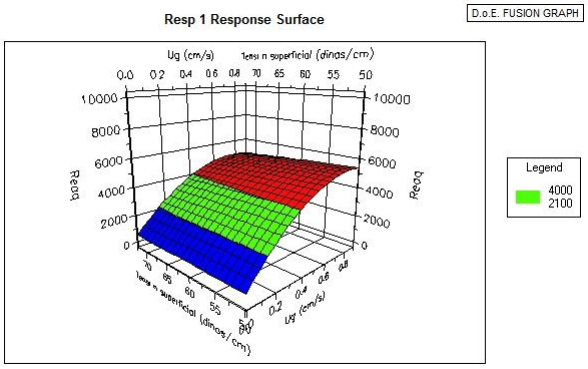

2 (a)

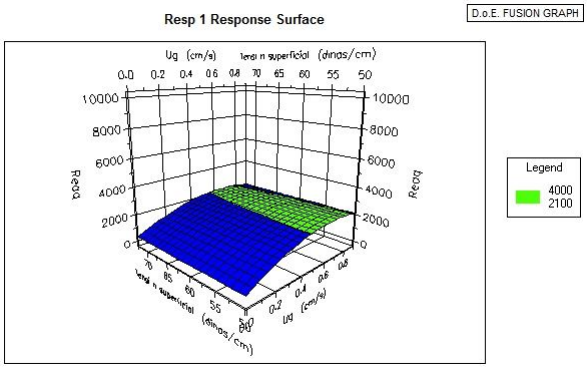

2 (b)

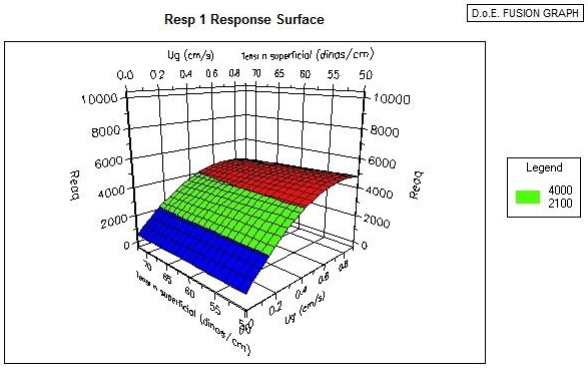

3 (a)

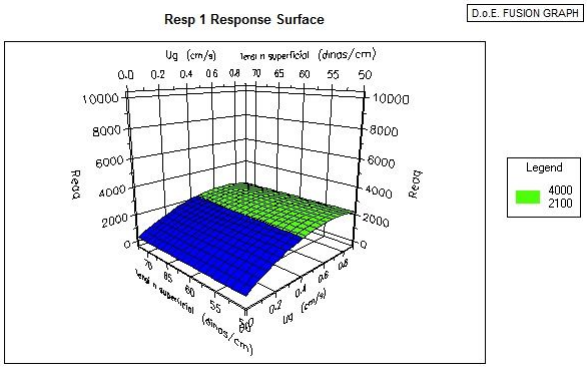

3 (b)

Figura 8.1 Re_{aq} en función de la velocidad superficial de la fase gaseosa (Ug) y de la tensión superficial (σ), tanto para la zona de ascenso (a) como el descenso (b). L2/L1 = 0.60, D2/D1 = 0.55 (1), 0.58 (2) y 0.65 (3).

Con el objetivo de investigar el efecto de aumentar la altura del tubo concéntrico del BAL se presenta la Figura 8.2, en ella se muestran las variaciones de Re_{aq} en función de Ug y σ, tanto para la zona de ascenso (a) como el descenso (b). La relación L2/L1 se mantuvo en 0.77 (mayor que el 0.60 de la Figura 8.1) mientras que la relación D2/D1 fue variable 0.55 (1), 0.58 (2) y 0.65 (3).

Ug y σ fueron ensayadas en los mismos rangos que en la Figura 8.1. Las configuraciones de tubo concéntrico ensayadas en la Figura 8.2 exhibieron en general Re_{aq} mayores que los mostrados en la Figura 8.1, tanto para la zona de ascenso ($7000 < Re_{aq} < 9000$ para $0.15 < Ug < 0.76$ cm s^{-1}), como para el descenso ($2500 < Re_{aq} < 3700$), posiblemente debido a que la mayor altura de la columna permite una mayor cantidad de burbujas en la zona de ascenso, mayor εg y con ello una mayor velocidad de recirculación de la fase acuosa.

El aumento en el diámetro del tubo concéntrico y la disminución en σ tuvieron el mismo efecto que el mostrado en la Figura 8.1 (aumento en el Re_{aq} de la zona de descenso y un ligero aumento en Re_{aq} tanto en la zona de ascenso como en el descenso respectivamente).

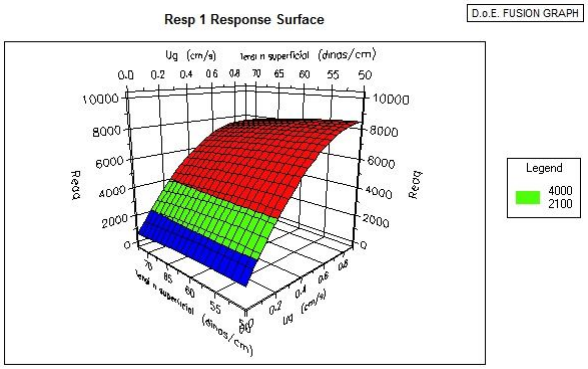

1 (a)

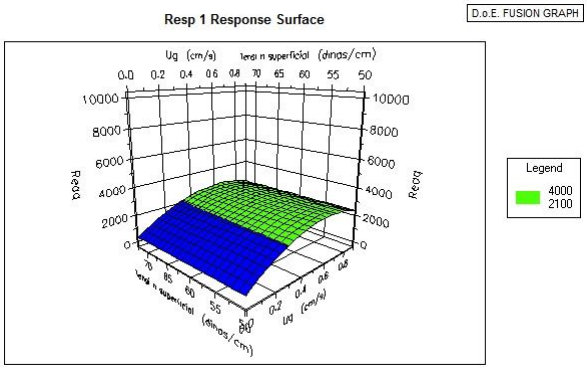

1 (b)

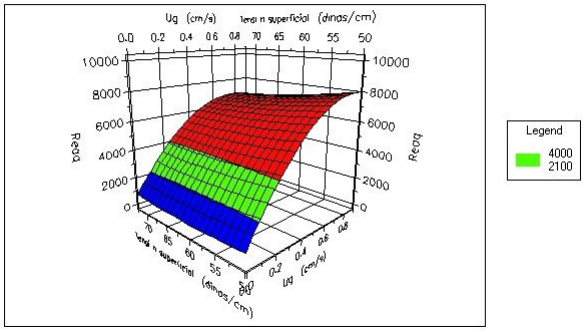

2 (a)

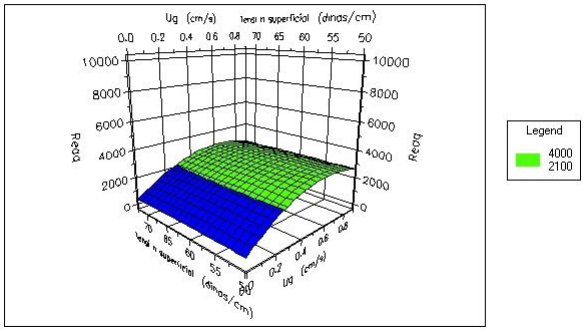

2 (b)

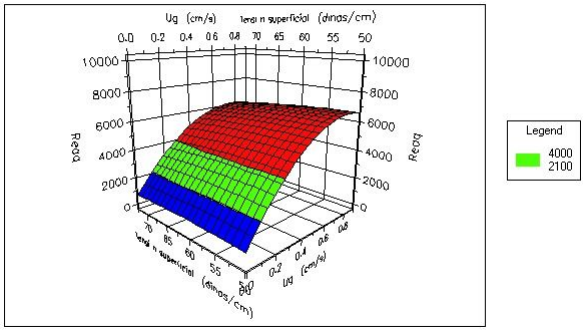

3 (a)

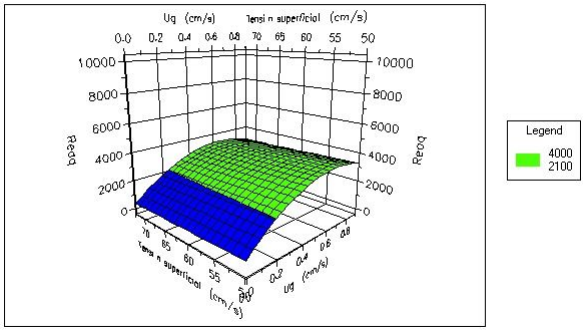

3 (b)

Figura 8.2 Re_{aq} en función de la velocidad superficial de la fase gaseosa (Ug) y de la tensión superficial (σ), tanto para la zona de ascenso (a) como el descenso (b). L2/L1 = 0.77, D2/D1 = 0.55 (1), 0.58 (2) y 0.65 (3).

Para terminar de evaluar el efecto del aumento de altura del tubo concéntrico se muestra la Figura 8.3, en la cual se presentan las variaciones de Re_{aq} en función de Ug y σ, tanto para la zona de ascenso (a) como el descenso (b). La relación L2/L1 se mantuvo en 0.90 mientras que la relación D2/D1 fue variable 0.55 (1), 0.58 (2) y 0.65 (3). Ug y σ fueron ajustadas como en las Figuras 8.1 y 8.2. Esta configuración de tubo concéntrico exhibió Re_{aq} ligeramente menores que los mostrados en la Figura 8.2, tanto para la zona de ascenso ($6800 < Re_{aq} < 8300$ para $0.15 < Ug < 0.76$ cm s^{-1}), como para el descenso ($2400 < Re_{aq} < 3200$). El aumento en el diámetro del tubo concéntrico implicó, como en las Figuras 8.1 y 8.2 un aumento en el Re_{aq} de la zona de descenso y una disminución de éste en la zona de ascenso. Los Re_{aq} fueron menores que en la configuración mostrada en la Figura 8.2 posiblemente debido a que la mayor altura de la columna aunque permite una mayor cantidad de burbujas en la zona de ascenso, no deja prácticamente espacio en la zona del separador gas-líquido para la recirculación, generando una fricción muy elevada, haciendo más lenta la circulación de la fase acuosa. Por otra parte, la disminución en σ provocó el mismo efecto que el mostrado en las Figuras 8.1 y 8.2.

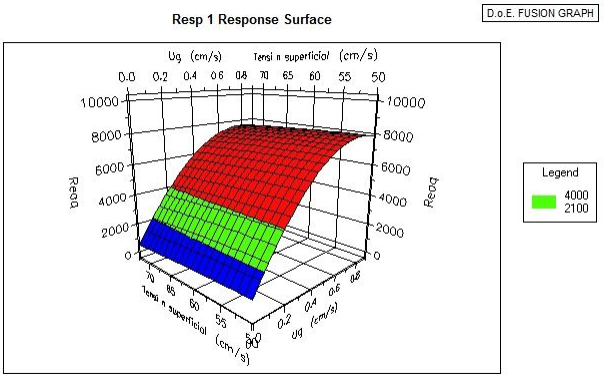

1 (a)

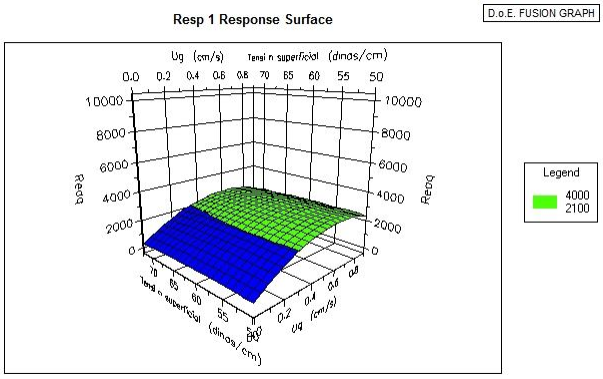

1 (b)

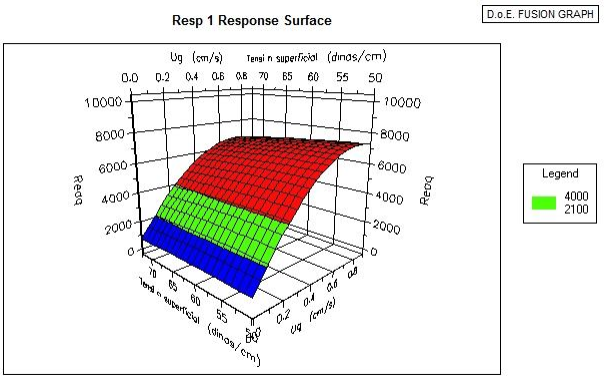

2 (a)

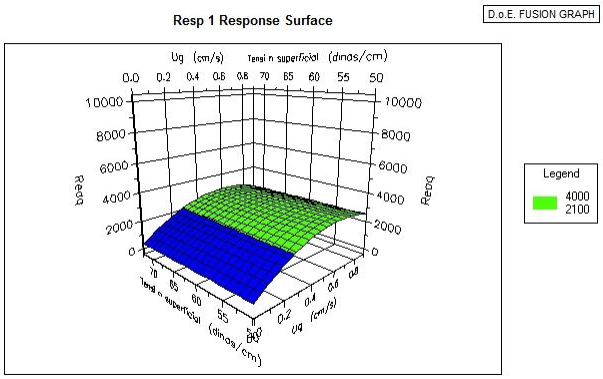

2 (b)

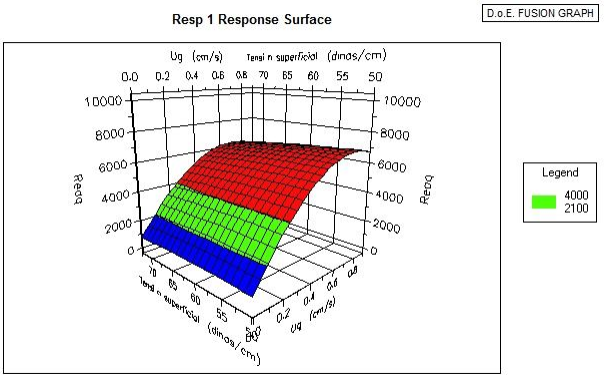

3 (a)

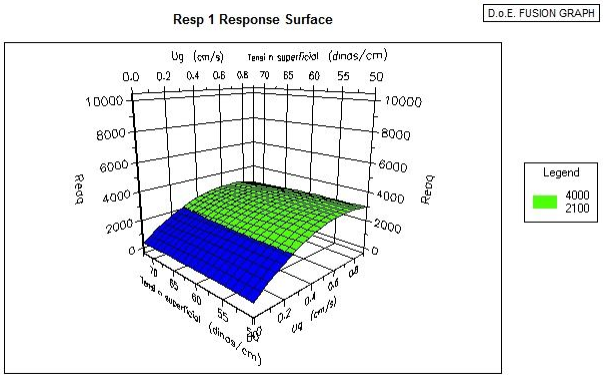

3 (b)

Figura 8.3 Re_{aq} en función de la velocidad superficial de la fase gaseosa (Ug) y de la tensión superficial (σ), tanto para la zona de ascenso (a) como el descenso (b) L2/L1 = 0.90, D2/D1 = 0.55 (1), 0.58 (2) y 0.65 (3).

Para todas las configuraciones del tubo concéntrico la zona de ascenso exhibió flujo turbulento ($4000 < Re_{aq} < 9000$ para $0.15 < Ug < 0.76$ cm s^{-1}) mientras que la zona de descenso presentó valores de Re_{aq} más bajos ($Re_{aq} < 4000$). Para todas las configuraciones el aumento en el diámetro del tubo concéntrico implicó un aumento en el Re_{aq} de la zona de descenso y una disminución de esté en la zona de ascenso. Por otro lado la disminución en la tensión superficial provocó un ligero aumento en Re_{aq} tanto en la zona de ascenso como en el descenso para las configuraciones ensayadas. La relación de altura del tubo concéntrico/altura del BAL que generó Re_{aq} mayores en la zona de descenso fue 0.77. La relación diámetro del tubo concéntrico/diámetro del BAL que generó mayores Re_{aq} en la zona de descenso fue 0.65. Dado que la zona de ascenso siempre exhibió flujo turbulento y la zona de descenso valores más bajos, seleccionamos la zona de descenso como la zona objetivo para seleccionar la configuración que ofrezca los más altos Re_{aq}.

Selección de la configuración geométrica

Para las relaciones geométricas D2/D1 = 0.65 y L2/L1 = 0.77 se observaron los mayores valores de Re_{aq} en la zona de descenso (*i.e.* cerca de 4000 para Ug = 0.76 cm s^{-1}) y por lo tanto se seleccionó esta configuración para los experimentos posteriores. La selección de está configuración está parcialmente de acuerdo con un estudio previo (Mehrnia y col., 2005), que trabajó con derivados del petróleo y un tubo perforado como distribuidor de aire; En ese estudio usaron una relación D2/D1 = 0.66, prácticamente igual que en nuestro trabajo, sin embargo su relación L2/L1 (0.90) fue mayor que la nuestra (0.77). Con el objetivo de determinar no sólo la hidrodinámica de la fase acuosa sino también la de la fase hidrocarburo se evaluó la hidrodinámica local para cada especie (agua y HXD).

8.2. Evaluación de las zonas hidrodinámicas locales en un reactor airlift trifásico: buscando el Re de fase líquida más bajo (Artículo publicado en RMIQ)

Resumen del artículo:

Se evaluó la hidrodinámica en las principales zonas (ascenso y descenso) de un reactor airlift (ALR) trifásico para encontrar el número de Reynolds (Re) de fase líquida más bajo. Las fases del estudio fueron: una gaseosa (aire) y dos líquidas (hidrocarburos y agua). Se definieron dos Re en las fases líquidas: Re_{aq} y Re_{HXD} correspondientes a las fases acuosa y oleosa. La fase gaseosa fue considerada por medio del coeficiente de retención (εg). En el ALR (10 L) la zona de ascenso mostró flujo turbulento ($4000 < Re_{aq} < 9000$) mientras que en la zona de descenso no se observó flujo turbulento ($1250 < Re_{aq} < 4000$). El Re_{HXD} en la zona de ascenso ($5000 < Re_{HXD} < 10000$) fue mayor que el Re_{aq}; mientras que en la zona de descenso fue menor ($200 < Re_{HXD} < 2200$). La fase oleosa en la zona de descenso fue la limitante hidrodinámica y consecuentemente se debería esperar una limitación en la transferencia de masa. La complejidad del flujo trifásico y las limitadas tecnologías para su medición han generado pocos estudios relacionados con las propiedades hidrodinámicas locales restringiendo la optimización y comercialización de los reactores trifásicos; nuestro estudio es una contribución a la identificación de este tipo de restricciones.

Revista Mexicana de Ingeniería Química

Volume 10 (2011) 59-65

ASSESSMENT OF THE LOCAL HYDRODYNAMIC ZONES IN A THREE-PHASE AIRLIFT REACTOR: LOOKING FOR THE LOWEST LIQUID-PHASE RE

Evaluación de las zonas hidrodinámicas locales en un reactor airlift trifásico: Buscando el Re de fase líquida más bajo

Lizardi-Jiménez M. A.[1]* and Gutiérrez-Rojas M.[1]

[1]Departamento de Biotecnología, Universidad Autónoma Metropolitana-Iztapalapa, Av. San Rafael Atlixco No. 186 Col. Vicentina, C.P. 09340, Ciudad de México, México.

*Corresponding author e-mail: cbs204381858@xanum.uam.mx

TEL: + 52 (55) 5804 6505

FAX: + 52 (55) 5804 6407

ABSTRACT

Hydrodynamic in main airlift reactor (ALR) zones (riser and downcomer) was evaluated in order to find the lowest Reynolds number (Re) in a three-phase ALR. In our study, three phases were identified: one gaseous (air) and two liquids (oil and aqueous). Two Re of the liquid species, one for each phase, were defined: Re_{aq} and Re_{oil} corresponding to the aqueous and oil phase, respectively. Since gas phase was considered by hold up (εg) in our work. In 10 L ALR, riser showed turbulent aqueous phase flow ($4000 < Re_{aq} < 9000$) whereas downcomer exhibited non-turbulent flow ($1250 < Re_{aq} < 4000$). Re_{oil} in riser ($5000 < Re_{oil} < 10000$) was higher than Re_{aq}; whereas in downcomer, Re_{oil} was lower than Re_{aq} ($200 < Re_{oil} < 2200$). The oil phase into the downcomer zone was demonstrated to be the most important hydrodynamic constraint and consequently limited mass transfer should be expected. The complexity of three-phase flow and the limited measurement technologies have generated few studies

regarding the local hydrodynamics properties restricting three-phase reactors optimization and commercialization; our study is a contribution to identify such restrictions.

KEYWORDS

Airlift, hydrodynamics, riser, downcomer, three-phase, Re.

INTRODUCTION

Airlift reactor (ALR) is a pneumatic reactor agitated with a continuous gas phase provided in form of bubbles, breaking-up towards the liquid phase resulting in an isothermal expansion to keep homogeneity (Chisti, 1989). In case of ALR performance, attention has been focused on two fundamental phenomena: (i) agitation for well mixed liquid phases (Gumery *et al.*, 2009) and (ii) oxygen mass transfer considering geometrics in internal loop reactors (Cerri *et al.*, 2010a) and CFD simulations (Huang *et.al*, 2010; Luo and Al-Dahhan, 2011). Agitation and mixing is often related to the Reynolds number (Re) as a global hydrodynamic parameter *i.e.* a bulk Re or a liquid phase Re (Wongsuchoto and Pavasant, 2004). Recent studies in ALR allow emphasizing the role of aqueous phase Re in two-phase ALR performance. Unfortunately, none of the works is oriented to study the different local hydrodynamic zones. For all types of ALR, it is possible to distinguish four different local hydrodynamic zones: riser, downcomer, top and bottom clearance (see Fig. 1). Although the hydrodynamic importance of zones in ALR performance is well documented (Sánchez-Mirón *et al*, 2004; Kilonzo *et al.*, 2006) most of ALR studies neither take into account zones or non-soluble aqueous substrates (*e.g.* oil) in three-phase systems. Studying aqueous and oil phase hydrodynamics in main three-phase ALR zones is very important because hydrodynamic is strongly implicated in both, aqueous soluble and non-soluble substrates and mass transfer phenomena and the resulting ALR performance; for example, bioengineering and oil biodesulfuration purposes (Mehrnia *et. al*., 2005; Shariati *et. al.*, 2007) or using silicone oil as an effective mass transfer vector (Quijano *et. al.*, 2009). The aim of this work is to assess, in a trhee-phase ALR, the local hydrodynamic zone (riser or downcomer) with lower Re by measuring fluid velocities in the aqueous and oil phases.

MATERIALS AND METHODS

Reactor

A 10-L operation volume airlift reactor (ALR) was used. The ALR cylindrical vessel was built in Pyrex glass (0.005 m of wall thickness). Gas phase was introduced into the ALR draft tube. Draft tube was located 0.035 m above the bottom. Geometrical relations and the flow pattern are shown in Fig. 1, in brief: D1 and D2 are reactor (0.14 m) and draft tube (0.09 m) diameter, respectively; L1 and L2 represent reactor (0.70 m) and draft tube (0.54 m) height; riser, top clearance, downcomer and bottom clearance are identified. Geometrical relations: D2/D1 = 0.65, L2/L1 = 0.77 and L1/D1 = 5 were used.

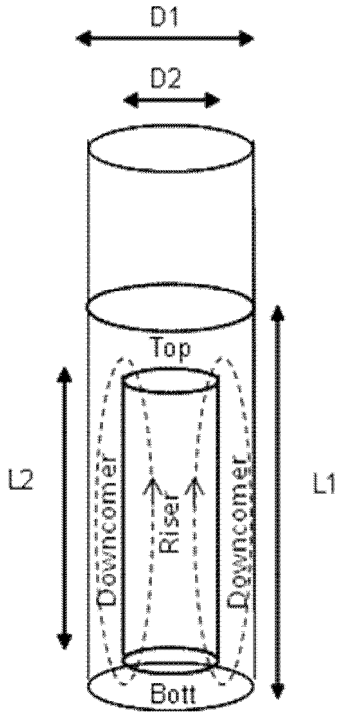

Figure 1. Geometrical relations and flow pattern in our three-phase airlift reactor

Gas sparger

Air was sparged through the draft tube with an L-form perforated (7 orifices; 0.001 m of diameter and 0.004 m of separation) stainless steel tubing (0.006 m internal diameter) driving out air downwards.

Two-liquid phase model medium

In order to adjust surface tension (σ), a model medium was designed using reference values (50 – 65 dynes cm^{-1}) as suggested elsewhere (Bai *et.al.*, 1997; Quijano *et. al*., 2010) by adding different Tween 20 (0-0.15 mL L^{-1}) concentrations and 13g L^{-1} of hexadecane (HXD). σ was measured with a Manual Fisher Surface Tensiometer Model 20 (Fisher Scientific International, Wisconsin, USA). Viscosity (μ) was determined by using a viscometer Physica MCR Model 300 (Sttuttgart, Germany).

Hydrodynamic parameters

Gas hold up

Gas hold up (εg) was evaluated into riser and downcomer by photographic method (Ribeiro and Lage, 2004) using a digital camera (Pentax Optio 50) and image analysis software (Image Pro plus 4.1).

Aqueous and oil phase hydrodynamic

Three phases (air, aqueous and oil) were involved in ALR, the two slow-moving phases (aqueous and oil) velocities were experimentally evaluated. In order to clearly follow flow patterns thorough model medium, we used two substances simulating water (sodium polyacrylate hydrogel; ρ=1.0 g cm^{-3}) and oil (oligosyloxane stained spheres; ρ = 0.77 g cm^{-3}). A digital videocamera (Sony HD) and on-line chronometer (StopWatch software) were used to

monitoring velocities of single spheres as path length/elapsed time ratio in both ALR zones: riser and downcomer. In order to contrast sphere images, HXD was previously stained with red chillies (*Capsicum annuum*) oleoresin (Montoya-Ballesteros *et. al.,* 2010), also known as rodophile (Bioquimex-Reka, México; 25.1 g of carotenoid kg^{-1}) (see Fig. 2). The resulting velocities were used to calculate two individual Reynolds numbers (Nielsen *et. al.,* 2003) as follows:

$$\mathrm{Re}_{aq} = \frac{DV_{aq}\rho_{aq}}{\mu} \qquad (1)$$

$$\mathrm{Re}_{oil} = \frac{DV_{oil}\rho_{oil}}{\mu} \qquad (2)$$

Where: Re_{aq} and Re_{oil} are aqueous and oil phase Reynolds number, respectively. D = D2 for riser zone; and D = (D1-D2) for downcomer zone; D1 is the ALR diameter, cm; D2 draft tube diameter, cm; V_{aq} aqueous phase velocity, cm s^{-1}; V_{oil} oil phase velocity, cm s^{-1}; ρ_{aq} aqueous phase density, g cm^{-3}; ρ_{oil} oil phase density, g cm^{-3}; μ bulk viscosity (oil in water emulsion), g cm s^{-1}. In order to validate our method, the V_{aqd} values obtained were compared with acid pulse method (Sanchez- Miron *et. al.,* 2004) . Chisti model (Chisti *et. al*., 1988; Abashar *et. al*., 1998) and the continuity criterion (Chisti, 1989) was used in order to predict superficial aqueous phase velocity (V_{aqd}) into downcomer using εg as follows:

$$V_{aqd} = \frac{A_r}{A_d}\left[\frac{2gL_D\left(\varepsilon g_r - \varepsilon g_d\right)}{K\left(\frac{1}{\left(1-\varepsilon g_r\right)^2} + \frac{\left(\frac{A_r}{A_d}\right)^2}{\left(1-\varepsilon g_d\right)^2}\right)}\right]^{0.5} \qquad (3)$$

Where: A_r and A_d are cross section area for riser and downcomer, m^2, respectively. εg_r and εg_d are gas hold up in riser and downcomer, dimensionless, respectively, K is the loss friction coefficient, dimensionless, g is the gravitational acceleration constat, $m\ s^{-2}$ and L_D is the draft tube lenght, m.

The model assumes the following: (1) steady-state conditions, (2) isothermal conditions, (3) the energy losses terms due to the skin friction in the riser and the downcomer are negligible in comparison to the others dissipation terms, (4) the presure drop due to acceleration is negligible.

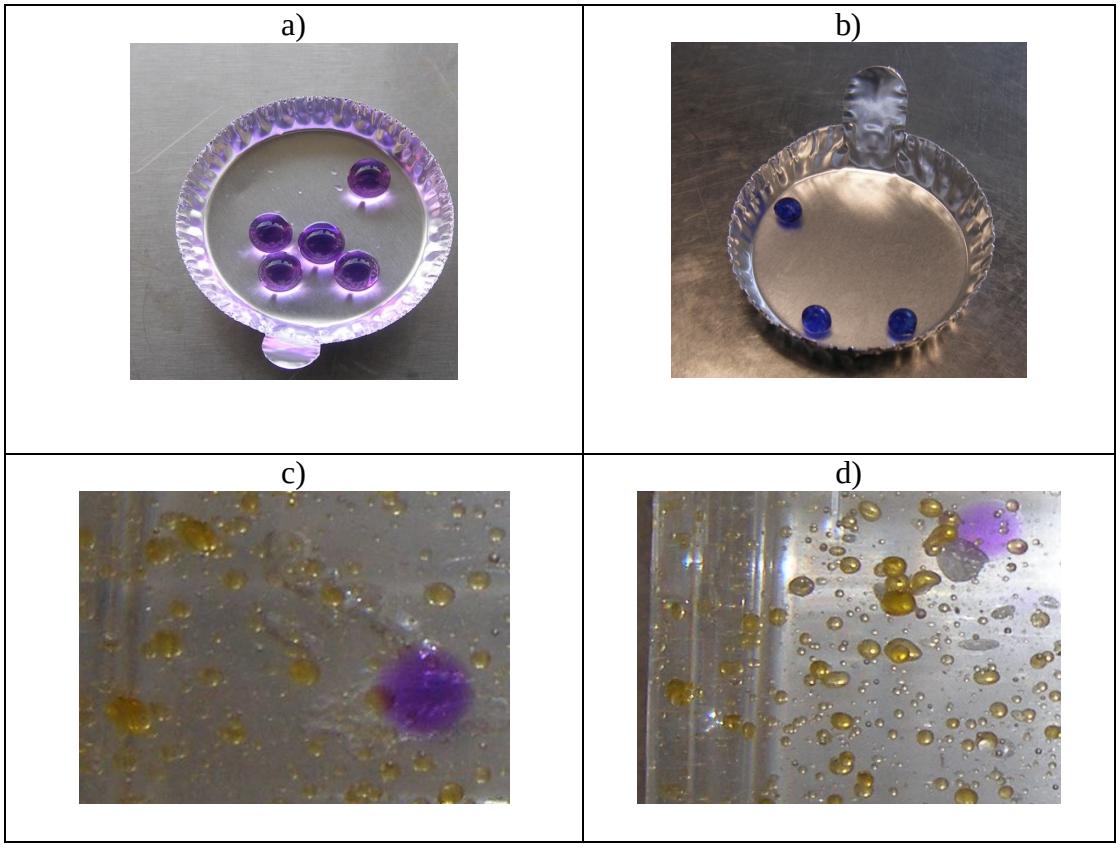

Figure 2. Polyacrilate (a) and olygosyloxane (b) spheres. Polyacrilate sphere in downcomer (c) and riser (d) clearly distinguished from air bubbles and HXD yellow stained droplets.

Statistical analyses

Data analyses were carried out by using NCSS-2000, version 2001 (Copyright 2001 by Jerry Hintze). Analysis of variance (ANOVA) was performed by comparing tests with $p < 0.05$.

RESULTS AND DISCUSSION

In order to evaluate hydrodynamic behavior in our three-phase ALR, εg, liquid phases velocities, Re_{aq} and Re_{oil} were measured using geometrical relations D2/D1 = 0.65 and L2/L1 = 0.77. The choice of this configuration is partially according to a similar hydrocarbon/liquid ALR (Gumery *et.al.*, 2005) studying dynamics and macro-mixing for design and scale-up purposes. Fig. 3 shows εg as a function of Ug into riser and downcomer. The εg in the riser was slightly higher than in the downcomer. A potential model: $\varepsilon g = a\mathrm{Ug}^b$ (where a and b depend on local hydrodynamic) was used for both: riser (a = 0.053 and b = 0.74; R^2 =0.99) and downcomer (a = 0.045 and b =0.72; R^2 = 0.98). The differences between εg in riser and downcomer caused liquid phases circulation. The potential model data obtained from Fig. 3 were used in order to predict superficial aqueous phase velocities into downcomer (V_{aqd}) using the Chisti model, see Eq. 3. Fig. 4 shows experimental data of V_{aqd} as a function of Ug in addition to V_{aqd} values predicted by the Chisti model. A good fitting value for the loss friction coefficient (K) of 4, close to other work (1.8) with water and kerosene (Abashar et. al., 1998), was found.

Fig. 5 shows Re_{aq} as a function of Ug and σ, for the selected configuration in riser (5a) and downcomer (5b). As expected, in riser and downcomer, Re increased as Ug increased. On the other hand Re_{aq} slightly decreased as σ increased. A similar performance was also observed in other pneumatic reactors working with two-phase systems (Kantarci *et al.*, 2005). Riser shows turbulent flow (Re_{aq} > 4000; see red zone in Fig. 5a) when Ug was higher than 0.4 cm s^{-1}, whilst downcomer do not (red zone is absent in Fig. 5b). Re_{aq} increased as Ug probably due to differences in gas hold up between riser and downcomer, which produces differences in hydrostatic pressure at the ALR bottom, these differences in hydrostatic pressure produce the

liquid phase being in continuos movement. The Re_{aq} decreasing as surface tension increased could be explained by reason of gas hold up decreased as a result of larger bubbles with lower residence time and the resultant decreasing in the differences in hydrostatic pressure. Moreover, lower Re_{aq} in downcomer (not turbulent) supposes a hydrodynamics limitation for mixing probably imposing mass transfer limitation (Nielsen *et al.,* 2003); this limitation is worst for oil phase as can be seen in Figs 5c and 5d. Figures show Re_{oil} as a function of Ug and surface tension. Re_{oil} in riser ($5000 < Re_{oil} < 10000$) (Fig. 5c) was higher than Re_{aq}; whereas in downcomer was lower ($200 < Re_{oil} < 2200$) (Fig. 5d). Re_{oil} in riser and downcomer were higher and lower than Re_{aq}, respectively, due to densities differences. Lower Re_{oil} values in downcomer involve an increasing in boundary layer between oil and aqueous phase, probably resulting in mass transfer constraints (Cerri *et al.,* 2010a). Our results suggest that a carefully evaluation of the two Re species, involved in performance of three-phase ALR was needed since oil phase into the downcomer supposed a clear hydrodynamic and probably mass transfer limitation. Traditional two-phase model that considers only aqueous phase is not enough to explain oil in water reactors. For example, oil-degrading microorganism growth (Medina-Moreno *et al.,* 2009) should consider oil transfer constraints in the bulk. The complexity of three-phase flow and the limited measurement technologies have generated few studies regarding the local hydrodynamics properties restricting three-phase reactors optimization and commercialization.

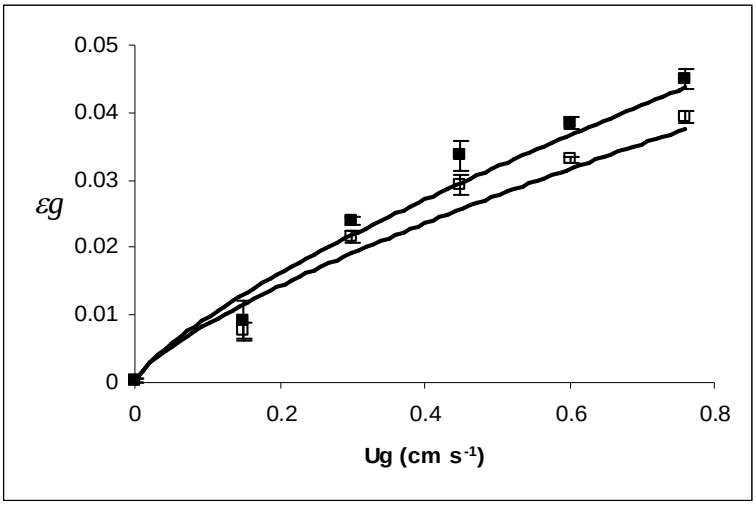

Figure 3. Gas hold up (εg) as a function of superficial gas velocity (Ug): (■) riser and (□) downcomer. Continuos line represents potential model with R^2 higher than 0.98. Error bars represent the standard error for triplicate samples.

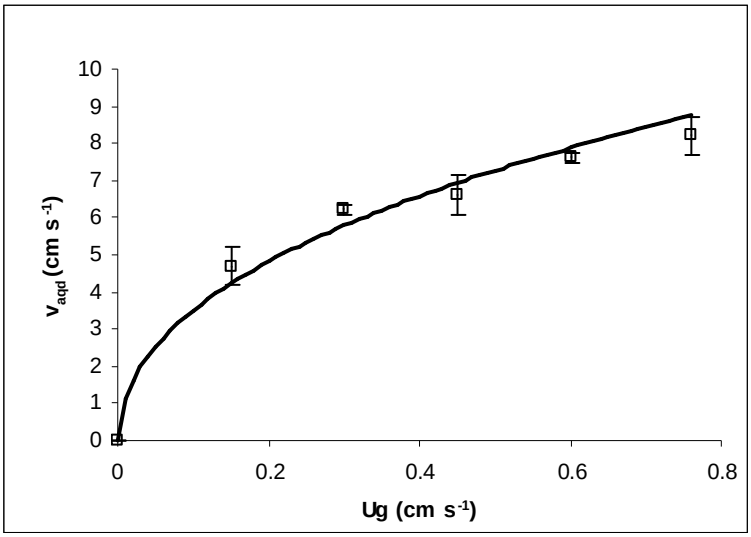

Figure 4. Superficial aqueous phase velocity into the downcomer (V_{aqd}) as a function of superficial gas velocity (Ug). Continuous line represents Chisti model with R^2 higher than 0.96. Error bars represent the standard error for triplicate samples.

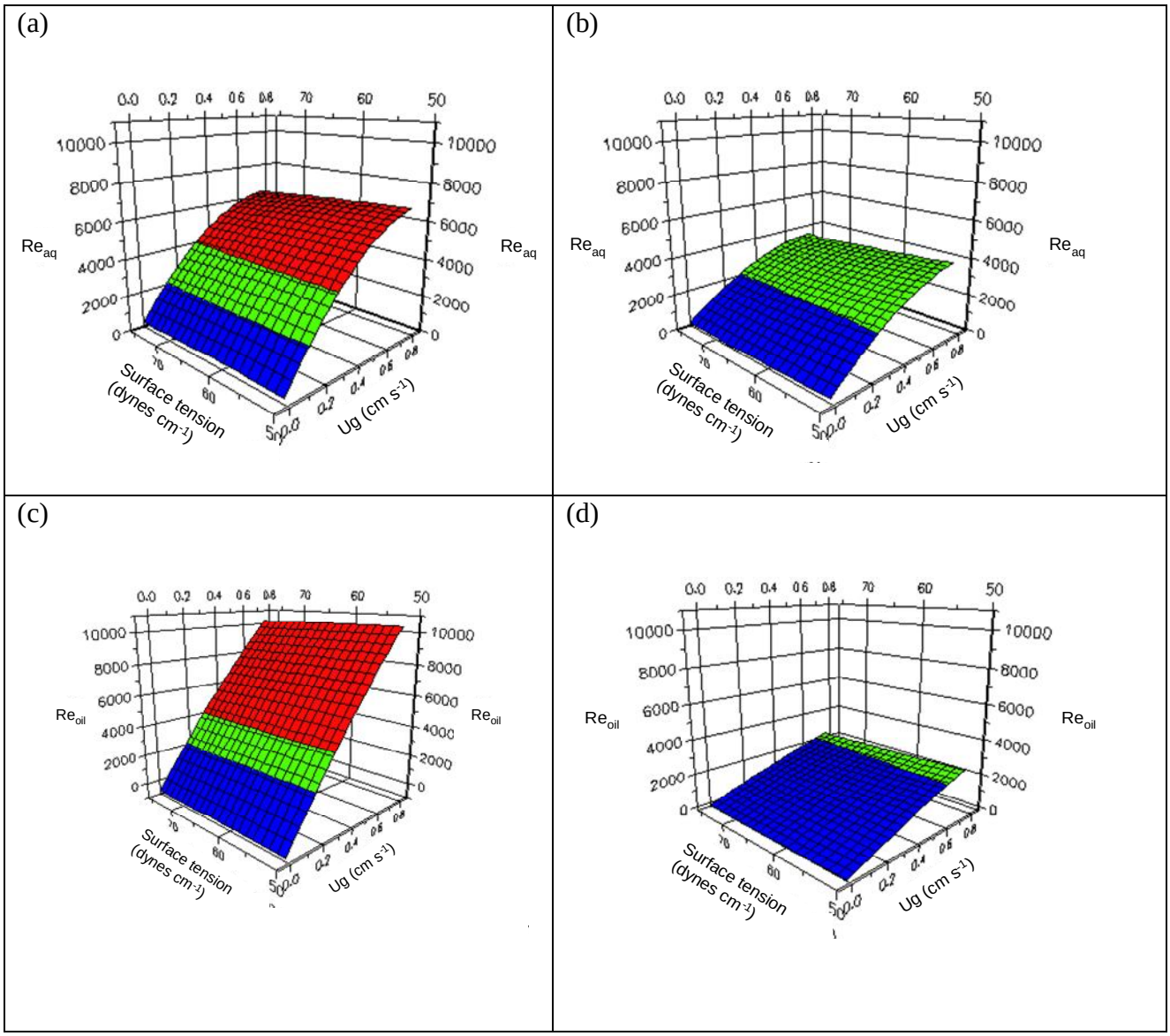

Figure 5. Re_{aq} as function of superficial gas velocity (Ug) and surface tension (σ) in riser (a) and downcomer (b); Re_{oil} as function of Ug and σ in riser (c) and downcomer (d). Red zone: Re ≥ 4000; turbulent flow. Green zone: 4000 ≥ Re ≥ 2000; transient flow. Blue zone: Re ≤ 2000 ; laminar flow.

CONCLUSIONS

Aqueous and oil phase Re for main ALR local hydrodynamics zones, riser and downcomer, in a three-phase ALR were evaluated in this work. Riser shows turbulent aqueous phase flow: $4000 < Re_{aq} < 9000$ for $0.15 < Ug < 0.76$ cm s^{-1} whereas downcomer shows non-turbulent aqueous phase flow: $1250 < Re_{aq} < 4000$ at the same above mentioned Ug values. Oil phase Re in riser ($5000 < Re_{oil} < 10000$) was higher than Re_{aq}; whereas in downcomer, Re_{oil} was lower than Re_{aq} ($200 < Re_{oil} < 2200$). Re_{oil} into downcomer zone is supposed to be the most important hydrodynamic constraint allowing us to identify the downcomer as a relevant mass transfer limitation zone.

ACKNOWLEDGEMENTS

We acknowledge CONACYT (Consejo Nacional de Ciencia y Tecnología) by scholarship to M. A. Lizardi-Jimenez and PEMEX-Refinación for partial support. Thanks are due to Dr. J. Vernon in providing rhodophile pigment solution.

El artículo publicado se muestra en su formato original en el Anexo 1.

Otro tipo de restricción para la optimización y comercialización de los reactores trifásicos es la transferencia de masa y el consumo del sustrato menos soluble (HXD). En la siguiente sección (8.3.) se caracterizó la emulsión de HXD en agua con el objetivo de determinar el área de transferencia de HXD (a_{HXD}).

8.3. Caracterización de la emulsión de hexadecano en agua y evaluación del consumo de las formas emulsificadas y libre por un consorcio microbiano

El objetivo de esta sección es caracterizar el tamaño de las gotas de las formas emulsificadas del HXD en emulsiones acuosas y evaluar el consumo de las formas emulsificadas y libre por el consorcio microbiano.

Caracterización de la emulsión

Con el objetivo de caracterizar la emulsión se determinó el tamaño de las gotas del sustrato menos soluble, la fase HXD. Los primeros experimentos realizados con el objetivo de caracterizar la emulsion fueron abióticos. Se utilizó el medio mineral ajustando la tensión superficial (σ) y viscosidad (μ) a los valores que presenta el medio biótico en donde crece el consorcio microbiano degradador de petróleo, 68 dinas cm^{-1} y 1.02 cP respectivamente. La Figura 8.4 muestra que se encontraron dos tamaños de gotas: microgotas mayores de 0.5 μm y microgotas de alrededor de 0.1 μm En un porcentaje de volumen de 80/20 (% V/V) respectivamente (Figura 8.5).

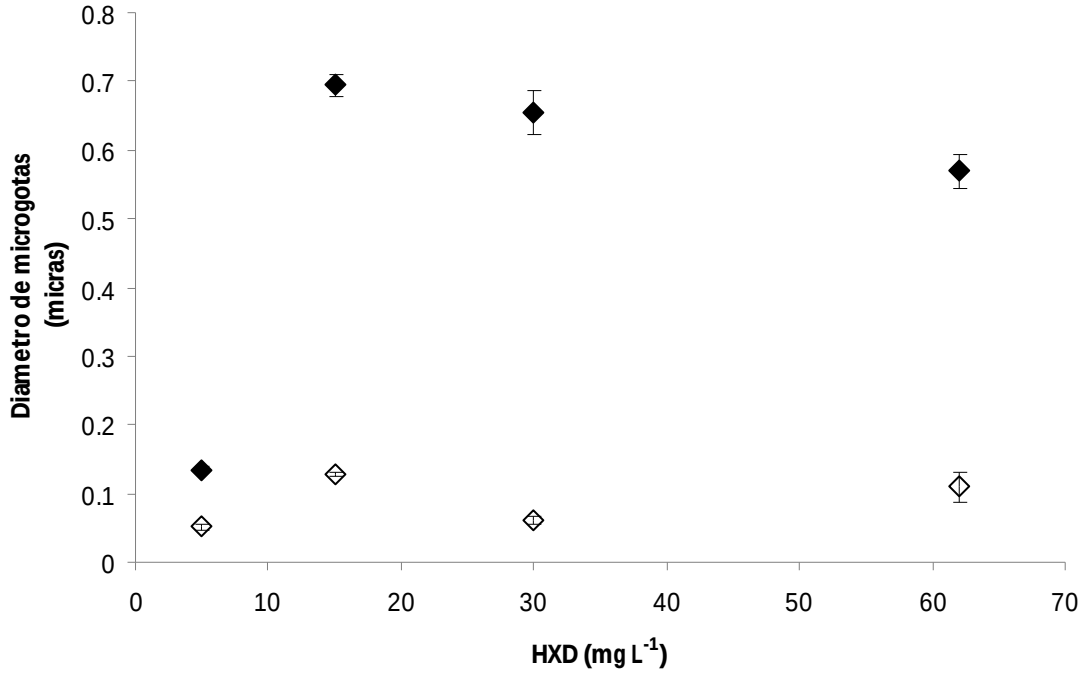

Figura 8.4. Diámetro de partículas de las formas emulsificadas en función de la concentración de saturación de HXD: (♦) gotas de 0.5 μm y (◊) gotas de 0.1 μm.

Con la determinación de los tamaños relativos de las formas emulsificadas del HXD y del volumen que ocupan se obtuvo el área especifica para cada forma: microgotas de 0.5 μm, 2, 000 cm^{-1} (cm^2 de superficie de la gota de HXD por cm^3 de la emulsión HXD en agua), microgotas de 0.1 μm, 10, 000 cm^{-1}.

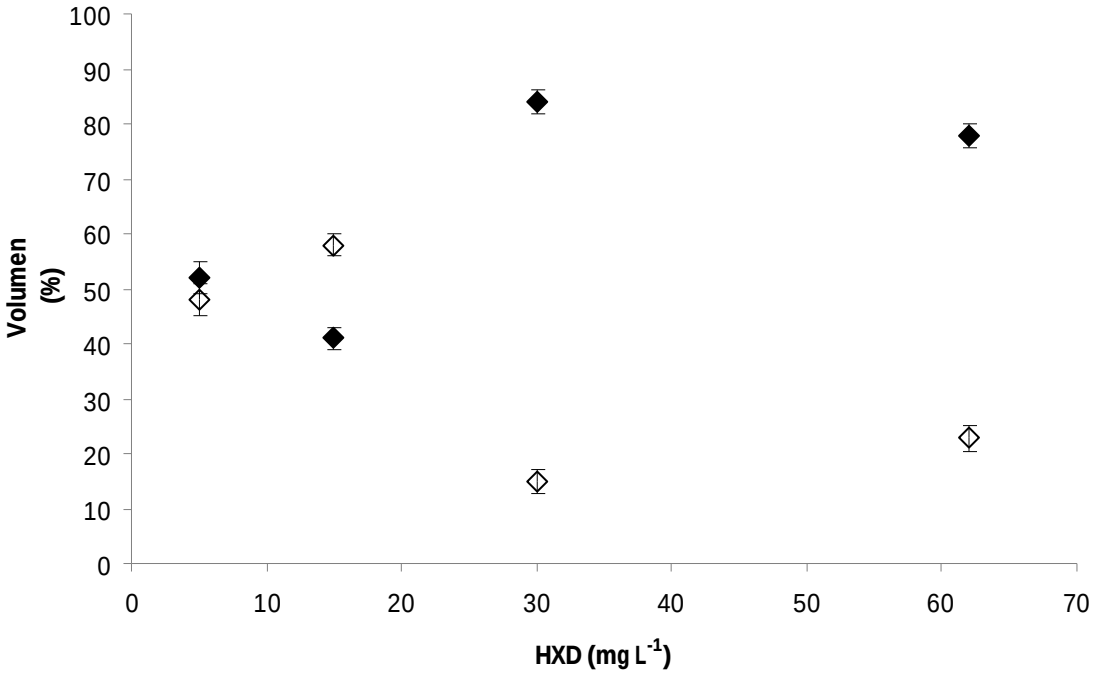

Figura 8.5 Porcentaje en volumen de las formas emulsificadas en función de la concentración de saturación de HXD. (♦) gotas de 0.5 µm y (◊) gotas de 0.1 µm.

En los experimentos bióticos, en presencia del consorcio microbiano degradador de petróleo, para concentraciones iniciales de 62, 45, 30, 15 y 5 mg HXD L^{-1} (sin formas libres) se encontraron los mismos dos tamaños de gota que en los experimentos abióticos: 0.5 y 0.1 µm (Figura 8.6), por lo cual se denomina microemulsión (Shariati y col., 2007) La coincidencia en los resultados del tamaño de microgotas en la microemulsión indicaron el acierto en el diseño del medio modelo abiótico además de que permitió validar el uso del surfactante químico Tween 20 (1227 g mol^{-1}), con fórmula química condensada $C_{55}H_{114}O_{26}$, como molécula simuladora del biosurfactante producido por al menos una cepa del consorcio, *Acinetobacter bouvetii,* (probablemente emulsan, con fórmula química condensada $C_{55}H_{99}O_{19}$) (Tzintzun-Camacho y col., 2011).

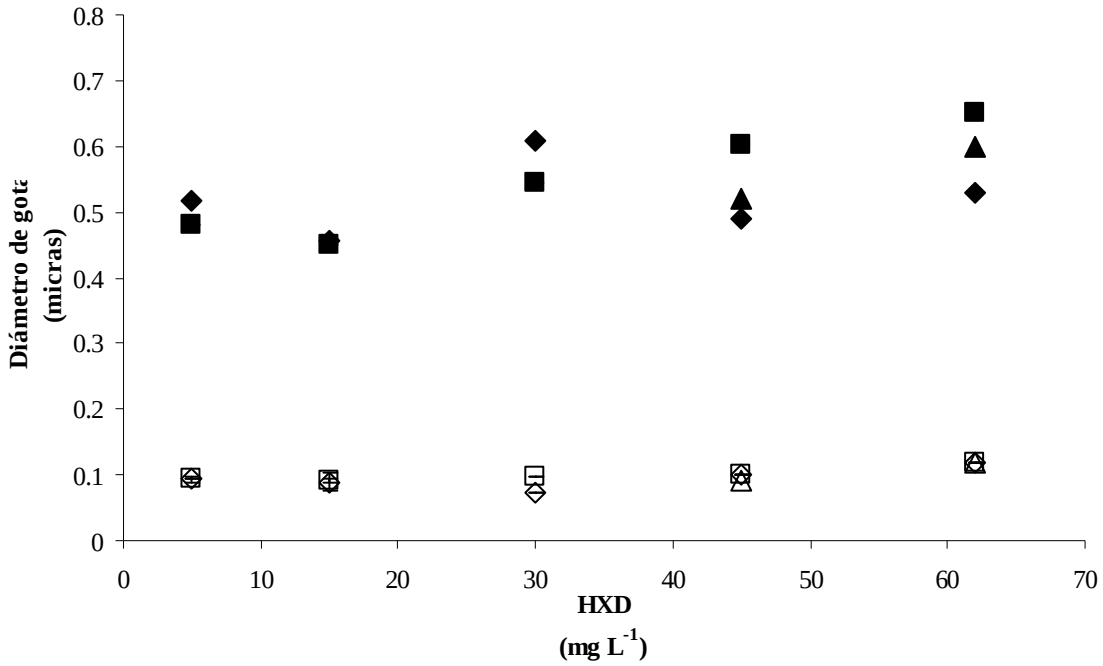

Figura 8.6 Tamaños de gota a distintos tiempos de cultivo en función de la concentración inicial de HXD: (◊) 0 h gotas de 0.1 µm (□) 2 h gotas de 0.1 µm (Δ) 4 h gotas de 0.1 µm (♦) 0 h gotas de 0.5 µm (■) 2 h gotas de 0.5 µm (▲) 4 h gotas de 0.5 µm.

El área específica de las formas emulsificadas (2, 000 cm^{-1} para microgotas de 0.5 µm y 10, 000 cm^{-1} para microgotas de 0.1 µm,) fue mayor que la del HXD libre, obtenida por técnicas fotográficas (0.87 cm^{-1} para gotas de 1.3 mm) y que se detalla en la Sección 8.4. Por lo tanto es correcto usar el área específica del HXD libre para estimar la tasa de transferencia de HXD (utilizada en la Sección 8.4. y la Sección 8.5.). La emulsión presentó una tendencia a la estabilidad de estos tamaños de partícula independientemente del tiempo de cultivo en el que se tomó la muestra y siempre en una proporción de 95/5 (% V/V) para las microgotas de 0.5 y 0.1 µm respectivamente, lo que sugirió que no hay una preferencia en el consumo entre los dos tamaños de microgotas.

Evaluación del consumo de las formas de HXD

El HXD residual disminuyó a lo largo del tiempo de cultivo, agotándose a las 10 h para todas las concentraciones iniciales de las formas emulsificadas ensayadas (Figura 8.7).

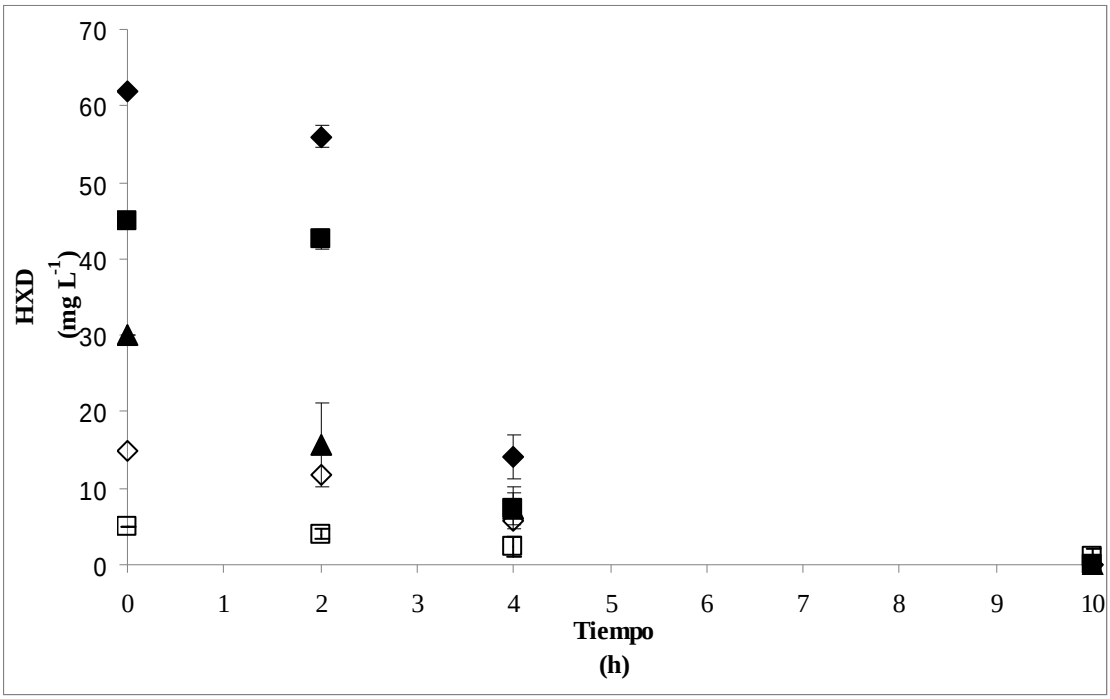

Figura 8.7 HXD residual en función del tiempo de cultivo (mg L^{-1}): (♦) 62, (■) 45, (▲) 30, (◊) 15, (□) 5.

La tasa de consumo máxima (q_{max}) de las formas emulsificadas aumentó con la concentración inicial de HXD (Tabla 8.1). Las q_{max} obtenidas sin HXD libre fueron siempre menores a las que se obtuvieron cuando estuvo presente el HXD libre (89 mg HXD L^{-1} h^{-1} para una concentración de HXD de 13 000 mg HXD L^{-1}) lo cual sugiere que el consumo de HXD puede ser por: a) contacto directo de la forma no emulsificada, y b) consumo de las formas emulsificadas que se estarían continuamente formando a partir del HXD libre (el que se encuentra en las gotas macroscópicas) que se encuentra en equilibrio dinámico con las formas emulsificadas de tal manera que el HXD libre está funcionando continuamente como reservorio del HXD. Estudios recientes en nuestro laboratorio sugieren que el consumo de la

forma libre se puede deber a la cepa *Defluvibacter lusatiensis* identificada en el consorcio microbiano que se utiliza en este trabajo y que consume hasta el 30 % del HXD. Sin embargo, una comparación de la tasa especifica de consumo máxima ($q_{esp\text{-}max}$) expresada como el cociente de la tasa máxima de consumo de HXD entre la cantidad de biomasa formada, en nuestro caso medida como sólidos suspendidos (SS), indicó que tanto para el caso en el que sólo hay formas emulsificadas como para el caso en que se encuentra presente el HXD libre la $q_{esp\text{-}max}$ fue similar, alrededor de 0.37 mg HXD mg SS^{-1} L^{-1}, lo que sugiere que el consumo de HXD se realiza preferentemente a partir de las formas emulsificadas. La preferencia del consorcio por el consumo de las formas emulsificadas parece ser apoyado por la evidencia de que las cepas de *Acinetobacter bouvetii y Xantomonas sp* identificadas en el consorcio microbiano son capaces de degradar hasta el 85 % del HXD según se ha demostrado en trabajos recientes en nuestro laboratorio. Más aun, es probable que en presencia de surfactantes biológicos incluso la cepa de *Defluvibacter lusatiensis* consuma preferentemente las formas emulsificadas y por esa razón la contribución de las formas libres no se vea reflejada en un aumento de la $q_{esp\text{-}max}$. Sin embargo, hacen falta estudios concluyentes al respecto que involucren observaciones microscópicas (fotográficas o videográficas) directas sobre las gotas de HXD y los consorcios microbianos en la emulsión (Dorobantu y col., 2004). Con el objetivo de estimar el consumo de las formas emulsificadas del HXD fue pertinente proponer una novedosa técnica que permita evaluar la transferencia del HXD libre a las formas emulsificadas (como se detalla en la Sección 8.4.) adicionalmente a la transferencia de oxígeno en el BAL trifásico y compararla con el cociente de consumo estequiométrico (como se muestra en la Sección 8.5.).

Tabla 8.1 Tasas máximas de consumo de HXD

Concentración inicial (mg HXD L^{-1})	Tasas máximas de consumo (q_{max}) (mg HXD L^{-1} h^{-1})
13 000	**89***
62	**23**
45	**20**
30	**12**
15	**2**
5	**1**

***** Presencia de las formas libres de HXD

8.4. Desarrollo de una nueva técnica dinámica para la determinación de la tasa de transferencia de HXD (TTH) (Artículo publicado en el IJCRE)

Resumen del artículo:

La determinación de las tasas de transferencia de sustratos no solubles es una importante limitación en los bioreactores airlift trifásicos. Una nueva técnica dinámica para medir la tasa de transferencia de hidrocarburo (TTH) se presenta en este trabajo. La técnica de análisis de imágenes permitió la medición del área de transferencia específica resultante (a_{HXD}). La técnica de cromatografía de gases fue usada para medir el HXD transferido con el tiempo y por lo tanto $k_{LHXD.}$ Finalmente, TTH fue calculada usando la ecuación $TTH = k_L a_{HXD}(C^*_{HXD}-C_{HXD})$ en donde C_{HXD}* y C_{HXD} son la concentración de saturación en la emulsión en la interfase HXD-agua y la concentración del HXD en la emulsión respectivamente.

Como un estudio de caso, aplicamos exitosamente está técnica para medir TTH durante un el cultivo de un consorcio microbiano. Está técnica fue usada más adelante (Sección 8.5.) para comparar parámetros de transferencia de masa que limitan simultáneamente al BAL trifásico

El artículo publicado se muestra en su formato original en el Anexo 2.

International Journal of Chemical Reactor Engineering

Volume 9 (2011) Note S3

DYNAMIC TECHNIQUE TO DETERMINE HEXADECANE TRANSFER RATE FROM ORGANIC PHASE TO AQUEOUS PHASE IN A THREE-PHASE BIOREACTOR

Lizardi-Jiménez M. A.[1], Saucedo-Castañeda G.[1], Thalasso F.[2] and Gutiérrez-Rojas M.[1]*

[1]Departamento de Biotecnología, Universidad Autónoma Metropolitana-Iztapalapa, Av. San Rafael Atlixco No. 186 Col. Vicentina, C.P. 09340, Ciudad de México, México. [2] CINVESTAV

*Corresponding author e-mail: mgr@xanum.uam.mx

TEL: + 52 (55) 5804 6505

FAX: + 52 (55) 5804 6407

ABSTRACT

Determination of mass transfer of non-water soluble substrates, as hexadecane (HXD), is an important constraint in three-phase airlift bioreactor. A new simple dynamic technique able to measure the hexadecane transfer rate (HTR) in a three-phase airlift bioreactor (ALB) was studied in this work. The image analices technique allowed measuring the resulting specific mass transfer area (a_{HXD}). Gas chromatography was used to measure time-dependent transferred HXD and therefore the HXD transfer coefficient (k_{LHXD}). Finally, HTR was calculated by using the equation $HTR = k_L a_{HXD}(C_{HXD}^* - C_{HXD})$ where C_{HXD}^* and C_{HXD} are the saturation HXD-aqueous interphase and HXD aqueous phase concentration, respectively. As case study, we successfully applied to the measurement of HTR during a typical ALB microbial consortium culture; values from 0.010 to 0.042 mg HXD $(L\ h)^{-1}$ were found. This

technique could be used to compare similar simultaneously occurring parameters to assess mass transfer constraints in three-phase systems.

KEYWORDS: airlift, three-phase system, mass transfer, technique, hexadecane.

INTRODUCTION

Most of airlift bioreactor (ALB) studies, concerning three-phase systems, hydrocarbons in water emulsion included, usually consider only oxygen transfer and do not take into account water-insoluble liquid substrates (Medina-Moreno *et al.,* 2005; Mehrnia *et al.*, 2005; Shariati *et al.*, 2007). To determine volumetric oxygen transfer coefficient (k_La_{O2}) from the gas to the water phase and consequently oxygen transfer rate, dynamic and steady state methods can be used (Fujio *et al.,* 1973; Cerri *et al.,* 2010a). In the dynamic method, the change of the dissolved oxygen concentration is monitored in time after a step-change of the concentration in the inlet gas. In the steady-state method, the concentration measurements are done at one moment after steady state has been reached (Cesario *et al.,* 1996). In order to use the dynamic method a quick and accurate measurement of the concentration is critical; for example in case of oxygen, where a continuous monitoring of the dissolved oxygen can be accomplished by using an oxygen probe. It is more difficult when an organic water-insoluble compound such as hexadecane (HXD) is used. Moreover, when HXD is the main substrate to be consumed as sole source of carbon and energy, the transport towards the aqueous phase is often the rate-limiting step in many microbial cultivation processes (Cesario *et al.,* 1996). Whilst the product k_La_{O2} is usually measured, such parameter characterizes the transport from gas to aqueous phase, the evaluation of oxygen transfer coefficient (k_{LO2}) and oxygen specific transfer area (a_{O2}) in pneumatic reactors has been recently studied (Cerri *et al.* 2010b); unfortunately, there is no HXD probe available allowing any similar evaluation, it was necessary to measure both the HXD specific mass transfer area (a_{HXD}) and the HXD transfer coefficient (k_{LHXD}) separately. A new simple dynamic technique to determine the volumetric hexadecane transfer coefficient (k_La_{HXD}) and consecuently hexadecane transfer rate (HTR) is here proposed. The aim of this work was to propose an experimental technique able to determine HTR in a three-

phase (air, aqueous, HXD) airlift bioreactor. The technique was applied to a HXD degrading bacterial consortium culture.

MATERIALS AND METHODS

Microbial consortium culture

A bacterial consortium (*Xanthomonas sp, Acinetobacter bouvetii, Shewanella sp* and *Defluvibacter lusatiae)* was cultured in a previously reported mineral medium (Medina-Moreno *et al*., 2005) added with 13 g L^{-1} of HXD (Sigma-Aldrich, 99.7 %).

Bioreactor

A 10-Liters airlift bioreactor (ALB) was used in this work. ALB cylindrical vessel was made of Pyrex glass (0.14 m diameter; 1.0 m height) provided with a draft tube (0.09 m diameter; 0.54 m height) located 0.035 m above the bottom; air was sparged through the draft tube with a L-shaped perforated (7 orifices; 1.0 mm diameter) stainless steel 1/4 inch internal diameter.

Abiotic medium

In order to adjust the bulk HXD concentration under saturation (C_{HXD}^{*}) up to 65 mg HXD L^{-1}, as published elsewhere (Bai *et al.*, 1997; Quijano *et al.,* 2010), an abiotic medium was designed by adding different Tween 20 (0-0.15 mL L^{-1}) concentrations and HXD (13g L^{-1}). Surface tension was measured in order to compare the chemical surfactant (Tween 20) to biosurfactant emulsification ability. The subsequent experiments were performed using the abiotic medium.

HXD specific area

The HXD specific mass transfer area (a_{HXD}) was calculated by Equation 1 (Torres-Martinez *et al.*, 2009).

$$a_{HXD} = \frac{6}{d_{32HXD}}\phi \qquad (1)$$

where d_{32HXD} is the Sauter mean diameter of HXD droplets (cm) and ϕ is the HXD dispersed phase fraction (dimensionless); it was measured in the downcomer, located in annular zone in our ALB, through d_{32HXD} measurement with a digital camera and image analysis software (Image Pro Plus 4.1., Media Cybernetics, USA). In order to contrast droplet images, HXD was previously stained with red chillies (Capsicum *annuum)* oleoresin, also known as rodophile (Bioquimex-Reka, México; 25.1 g of carotenoid kg^{-1}). Assays were carried out by triplicate. d_{32HXD} was measured in triplicate. In each experiment, from 500 to 600 HXD droplets were measured. This number was always greater than 500 as recommended elsewhere (García-Salas *et.al*, 2008) for reliable results.

HXD transfer parameters

k_La_{HXD} was evaluated as follows: abiotic medium (10 L) was added to ALB. A stainless steel cylinder (1 cm diameter; 3.5 cm height) was filled with HXD and introduced with the open side downward into the downcomer. The filled stainless steel cylinder was introduced into the medium before start aeration. Air supply was turned on and superficial gas velocity (Ug) was adjusted to any desired working value of 0.15 to 1.6 cm s^{-1}. Once aeration was steady, 5 mL samples were extracted each 60 min. Transferred HXD from organic to aqueous phase was recovered by three successive extractions with a sample to solvent ratio of 1:5 (*v/v*) using a hexane (J.T. Baker, 99.6%)/isotonic solution (1:3 *v/v*) as solvent. The organic phases containing transferred HXD were pooled and stored into vials (30 mL; 4°C) for further

analysis. The HXD transfer coefficient (k_{LHXD}) was obtained from the stainless steel cylinder (cross section) mass transfer area as the one responsable for all HXD delivered to the medium. And we used, by analogy to oxygen transfer principles, the clasical dynamic method (Fujio *et.al*., 1973); whilst, k_La_{HXD} was obtained as the product of k_{LHXD} and specific mass transfer area of the HXD droplets (a_{HXD}). Finally, HXD transfer rate (HTR) was calculated with the equation $HTR = k_La_{HXD} (C_{HXD}^* - C_{HXD})$; where, C_{HXD} is the measured HXD concentration into the bulk.

RESULTS AND DISCUSSION

Abiotic medium

In order to find the Tween 20 concentration providing C_{HXD}^* up to 65 mg HXD L^{-1} assays at different concentrations were done. Surface tension was measured to compare with biotic medium characteristics (65-47 dynes cm^{-1}) (Quijano *et al.,* 2010). Figure 1 shows C_{HXD}^* (right-hand ordinate) and surface tension (left ordinate) profiles as a function of Tween 20 concentration. As we expected, surface tension values decreased as Tween 20 concentration was increased. In opposition, the increase in Tween 20 allowed increasing C_{HXD}^* up to 100 mg HXD L^{-1}. According to Figure 1, 0.08 mL of Tween 20 per liter of mineral medium are needed to reach 65 mg HXD L^{-1} and the resulting surface tension was 65 dynes cm^{-1}. Such surface tension values associated to C_{HXD}^* (65 mg HXD L^{-1}) were similar to those previously published (Quijano *et al.,* 2010) in bubble columns. The experimental abiotic medium was able to reproduce similar C_{HXD}^* values to those observed with biotic medium. The designed abiotic medium was used for HXD specific area and mass transfer parameters determination. The designed abiotic medium was used for HXD specific area and mass transfer parameters determination.

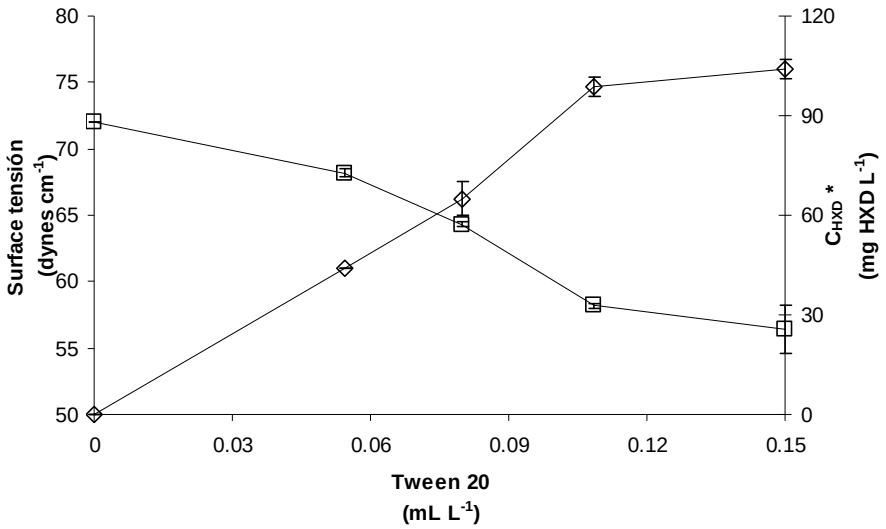

Figure 1. Surface tension (□) and C^*_{HXD} (◊) as a function of Tween 20 concentration

HXD specific area

With the purpose of clearly distinguish between air bubbles and the HXD droplets, HXD was stained with rhodophile and image analyses were applied toward HXD. Figure 2 shows two kinds of HXD droplets: (a) non-stained and (b) stained. In Figure 2b all air bubbles were translucent and excluded during the image analysis. Droplets were easily contrasted when rhodophile pigment was used and d_{32HXD} was measured without doubt.

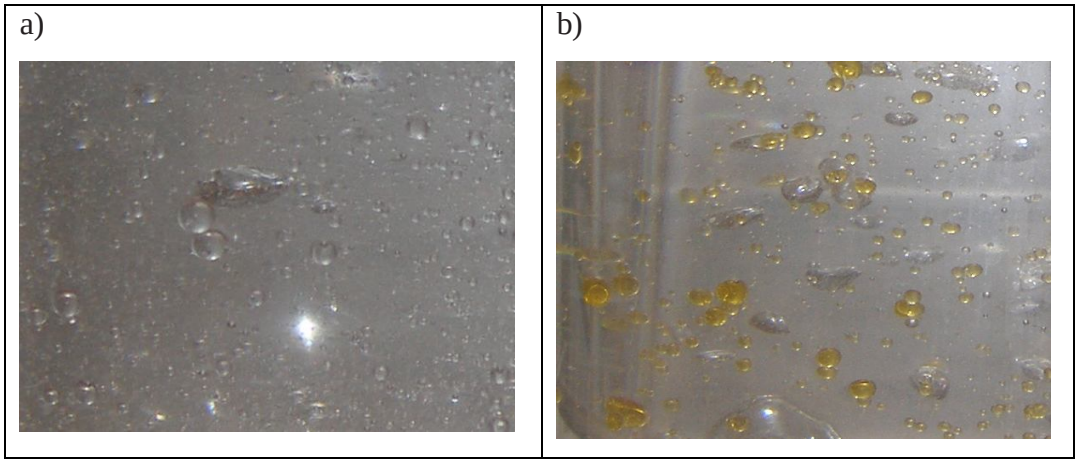

Figure 2. HXD droplets: (a) non-stained and, (b) rhodophile stained.

Table 1 shows d_{32HXD}, a_{HXD} and HXD transfer parameters as a function of Ug. a_{HXD} increased (0.35 – 0.87 cm^2 cm^{-3}) as Ug rose from 0.15 to 1.54 cm s^{-1} as can be seen in 3rd column. All a_{HXD} were used to calculate HXD transfer parameters.

HXD transfer parameters

HXD transfer coefficient (k_{LHXD}), HXD volumetric transfer coefficient (k_La_{HXD}) and HXD transfer rate (HTR) were evaluated as the main mass transfer parameters (Lemoine and Morsi, 2005). k_{LHXD} as a function of Ug is shown in Table 1. The increase in k_{LHXD} values could be due to rapid aqueous phase movement which diminished HXD-water boundary layer (Nielsen et al., 2003). The product of k_{LHXD} by aHXD was computed with the intention to obtain the mass transfer parameter k_La_{HXD}. k_La_{HXD} as a function of Ug is shown in Table 1. As expected, k_La_{HXD} increased (0.005 - 0.023 h-1) with increasing Ug. Higher k_La_{HXD} values (0.8 - 1.3 h^{-1}) were estimated in a 1-Liter bubble column reactor working with constant Ug (1.0 cm s^{-1}) for different culture times involving HXD-water emulsions (Quijano *et al*., 2010). Our data show at least two magnitude order lower; however, they did not evaluate a_{HXD} as a function of experimental d_{32HXD}. Finally, HTR from HXD droplets to the aqueous phase can be calculated by the product $k_La_{HXD}\cdot (C_{HXD}^* - C_{HXD})$; where C_{HXD}^* and C_{HXD} are the saturation HXD-

aqueous interphase and HXD aqueous phase concentration, respectively. As an example, Table 1 shows maxima HTR (HTRmax; when C_{HXD} = 0) for all assayed Ug. HTRmax increased (0.32 – 1.52 mg HXD (L h)$^{-1}$) as Ug was increased. Higher HTRmax values (30 - 55 mg HXD (L h)$^{-1}$) were previously observed in bubble column (Quijano et al., 2010). Our data show at least two magnitude order lower. Since C_{HXD} is not zero during a typical culture, it was necessary to determine HTR by measuring C_{HXD} on the bulk.

Table 1. Sauter mean diameter (d_{32HXD}), HXD droplets specific area (a_{HXD}), HXD transfer coefficient (k_{LHXD}), HXD volumetric transfer coefficient (k_La_{HXD}) and maximum hexadecane transfer rate (HTRmax) as a function of Ug.

Ug (cm s^{-1})	d_{32HXD} (cm)	a_{HXD} (cm^2 cm^{-3})	k_{LHXD} (cm h^{-1})	k_La_{HXD} (h^{-1})	HTRmax[1] (mg HXD (L h)$^{-1}$)
0.15	0.32 ± 0.01	0.35 ± 0.02	0.014 ± 0.005	0.005 ± 0.0004	0.32 ± 0.03
0.46	0.25 ± 0.02	0.45 ± 0.02	0.016 ± 0.005	0.007 ± 0.001	0.46 ± 0.02
0.61	0.22 ± 0.03	0.51 ± 0.01	0.023 ± 0.003	0.011 ± 0.009	0.76 ± 0.04
0.76	0.18 ± 0.06	0.79 ± 0.06	0.026 ± 0.002	0.020 ± 0.003	1.33 ± 0.11
1.54	0.13 ± 0.04	0.87 ± 0.01	0.027 ± 0.005	0.023 ± 0.001	1.52 ± 0.13

[1] Values calculated for C_{HXD} = 0

Hexadecane transfer rate

As case study, HTR was determined in a 10 L ALB-bacterial culture. Figure 3 shows HTR and the C_{HXD} measured during a 10-day culture at constant Ug = 0.76 cm s-1. At the beginning of culture C_{HXD} and HTR were 62.0 mg HXD L^{-1} and 0.042 mg HXD (L h)$^{-1}$, respectively; after day three C_{HXD} was close to 61.2 mg HXD L^{-1} keeping constant values (error bars did not allow us to observe differences) up to the end of culture. HTR decreased to 0.010 mg HXD (L h)$^{-1}$ up to the end of culture. HTR was around 33-fold lower than HTRmax. Our results suggested a possible dominant mass transfer constraint related to the HXD phase to be overcome.

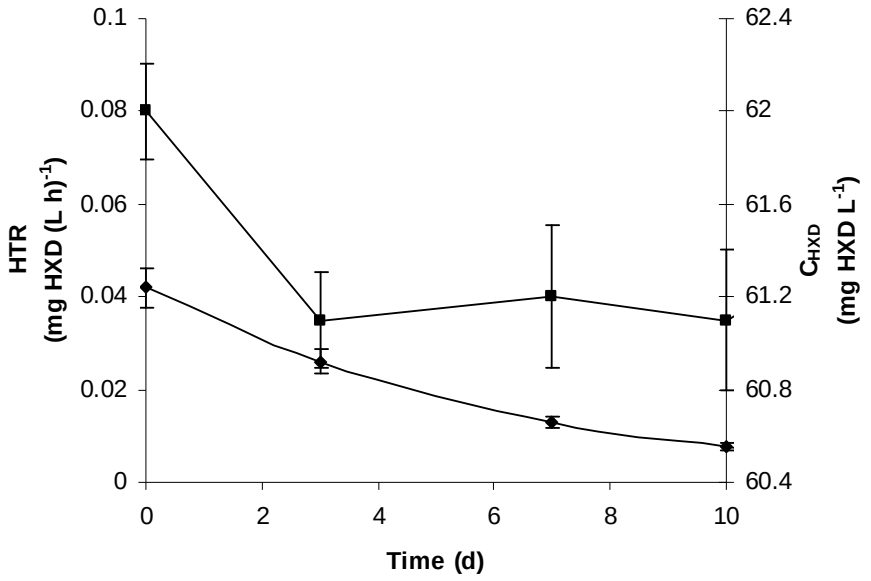

Figure 3.HTR (♦) and C_{HXD} (■) during a 10-day culture of a bacterial consortium at constant Ug = 0.76 cm s^{-1}.

CONCLUSIONS

In this work, a new simple dynamic technique that allows the accurate HTR determination in a three-phase (air, aqueous and HXD) airlift bioreactor was developed. The technique was successfully applied to the determination of HTR in a bacterial culture grown in an airlift bioreactor. Our results suggested a possible dominant mass transfer constraint related with HXD transfer to aqueous phase as the limiting step. HTR seems to be a good criterion for the control of processes where the biodegradation of HXD or other oils is involved.

ACKNOWLEDGEMENTS

We acknowledge CONACYT (Consejo Nacional de Ciencia y Tecnología), scholarship to M. A. Lizardi-Jimenez, and PEMEX-Refinación for partial support. Thanks are due to Dr. J. Vernon in providing HXD droplets pigment solution.

8.5. Evaluación simultánea de las tasas de transferencia de HXD y oxígeno en la producción de un consorcio microbiano degradador de petróleo en un birreactor airlift trifásico (Artículo enviado al CEJ)

Resumen del artículo:

La eficiencia de la tasa de transferencia de hexadecano (TTH) adicionalmente a la tasa de transferencia de oxígeno (TTO) fue evaluada como un criterio para mejorar la productividad del consorcio microbiano rizosférico degradador de petróleo en un biorreactor airlift (BAL) trifásico. Los valores del coeficiente volumétrico de transferencia de oxígeno (k_La_{O2}) variaron entre 25 y 49 h^{-1} para el rango de velocidad superficial (Ug) del gas ensayadas (0.15 – 2.7 cm s^{-1}). El coeficiente volumétrico de transferencia de HXD (k_La_{HXD}) varió entre 0.005 a 0.041 h^{-1} al mismo rango de Ug. TTO y TTH fueron ambas calculadas como el producto de por el gradiente de concentración respectivo. Durante experimentos de 14 d en BAL de 10 L usando Ug constante. La más alta productividad a Ug constante (2.7 cm s^{-1}) fue 1.02 ± 0.03 g SS $(L\ h)^{-1}$. Propusimos una estrategia de Ug variable, cambiando la Ug de 0.61 a 2.7 cm s^{-1}, lo que permitió alcanzar la mayor productividad del consorcio con un bajo gasto de energía. En este artículo se muestra que el desempeño de un BAL mejorado con éxito usando simultáneamente consideraciones de transferencia de HXD y oxígeno.

El artículo enviado se muestra en su formato original en el Anexo 3.

Chemical Engineering Journal

Enviado 3 de Mayo de 2011

SIMULTANEOUS HEXADECANE AND OXYGEN TRANSFER RATE ON THE PRODUCTION OF AN OIL-DEGRADING CONSORTIUM IN A THREE-PHASE AIRLIFT BIOREACTOR.

Lizardi-Jiménez M. A., Saucedo-Castañeda G., [1] Thalasso F. and *Gutiérrez-Rojas M.

Departamento de Biotecnología, Universidad Autónoma Metropolitana-Iztapalapa, Av. San Rafael Atlixco No. 186, Col. Vicentina, Iztapalapa, México, D.F. C.P. 09340, México.
[1] Departamento de Biotecnología y Bioingeniería, Centro de Investigación y Estudios Avanzados, México.
* Corresponding author:

TEL: + 52 (55) 5804 6505

FAX: + 52 (55) 5804 6407
e-mail: mgr@xanum.uam.mx

ABSTRACT

The hexadecane (HXD) transfer rate (HTR) and the oxygen transfer rate (OTR) were simultaneously evaluated as a single engineering criterion to enhance the production of an oil-degrading bacterial consortium. In order to accomplish the task, a 10-L three-phase airlift bioreactor (ALB) was used. Oxygen transfer volumetric coefficient (k_La_{O2}) values of 25 – 49 h^{-1} were found for several superficial gas velocities (Ug 0.15 – 2.7 cm s^{-1}). HXD transfer volumetric coefficient (k_La_{HXD}) values of 0.005 – 0.041 h^{-1} were obtained for the same range of Ug values. OTR and HTR were calculated as the product of k_La_{O2} or k_La_{HXD} and the respective concentration gradient. HXD transfer parameters were evaluated by using an early reported novel technique. During 14 days culture, using constant Ug values, the ratio of HTR to OTR (HTR/OTR) never reached the stoichiometric ratio (0.41 ± 0.05 g

HXD (g O2)$^{-1}$). However, the productivity at the higher assayed constant Ug (2.7 cm s^{-1}) was as good as 1.02 ± 0.03 g SS (L d)$^{-1}$. We propose a variable Ug strategy that consumes 33 % less energy than a higher constant Ug strategy to achieve the same yield and productivity. In this study, the oil-degrading consortium, able to remediate contaminated soils and water, productivity was successfully enhanced with simultaneous HXD and oxygen transfer considerations.

Keywords: Oxygen, Hydrocarbon, Mass transfer, Oil-degrading consortium, Airlift bioreactor, bioremediation.

1. INTRODUCTION

An airlift bioreactor (ALB) is a pneumatic bioreactor agitated with a continuous gas phase in the form of bubbles that break towards the liquid phase, resulting in an isothermal expansion that maintains homogeneity within the reactor (Chisti *et.al.*, 1989). The main advantages of the ALB compared to conventional bioreactors (bubble column and stirred tank) are efficient mixing and higher aeration rates at lower energy consumption (Lin and Chen, 2005). ALBs are used for the industrial production of lactic acid by fungi (Liu *et.al.*, 2006) and the degradation of phenol compounds by bacteria in axenic cultures (Saravanan *et.al*. 2009). However, very little information is available about microbial consortia grown in water-insoluble liquid substrates in ALBs for environmental purposes (Medina-Moreno *et.al*., 2005). Water-insoluble contaminants in soil and water, oil in particular, are widely studied due to constant persistence, environmental impact and economical importance (Saval, 2000). The alkanes are important oil constituents; hexadecane (HXD) is an alkane that is widely used as a model for oil degradation because it is easy to monitor and yields high biomass values (Inakollu *et.al.*, 2004). Earlier studies (Medina-Moreno *et.al.*, 2005) with pneumatic bioreactors were focused on the production of oil-degrading biomass; however, they found levels of productivity as low as 0.2 g L^{-1} d^{-1}. Biomass productivity is strongly related to bioreactor hydrodynamics and the resulting mass transfer phenomena (Chisti *et.al.*, 1989; García-Ochoa and Gomez, 2009) and the resulting parameters (specific areas, coefficients and volumetric coefficients) (Lemoine and Morsi, 2005)**.** The importance of oxygen transfer in ALB performance is well documented (Lin and Chen,

2005; Mehrnia *et.al.*, 2005; Quijano *et.al.*, 2009). Numerous reports have used the volumetric oxygen transfer coefficient ($k_L a_{O2}$) as a practical single criterion to evaluate the oxygen transfer limitations; recent studies of the oxygen transfer rate (OTR) have been done to ensure an adequate delivery of oxygen from the gas stream to the culture broth (García-Ochoa and Gomez, 2009). However, most ALB studies concerning three-phase systems do not take water-insoluble liquid substrates into account. When HXD is used as the only source of carbon and energy, HXD plays an important role because a new mass transfer limitation is added to that imposed by oxygen; HXD solubility is several-fold lower (~10^{-7} mg L^{-1}) than that of oxygen (~6.6 mg L^{-1}). Stirred tank reactors studies have focused on macromixing (Martín *et.al.*, 2008), hydrodynamics and oxygen mass transfer in three-phase reactors (Torres-Martinez *et.al.*, 2009) or improving oxygen mass transfer by the addition of hydrocarbon (Clarke *et.al.*, 2006). However, there is little published work on oil-phase mass transfer phenomena; for instance, the hexadecane transfer rate (HTR), related to oxygen mass transfer and considering the stoichiometric consumptions of both. The aim of this study was to evaluate simultaneously hexadecane and oxygen transfer rates as a single criterion to enhance the productivity of an oil-degrading bacterial consortium in a three-phase ALB.

2. MATERIALS AND METHODS

2.1. Microbial consortium and culture medium

The indigenous oil-degrading bacterial consortium was isolated from the rhizosphere of *Cyperus laxus*, a native plant (Díaz-Ramírez et.al., 2003) growing in an oil-contaminated swamp in Mexico. The rhizospheric oil-degrading consortium was composed of four bacterial species: *Xanthomonas* sp., *Acinetobacter bouvetii, Shewanella* sp. and *Defluvibacter lusatiae*. The mineral medium was (g L^{-1}): 6.75, $NaNO_3$ (J.T. Baker, 99. 9%); 2.15, K_2HPO_4 (J.T. Baker, 99.3%); 1.13, KCl (J.T. Baker, 99.9%), 0.54, $MgSO_4 \cdot 5H_2O$ (J.T. Baker, 100.1 %), the pH was adjusted to 6.5 with 1.0 M HCl. The consortium was cultivated in mineral medium containing 13 g L^{-1} HXD (Sigma-Aldrich, 99.7 %).

2.2. Inoculum preparation

The four bacterial species were cultivated separately in 250 mL flasks containing 50 mL of nutritive broth (Bioxon), which were incubated at 30 ^{o}C for 24 h with agitation at 200 rpm in a shaker (model I26, New Brunswick Scientific, USA). Then 2.5×10^5 colony-forming units mL^{-1}; i.e. 0.01 mL and 1.0 mL from each bacterial strain culture were used to inoculate 1 L of medium.

2.3. Bioreactor set-up and operation

The cylindrical vessel (0.14 m diameter, 1 m length) in the ALB was made of Pyrex glass. A draft tube (0.09 m diameter, 0.54 m length) was located 0.035 m above the bottom. The ALB (working volume 10 L) was air-sparged into the draft tube through a perforated L-shaped stainless steel pipe (0.006 m internal diameter) with seven perforations (0.001 m diameter, 0.004 m separation). The ALB was operated as a 14-day batch at 28 ^{o}C with HXD as the sole carbon and energy source. The first batch was inoculated as described in section 2.2. Subsequently, ALB batches were inoculated every 14 days with biomass (0.8 g L^{-1} dry weight) harvested from the preceding batch onto fresh culture medium where the initial culture conditions were restored. ALB was sampled (10 mL) at days 0, 3, 7, 10 and 14. The surface tension (σ) of the culture medium was measured with a surface tensiometer (SensaDyne, Chem-Dyne Research Corp., USA). Viscosity (μ) was measured with a viscometer (Physica MCR model 300, Germany).

2.4. Aqueous and HXD phase hydrodynamics

Three phases (air, aqueous and HXD) were involved in the ALB; the velocity of the two slow-moving phases (aqueous and HXD) was evaluated experimentally. We used sodium polyacrylate hydrogel (ρ_{aq} = 1.0 g cm^{-3}) and oligosyloxane-stained spheres (ρ_{HXD} = 0.77 g cm^{-3}) simulating the aqueous and the HXD phase, respectively, in order to follow flow patterns through the mineral medium. A digital video camera (Sony HD) and an on-line

chronometer (StopWatch software) were used to follow the velocity of single spheres as the ratio of path-length to elapsed time in both ALB zones: riser and downcomer. The resulting velocities were used to calculate two individual Reynolds numbers (Nielsen *et.al.*, 2003) and Re differences, as follows:

$$\mathrm{Re}_{aq} = \frac{D V_{aq} \rho_{aq}}{\mu} \quad (1)$$

$$\mathrm{Re}_{HXD} = \frac{D V_{HXD} \rho_{HXD}}{\mu} \quad (2)$$

$$\mathrm{Re}_{aq-HXD} = \frac{D}{\mu} \left| V_{aq} \rho_{aq} - V_{HXD} \rho_{HXD} \right| \quad (3)$$

where Re_{aq} and Re_{HXD} are the aqueous and HXD phase Reynolds number, respectively. *D* is for the riser zone is *D*2; *D* for the downcomer zone is *D*1–*D*2; *D*1 is the ALB diameter (m); *D*2 is the draft tube diameter (m); V_{aq} is the aqueous phase velocity (cm s^{-1}); V_{HXD} is the HXD phase velocity (cm s^{-1}); ρ_{aq} is aqueous phase density (g cm^{-3}); ρ_{HXD} is the HXD phase density (g cm^{-3}); and μ is the bulk viscosity of HXD in a water emulsion (g cm s^{-1}). Absolute values were used because the HXD phase has greater velocity through the riser zone than that observed in the aqueous phase; simultaneously, the aqueous phase has greater velocity through the downcomer zone than that observed in the HXD phase. In order to simulate the physicochemical properties of the culture medium, an abiotic medium was designed using biotic values for σ (65 dynes cm^{-1}) and μ (1.05 cP) by adding Tween 20 and HXD to a final concentration of 0.081 mg L^{-1} and 13 g L^{-1}, respectively. The abiotic medium was used in the hydrodynamics and mass transfer experiments.

2.5. Oxygen transfer parameters

The dynamic numerical method (Fujio et.al., 1973) was used to determine $k_L a_{O2}$. The concentration of dissolved oxygen (DO) was measured with a polarographic oxygen sensor (ADI dO2, Applisens, The Netherlands) and a DO meter (model DO-40, New Brunswick Scientific, USA). OTR was calculated as the product of $k_L a_{O2}$ and the oxygen gradient concentration.

2.6. HXD transfer parameters and specific area

$k_L a_{HXD}$ was evaluated essentially by using an earlier reported novel technique (Lizardi-Jiménez *et.al.*, 2011) as follows: abiotic medium (10 L) was added to the ALB; a stainless steel cylinder (2.8 mL) was filled with HXD and introduced into the downcomer with the open side downward. Once aeration was in the steady state, 5 mL of ALB was withdrawn every 60 min. The HXD transferred to the aqueous phase was recovered by successive extractions with a sample to solvent ratio of 1:5 (v/v) using a hexane/isotonic solution (1:3, v/v) as solvent. The HXD transfer coefficient (k_{LHXD}) was obtained from the stainless steel cylinder mass transfer area and the relative liquid phase (aqueous and HXD) velocity. We set Ug level so that the difference in velocities, and the resulting $Re_{aq\text{-}HXD}$, between steel cylinder (static) and aqueous phase were the same to those values produced between HXD droplets and aqueous phase in the ALB. $k_L a_{HXD}$ was obtained as the product of k_{LHXD} and specific mass transfer area of the HXD droplets, a_{HXD}, was calculted by Equation 4 (Torres-Martinez *et.al.*, 2009).

$$a_{HXD} = \frac{6}{d_{32HXD}}\phi \qquad (4)$$

where d_{32HXD} is the Sauter mean diameter of HXD droplets (cm) and ϕ is the HXD dispersed phase fraction (dimensionless), d_{32HXD} was measured with a digital camera and image analysis software (Image Pro Plus 4.1., Media Cybernetics, USA) at three different height levels (0.02 m, 0.25 m and 0.50 m from the bottom) in the downcomer. In order to contrast droplet images, HXD was stained with red chilli (*Capsicum annuum*) oleoresin, also known as rodophile (Bioquimex-Reka, Mexico). We added 25.1 mg of rodophile per 1 g of HXD. The Sauter mean diameter (d_{32HXD}) was obtained as the average of two measurements for each droplet. The hexadecane transfer rate (HTR) was calculated as the product of the volumetric mass transfer coefficient ($k_L a_{HXD}$) and the HXD gradient concentration measured in the aqueous phase. We did not consider it to be pertinent to take into account the effect of bubble hydrodynamics because: (i) bubble hydrodynamics is quite important in the riser and more important than it is in the downcomer; (ii) our

experimental method was implemented in the downcomer and we did not assay in the riser; and (iii) k_{LHXD} depends on $Re_{aq\text{-}HXD}$ in both zones (riser and downcomer).

2.7. Suspended solids

Samples (10 mL) from ALB were centrifuged (J2-HS, Beckman, USA) at 4000*g* for 30 min at 4 ºC. Three phases were formed: HXD, aqueous and solid. The suspended solids (SS), including the rhizospheric oil-degrading consortium, were determined in the solid phase after heating in a low-pressure oven at 60 °C for 48 h (Duo Vac, Lab-line Inc. Instruments, USA). The SS fraction that remained trapped in the HXD phase was recovered by three successive extractions, as described above. The organic phases, including residual HXD, were pooled and stored at 4 ºC in 30 mL vials.

2.8. Hexadecane

HXD in the pooled organic phases was measured by gas chromatography (Varian model 3900, USA) at 300 ^{o}C with a flame-ionization detector, a DB-Petro narrow-bore column (30 m × 0.00025 m; J & W Scientific) and helium as the carrier gas. The injector and detector temperatures were constant at 290 °C and 300 °C, respectively. The temperature program was: 120 °C for 1 min; increase by 10 °C min^{-1} until 150 °C (2 min); then by 15 °C min^{-1} until 170 °C (1.5 min).

2.9. Statistical analysis

Data analysis was done with NCSS-2000, version 2001 (copyright 2001 by Jerry Hintze). One-way analysis of variance (ANOVA) was used with the level of statistical significance set at p <0.05.

3. RESULTS AND DISCUSSION

3.1. HXD specific area and local Re differences

The HXD droplet Sauter mean diameter (d_{32HXD}) depends on surface tension (σ) and we measured the variation of σ with time in preliminary biotic ALB runs. For all Ug assayed, σ changed slightly from 72.6 ± 1.02 dynes cm^{-1} at day zero to 68 ± 1.30 dynes cm^{-1} at days 0, 3, 7, 10 and 14. When the abiotic medium was prepared using these two σ values, the diameters of the resulting droplets were not significantly different (d_{32HXD} = 0.157 ± 0.001 and 0.152 ± 0.01 cm for σ = 72.6 and 68 dynes cm^{-1}, respectively). By contrast, d_{32HXD} did change significantly with σ in bubble column reactors (Quijano et.al., 2009). In our study, d_{32HXD} depends only on variations of Ug.

In order to evaluate the effect of Ug on d_{32HXD} and the resulting a_{HXD}, measured in the downcomer, six different Ug values were assayed using the abiotic medium described in section 2.4. d_{32HXD} of macroscopic droplets, number of droplets and a_{HXD} as a function of Ug are given in Table 1. As expected, d_{32HXD} and Ug were negatively correlated and the number of droplets and Ug were positively correlated; therefore, for a given volume of HXD, a greater a_{HXD} is provided if HXD is dispersed into many small droplets rather than a few large drops. Finally, a_{HXD} increased with Ug and probably depends on local hydrodynamics (Table 1).

Table 1. Sauter mean diameter (d_{32HXD}) of macroscopic droplets, total droplets number and a_{HXD} in downcomer, as a function of Ug.

Ug ($cm\ s^{-1}$)	d_{32HXD} (cm)	Total droplets number	a_{HXD} ($cm^2\ cm^{-3}$)
0.15	0.32 ± 0.01	11 080 ± 69	0.35 ± 0.002
0.46	0.25 ± 0.02	23 236 ± 23	0.45 ± 0.020
0.61	0.22 ± 0.03	34 096 ± 97	0.51 ± 0.017
1.00	0.15 ± 0.03	110 000 ± 100	0.79 ± 0.060
1.54	0.13 ± 0.04	165 251 ± 65	0.87 ± 0.010
2.70	0.09 ± 0.01	498 021 ± 122	1.30 ± 0.024

Local Re differences between aqueous and hydrocarbon phase, according to equations (1), (2) and (3), in the riser and in the downcomer as a function of superficial gas velocity (Ug) are shown in Figure 1. Assays were done under abiotic conditions. $Re_{aq\text{-}HXD}$ follows the same increasing pattern for both zones except for Ug = 0.15 cm s^{-1}, where the HXD phase velocity is close to zero (HXD does not decrease). The results show also that $Re_{aq\text{-}HXD}$ was slightly higher in the riser than that in the downcomer in the range 0.46 – 0.76 cm s^{-1}, whereas $Re_{aq\text{-}HXD}$ between the riser and the downcomer were not significantly different for Ug >0.76 cm s^{-1}. Similar behavior in a bubble column has been reported (Kantarci *et.al.*, 2005). Nevertheless, most of the studies that have been done using a three-phase ALB have examined only the aqueous and gas phase hydrodynamics (Shariati *et.al.*, 2007; Mengxi *et.al.*, 2007; Olivieri *et. al.*, 2003). Our results suggest (see Figure 1) that $Re_{aq\text{-}HXD}$ values were similar for the two zones (riser and downcomer), particularly at Ug > 0.76 cm s^{-1} there were no significant differences. Therefore, since d_{32HXD} depends on Ug (see Table 1) it is possible to conclude that d_{32HXD} were similar for the two studied zones at Ug > 0.76 cm s^{-1}; the resulting HXD-specific area measured in the downcomer can be recognized as the mass transfer-specific area (a_{HXD}) in the whole bulk, riser included. In this study, a_{HXD} was used to calculate the HXD mass transfer parameters.

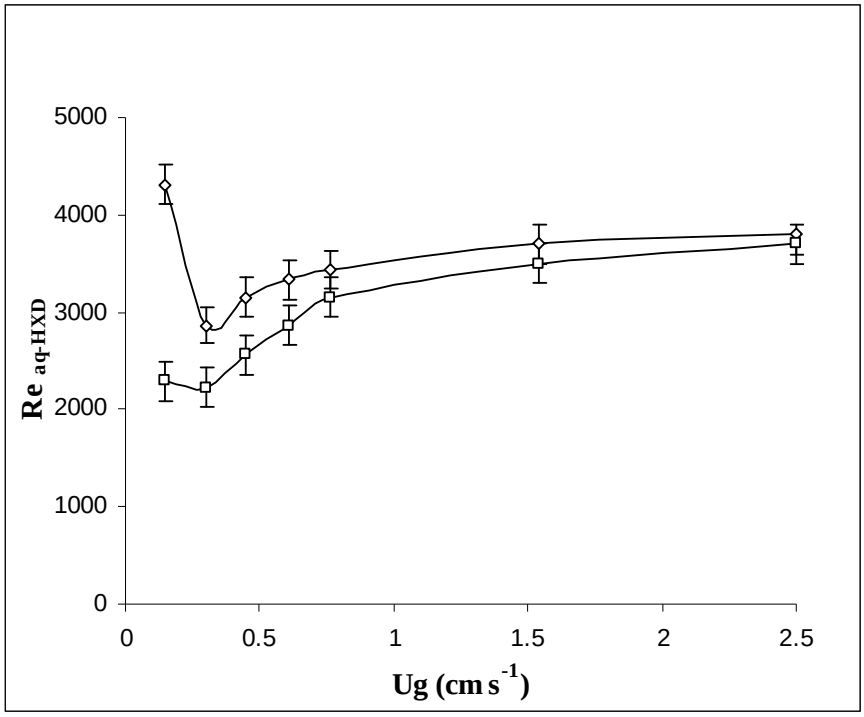

Figure 1. Local $Re_{aq\text{-}HXD}$ in riser (◊) and downcomer (□) as a function of Ug in 10 L airlift bioreactor.

3.2. Mass transfer parameters

Studies using three-phase pneumatic bioreactors (Medina-Moreno *et.al.,* 2005; Mehrnia *et.al.,* 2005) define the volumetric oxygen transfer coefficient (k_La_{O2}) as the only mass transfer parameter (as in a biphasic bioreactor). However, the hydrocarbon phase could be the limiting step in hydrocarbon-biodegrading processes. We studied k_La_{HXD} in order to consider both transfer phenomena.

3.2.1. Volumetric mass transfer coefficients

Owing to the difficulty of measuring the oxygen transfer coefficient (k_{LO2}) and the gas bubble-specific area (a_{O2}) separately, the product k_La_{O2} was measured, which is the parameter that characterizes transport from the gas phase to the aqueous phase. However, because there is no HXD probe available that would allow an evaluation similar to k_La_{O2}, it was necessary to measure a_{HXD} and k_{LHXD} separately; a_{HXD} was computed from

experimental values of d_{32HXD} (Table 1). Table 2 shows the measured k_La_{O2} and k_La_{HXD} values and the ratio of hexadecane to oxygen volumetric mass transfer coefficient ((k_La_{HXD}) (k_La_{O2})$^{-1}$) as a function of Ug. Five different Ug values in the range 0.15 – 2.7 cm s^{-1} were investigated. As expected, both volumetric coefficients were correlated positively with Ug: k_La_{HXD} ranged from 0.005 – 0.041h^{-1} and k_La_{O2} ranged from 26 – 46 h^{-1} for all Ug values assayed. These k_La_{O2} values are higher than those reported for bubble column bioreactor using petroleum and paraffins (Medina-Moreno *et.al.*, 2005) and similar to another ALB study with petroleum-based liquids (Mehrnia *et.al.*, 2005). The higher k_La_{O2} values in our ALB could be due to rapid circulation of the liquid phase, which would diminish the air boundary layer; but not enough to produce higher k_La_{HXD} values, as can be seen in Table 2 where (k_La_{HXD}) (k_La_{O2})$^{-1}$ was < 0.001 for all Ug values assayed, suggesting mass transfer limitation by HXD. k_La_{HXD} increased 8-fold, whereas k_La_{O2} did not achieve a 2-fold increase in the same increased range of Ug. However, studies regarding mass transfer rates are needed because oxygen and HXD consumption must be taken into account as described in the following section.

Table 2. Volumetric HXD transfer coefficient (k_La_{HXD}) and volumetric oxygen transfer coefficient (k_La_{O2}) at different Ug (day 0)

Ug (cm s^{-1})	k_La_{HXD} (h^{-1})	k_La_{O2} (h^{-1})	(k_La_{HXD}) (k_La_{O2})$^{-1}$
0.15	0.005 ± 0.00006	26.17 ± 2.62	0.0002
0.46	0.006 ± 0.00002	30.00 ± 2.00	0.0002
0.61	0.015 ± 0.00002	33.67 ± 3.37	0.0004
1.54	0.024 ± 0.00030	41.66 ± 3.10	0.0005
2.70	0.041 ± 0.00040	45.65 ± 2.09	0.0009

3.2.2. Mass transfer rates

In two-phase ALB studies, the OTR is commonly considered to be the unique mass transfer limitation. However, the HXD transfer rate (HTR) must be simultaneously taken

into account, in the three-phase ALB used in this study, and particular attention should be paid to the HTR/OTR ratio. In our work, HTR values were not computed as averages from the HXD transfer coefficient k_{LHXD} in ALB zones (riser and downcomer); instead we obtained k_{LHXD} from the downcomer by using steel cylinder and we used a generalized k_{LHXD} in the entire ALB due to $Re_{aq\text{-}HXD}$ was practically the same in both zones. The time profiles of the experimentally determined ratio for all constant Ug values are shown in Figure 2. For all Ug, the HTR/OTR value increased as Ug increased and all profiles decreased with time. In all cases, the maximum HTR/OTR value was obtained at the beginning of the culture and the minimum value was reached by day 7 and was constant to the end of culture, except for the Ug term of 2.7 cm s^{-1}; in this case, HXD was exhausted after day 6, so a_{HXD}, $k_L a_{HXD}$ and HTR were no longer applicable. The stoichiometric ratio between hydrocarbon and oxygen consumption values was obtained as:

$$CH_{2.125} + 0.056\ NO_3 + 1.06O_2 \rightarrow 0.33\ CH_{1.77}\ O_{0.55}\ N_{0.17} + 0.67CO_2 + 0.77H_2O$$

where the first left-hand term is 1 C-mol of HXD and the first right-hand term is 1 C-mol of biomass (Nielsen *et.al.*, 2003) and yields (biomass/HXD) were measured. Our stoichiometric approach shows that 0.41 g of HXD theoretically requires 1.0 g of oxygen. In Figure 2, all assayed Ug shows HTR/OTR at least ten times lower than 0.41 g HXD g of O_2^{-1} and three groups are distinguished; those at lower constant Ug (0.15 and 0.45 cm s^{-1}), middle Ug (0.61 and 1.54 cm s^{-1}) and higher Ug (2.7 cm s^{-1}). The three groups were selected on the basis of maximal slope computed for HTR/OTR versus time. The slope values were –0.002, –0.004 and –0.010 g HXD (g O2)$^{-1}$ d^{-1} for the lower, middle and higher Ug group, respectively. These slopes represent the maximum rate at which the HTR/OTR ratio decreased. The maximum HTR/OTR at lower Ug was ~ 0.006 g HXD (g O2)$^{-1}$; at middle Ug up to 0.012 g HXD (g O2)$^{-1}$ and at higher Ug up to 0.025 g HXD (g O2)$^{-1}$. Our results show that all HTR/OTR values lower than 0.41 g HXD (g O2)$^{-1}$ are due to HXD transfer limitation. Such mass transfer limitation should impact both HXD biodegradation and the production of suspended solids (SS). The HTR/OTR ratio is applicable to real cultivation conditions because k_{LHXD} values were evaluated by considering the relative velocity differences between the aqueous and HXD phases. In addition, we did not assume constant $k_L a_{HXD}$ during the culture, although slow changes in

surface tension did not affect d_{32HXD} (see section 3.1), because a_{HXD} diminished as culture proceed due to ϕ diminished too. The fact that HTR/OTR varies as a function of time was made clearer by examination of the HTR and OTR variations separately: (i) HTR is augmented with aeration owing to the decrease of droplet size with Ug; by contrast, culture time did not affect droplet size. (ii) OTR is augmented with aeration but the increasing values were lower than those observed for HTR; however, OTR was affected by culture time because the dissolved oxygen aqueous phase concentrations measured in the bulk differed with time, –6.5 to 4.6 mg O_2 L^{-1} (30 % variation); whereas HXD was dispersed into droplets and reached aqueous phase concentration values of 65 – 61 mg of HXD L^{-1} (7 % variation).

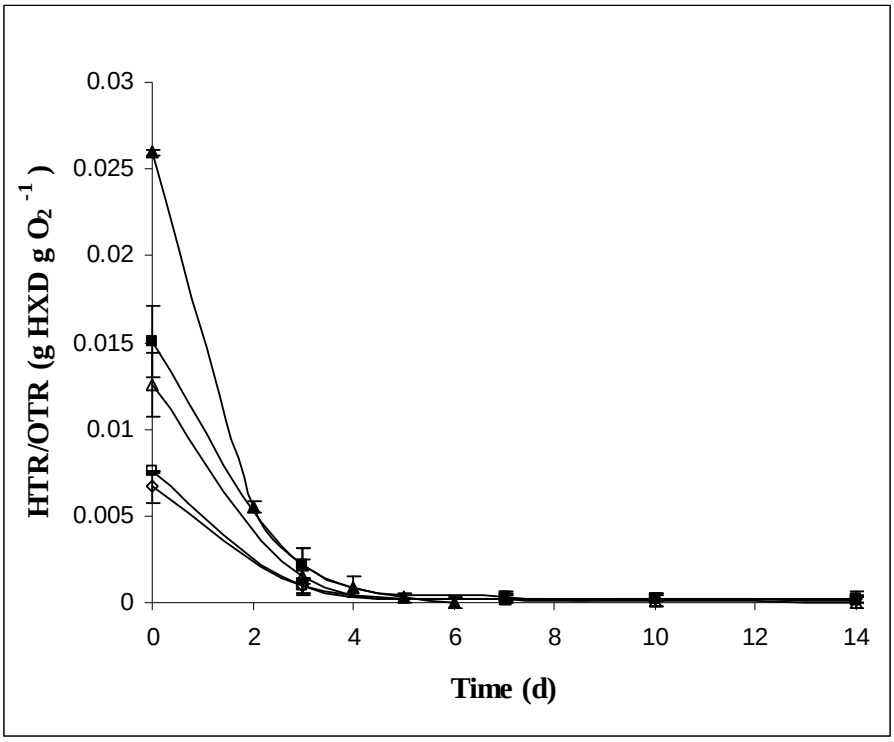

Figure 2. Ratio of hexadecane to oxygen transfer rate, HTR/OTR, along culture time as a function of constant Ug (cm s^{-1}): (◊) 0.15, (□) 0.46, (Δ) 0.61, (■) 1.54 and (▲) 2.7.

3.3. HXD biodegradation and SS production

In order to enhance the productivity of SS, including the rhizospheric indigenous oil-degrading consortium, we studied total HXD (non-soluble and soluble into the aqueous

phase) biodegradation following two different aeration strategies: constant Ug or variable Ug during the ALB culture.

3.3.1. HXD biodegradation and SS production using constant Ug

We measured SS production and HXD biodegradation at constant Ug in order to evaluate the effect of mass transfer limitations. Figure 3 shows total HXD biodegradation and SS production profiles as a function of culture time when five constant values of Ug (0.15, 0.45, 0.61, 1.54 and 2.7 cm s^{-1}) were used. Figure 3a shows that HXD was 98.47 ± 0.38 % degraded in only 6 days at higher constant values of Ug; HXD was practically exhausted within 14 days at middle constant values of Ug; whereas, 6 g L^{-1} of HXD remained at lower constant values of Ug. SS production (Figure 3b) increased as Ug increased; concentrations of SS were highest at the end of culture for middle and lower Ug and at day 6 for higher Ug. We considered it pertinent to compute batch culture productivity at higher Ug when the instant productivity, defined as the derivative of SS (g L^{-1}) with respect to time, was zero (day 7). In the case of middle and lower Ug, the derivative never was strictly zero and productivity was computed at the end of the batch. SS yield and productivity were 0.46 ± 0.01 g SS (g HXD)$^{-1}$ and 0.25 ± 0.01 g SS (L d)$^{-1}$, respectively, at lower Ug; 0.58 ± 0.09 g SS (g HXD)$^{-1}$ and 0.51 ± 0.05 g SS (L d)$^{-1}$, respectively, at middle Ug; and 0.58 ± 0.02 g SS (g HXD)$^{-1}$ and 1.01± 0.03 g SS (L d)$^{-1}$, respectively, at higher Ug. Productivity was evaluated at day 14 for lower and middle Ug, whereas for higher Ug, productivity was evaluated when HXD was exhausted. Earlier studies (Medina-Moreno *et.al.*, 2005) with sequential batch bubble column working at middle Ug (1 cm s^{-1}) gave similar SS yield values (0.45 g SS (g hydrocarbon)$^{-1}$) but lower productivity, 0.2 g SS (L d)$^{-1}$, as compared to our results at similar Ug. In our work, the oil-degrading consortium productivity was 2.5-fold enhanced. In those studies, it took nearly 21 days to degrade Maya crude oil and paraffins and those authors suggested oxygen transfer limitation. This study (Medina-Moreno *et.al.*, 2005) relates SS yield to mass transfer phenomena, describing a low biomass formation under mass transfer limitation and explain this fact due to the high transformation of initial hydrocarbon in more soluble carbon forms and non-soluble metabolite production. However, we show here that, at all assayed Ug, HXD transfer limitation is predominant during the culture, then HXD transfer becomes the

limiting phenomenon. Other work with fungi and HXD (Volke-Sepulveda *et.al.,* 2006) showed the relationship between yield and HXD concentration. Our results showed that SS productivity was not affected by HXD limitation, although other explanation is: the given stoichiometry is probably not valid, similar result was obtained in other work (Doing *et.al.*, 2002) studying OTR in lactone formation.

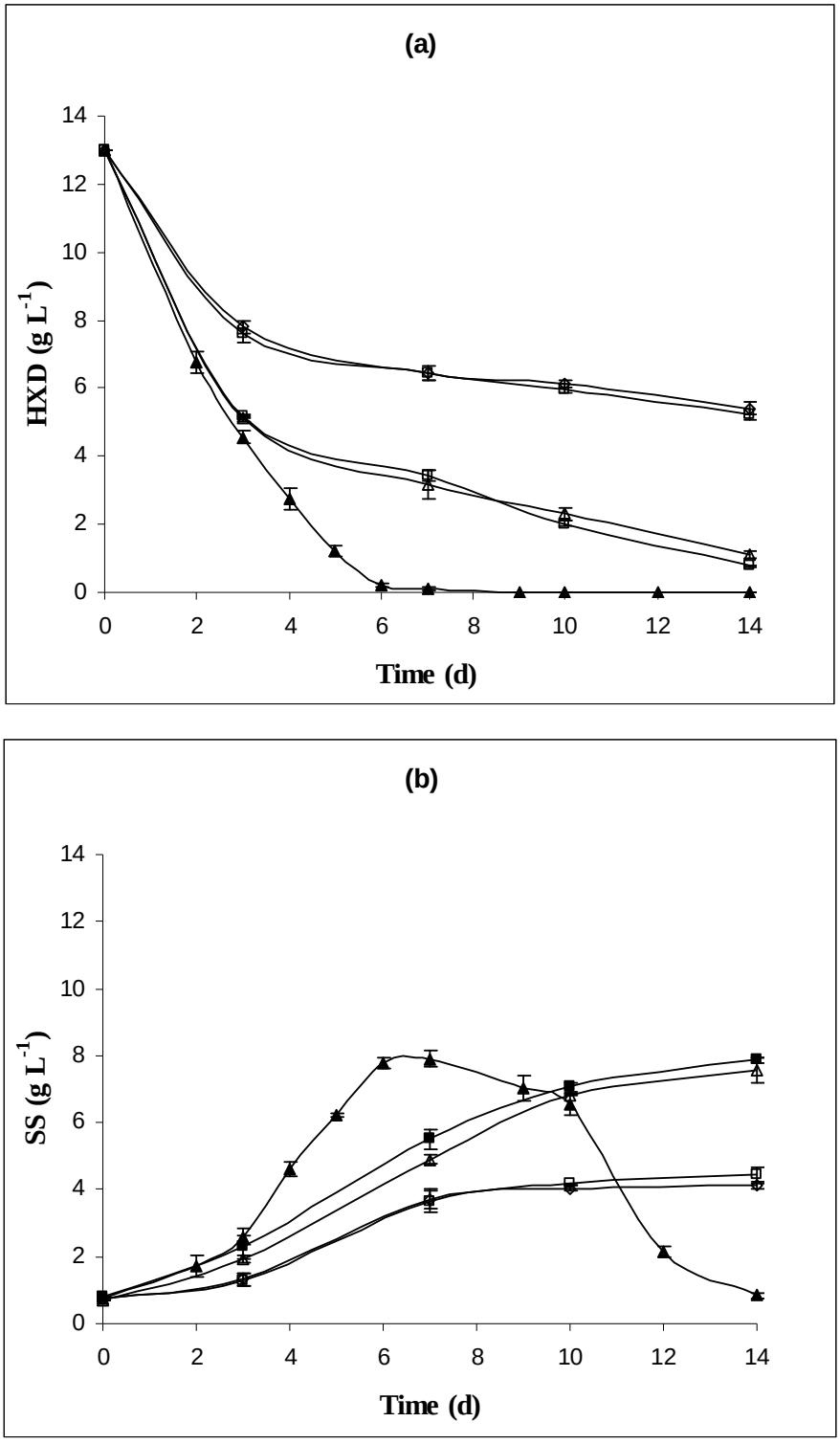

Figure 3. HXD biodegradation (a) and SS production (b) time profiles for different Ug (cm s^{-1}) assayed: (◊) 0.15, (□) 0.46, (Δ) 0.61, (■) 1.54 and (▲) 2.7.

The highest SS productivity achieved, working at constant Ug, was obtained when higher Ug values were imposed; however, two operation problems emerged: (i) SS reached a maximum at 8.1 g L^{-1} but was decreased by up to 0.9 g L^{-1}, suggesting that autolysis of suspended cells is probably due to the lack of energy and carbon source stimulated by the high aeration rate; and (ii) higher constant Ug values were associated with a higher energy consumption. Therefore, studies examining variable Ug strategies are needed in attempts to save energy and to avoid SS lysis.

3.3.2. HXD biodegradation and SS production using a variable Ug strategy

We propose a variable Ug strategy: to start using middle Ug (e.g. 0.61 cm s^{-1}; see Figure 2) up to day 3, then change to higher Ug (2.7 cm s^{-1}) until the end of culture. The effect of a selected variable Ug strategy on experimentally determined HTR/OTR is shown in Figure 4.

As we expected, initial HTR/OTR was close to 0.012 g HXD (g O2)$^{-1}$, decreasing to 0.0015 g HXD (g O2)$^{-1}$ by day 3. The increase in Ug (2.7 cm s^{-1}) allowed HTR/OTR to increase up to 0.0021 g HXD (g O2)$^{-1}$. HXD was exhausted after day 10 and, to avoid cell lysis, we decided to stop the culture at day 10 where SS reached the highest production level. Figure 5 shows HXD and SS profiles when the variable Ug strategy was used. Although it is not possible to guarantee that the initial population composition will be the same in each batch owing to the complex population dynamics after subsequent cultures, our results show that it is possible to guarantee stable HXD degradation and SS production patterns for each tested Ug value (error bars in Figure 5 are for independent triplicate batches). This variable Ug strategy consumed 33 % less energy than higher Ug but reached the same yield and productivity.

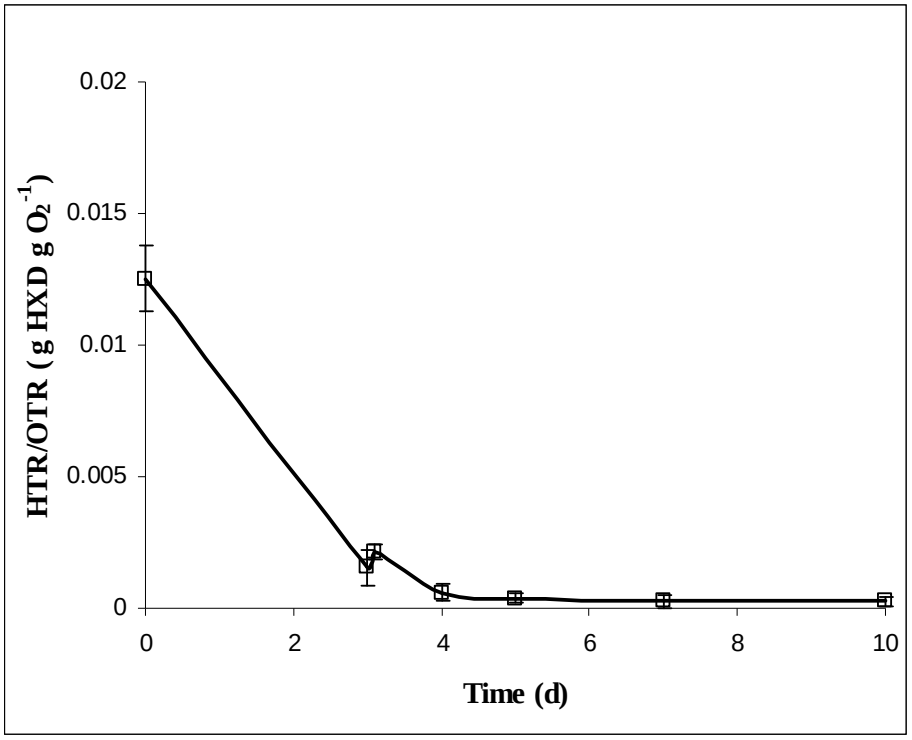

Figure 4. Ratio of hexadecane to oxygen transfer rate, HTR/OTR, along culture time with variable Ug strategy: Ug of 0.61 cm s^{-1} up to day 3; Ug of 2.7 cm s^{-1} up to the end of culture.

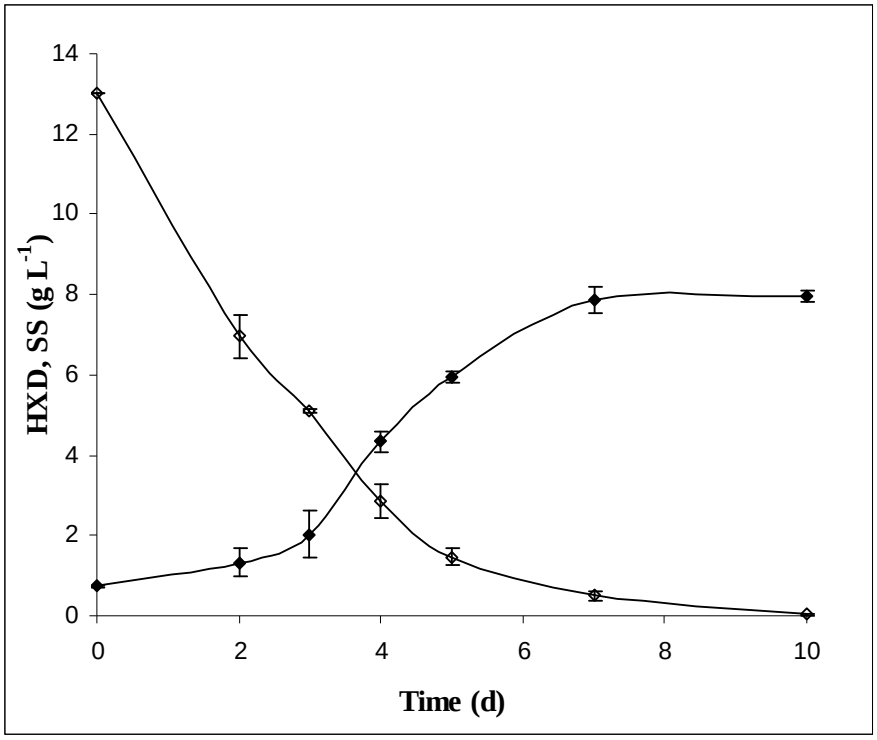

Figure 5. (◊) HXD or (♦) SS (g L^{-1}) with variable Ug strategy.

4. CONCLUSIONS

$Re_{aq\text{-}HXD}$ in the riser and the downcomer were the same within the range 0.76 – 2.7 cm s^{-1}. The HXD mass transfer area (a_{HXD}) increased with increased Ug and decreased as culture proceeded. For all Ug values tested, $k_L a_{O2}$ values were higher (up to 10^3-fold) than the $k_L a_{HXD}$ values. The stoichiometric ratio (0.41 g HXD (g O2)$^{-1}$) was never reached. In our work, HTR and OTR were simultaneously evaluated on the production of an oil-degrading bacterial consortium in a three-phase ALB. Our results show that all HTR/OTR values were due to HXD transfer limitations. At constant Ug, the highest consortium biomass productivity was reached with the highest Ug (7 days). This value was 2.5-fold higher than those reported only considering oxygen transfer phenomena. In our three-phase airlift bioreactor, the constant and the variable strategies provided similar biomass productivity-enhanced values.

ACKNOWLEDGMENTS

We acknowledge Consejo Nacional de Ciencia y Tecnología (CONACYT) for a scholarship to M. A. L-J.; and PEMEX-Refinación for partial support.

8.6. Producción de sólidos suspendidos y biodegradación de hexadecano en diferentes escalas utilizando la estrategia de Ug variable

El objetivo de esta sección fue evaluar la productividad y el rendimiento en el BAL cuando se realiza un escalamiento descendente con un factor de escala de 20:1 (0.5 y 10 L). En la Tabla 8.2 se muestra la producción de SS, rendimiento y productividad para las diferentes escalas utilizando la estrategia de Ug variable que se propuso en la Sección 8.5. (0.61 a 2.7 cm s^{-1}). La estrategia de Ug variable consistió en airear a Ug de 0.61 cm s^{-1} durante los primeros tres días del cultivo y a 2.7 cm s^{-1} desde el día cuatro hasta el final del tiempo de cultivo. El rendimiento en gramos de SS por gramo de HXD consumido es el mismo para las dos escalas utilizando la estrategia de Ug variable. En trabajos previos, trabajando con un biorreactor de columna de burbujas, la escala mayor (10.5 L) mostró rendimientos más bajos (Lizardi-Jimenéz, 2007). Otros investigadores (Nielsen y col., 2003) encontraron que el rendimiento de biomasa puede decrecer con el escalamiento de los biorreactores. En este trabajo se demostró que usar el cociente TTH/TTO como criterio de operación para la producción de un consorcio microbiano degradador de petróleo mantiene el rendimiento aún con un cambio de escala. Resultados similares fueron encontrados (Daugulis y Janikowski, 2002) trabajando la degradación de dos hidrocarburos poliaromáticos (fenantreno y naftaleno) por *Sphingomonas aromactivorans* en un escalamiento de 5 a 150 L encontrando que la producción de biomasa tenía el mismo comportamiento en ambas escalas.

Uno de los objetivos de nuestro trabajo es la producción de inoculantes (SS) que satisfagan el mercado de la biorremediación de agua y suelos contaminados con petróleo, en términos económicos no es conveniente que el reactor de la escala mayor consuma más sustrato (HXD), como ocurre con la columna de burbujas evaluada en nuestro trabajo previo,

(Lizardi-Jiménez, 2007). El escalamiento de BAL para la producción de consorcios microbianos degradadores de petróleo es eficiente y se puede llevar a cabo usando una estrategia de aireación con Ug variable que mantenga al biorreactor lejos de la limitación por oxígeno. En general, la consideración del cociente de tasas de transferencia de masa puede aplicarse a bioprocesos con transferencia de masa y reacción (degradación de HXD y crecimiento microbiano) simultánea.

Tabla 8.2 Producción de SS, rendimiento y productividad para las diferentes escalas con la estrategia de Ug variable.

UG	**ESCALA BAL (L)**	**PRODUCCIÓN DE SS**	**RENDIMIENTO**	**PRODUCTIVIDAD**
		(g SS) L^{-1}	g SS (g HXD)$^{-1}$	g SS (L d)$^{-1}$
Variable 0.61 y 2.7 cm s^{-1}	0.5	7.9 ± 0.21	0.55 ± 0.01	1.02 ± 0.03
	10	7.8 ± 0.23	0.55 ± 0.13	1.01 ± 0.05

9. Conclusiones y Recomendaciones

Conclusiones

1. El estudio de la hidrodinámica en biorreactores de 10 L tipo airlift (BAL) de tres fases mediante el número de Reynolds (Re) permitió: (i) seleccionar la configuración geométrica del BAL con mejores Re de la fase acuosa (Re_{aq}); mediante el ensayo de nueve configuraciones de tubo concéntrico se seleccionó la que presentó mayores Re_{aq} en la zona de descenso (identificada como zona con limitación hidrodinámica), (ii) proponer un Re representativo del BAL, que relacionó la hidrodinámica con la transferencia de masa de la fase HXD a la fase acuosa, como la diferencia entre el Re de la fase HXD (Re_{HXD}) y Re_{aq} ($Re_{aq\text{-}HXD}$); (iii) caracterizar las zonas de operación del BAL usando $Re_{aq\text{-}HXD.}$ $Re_{aq\text{-}HXD}$ fue similar para las zonas de ascenso y descenso.

2. El estudio de la transferencia de masa en biorreactores de 10 L tipo BAL de tres fases mediante el cociente TTH/TTO permitió: (i) desarrollar una nueva técnica dinámica para la determinación de la tasa de transferencia de HXD (TTH), utilizando análisis de imágenes y cromatografía de gases. Los valores de TTH fueron obtenidos entre 0.001 y 0.042 mg HXD $(L\ h)^{-1}$), (ii) proponer el cociente entre las tasas de transferencia de HXD y oxígeno TTH/TTO como el criterio de ingeniería que considera la tasa con la que se transfieren los dos sustratos involucrados en un proceso biotecnológico de degradación aerobia de HXD.

3. El uso del cociente TTH/TTO como criterio de operación que considera la hidrodinámica y transferencia de masa permitió: (i) incrementar la eficiencia (rendimiento de 0.55 g SS g HXD^{-1} y productividad de 1 g SS $(L\ d)^{-1}$) de la producción del consorcio microbiano y (ii) el escalamiento descendente (Factor de escala 20) de la producción del consorcio microbiano degradador de petróleo. Una de las aportaciones principales de este trabajo es el estudio de un bioproceso con transferencia de masa y reacción (degradación de HXD y crecimiento) simultánea. El uso del cociente TTH/TTO permitió mejorar la productividad del consorcio microbiano degradador de petroleo, que puede ser utilizado como inóculo para la remediación de agua y suelos contaminados.

Recomendaciones

1. Usar el modelo de biorreactor de tres fases (gaseosa, HXD y acuosa), estudiado en este trabajo, para abordar la problemática de contaminación por petróleo del agua de mar. Para cumplir con esto:

(i) Diseñar un biorreactor agitado por medio de la energía de las olas del mar: considerando la hidrodinámica por medio de $Re_{aq\text{-}HXD.}$

(ii) Determinar la dependencia que tiene la transferencia de masa de la hidrodinámica en este sistema.

(iii) Aplicar presión selectiva sobre el consorcio utilizado en este trabajo para generar resistencia a distintas concentraciones salinas (rango de agua dulce a agua de mar) y a la variación de temperatura.

(iv) Aplicar presión selectiva sobre el consorcio utilizado en este trabajo para generar resistencia a distintas concentraciones de HXD desde el rango de la concentración empleada en esté trabajo (13 g L^{-1}) hasta la que se encuentre presente en el sitio contaminado.

2. Aprovechar las ventajas del BAL para aplicarlo en otros bioprocesos que combaten problemas ambientales con fines industriales, por ejemplo, la reducción de cromo (VI) por *Aspergillus niger var. Tubingensis,* en otro biorreactor neumático (columna de burbujas) generó buenas tasas de reducción pero mostró baja reproducibilidad. Posiblemente el BAL, un biorreactor con un flujo más ordenado y cuya hidrodinámica y transferencia de masa estudiamos en este trabajo, corrija esta deficiencia.

3. Aplicar el cociente de tasas de transferencia simultánea de masa a otros bioprocesos que involucren sistemas trifásicos y en los cuales generalmente se considera sólo la transferencia de oxígeno. Particularmente para la producción de consorcios microbianos, estudiando su dinámica de poblaciones, con capacidad para remediar sitios contaminados.

10. Referencias y Anexos

[1] Abashar M.E., Narssing U. y Rouilliard A. E., (1998), Hydrodynamic Flow Regimes, Gas Holdup, and Liquid Circulation in Airlift Reactors, Industrial and Engineering Chemistry Research, **199**: 1251-1259

[2] Bai G., Brusseau M.L. y Miller R.M., (1997), Biosurfactant-enhaced removal of residual hydrocarbon from soil, Journal of Contaminant Hydrology, **25**: 157-170.

[3] Cerri M.O., Policarpo L.M. y Badino A. C., (2010a), Gas Hold-Up and mass transfer in three geometrically similar internal loop airlift reactors using newtonian fluids, International Journal of Chemical Reactor Engineering, **8:** 1-14.

[4] Cerri M.O., Baldacin J.C., Cruz A.J.G., Hokka C.O. y Badino A.C., (2010b), Prediction of mean bubble size in pneumatic reactors, Biochemical Engineering Journal, **53:** 12-17.

[5] Cesario M.T., de Wit H. L., Tramoer J. y Beefiink H.H., (1996), New technique for K_LA measurement between gas and water in aereated solvent-inwater dispersions, Biotechnology Techniques, **10:** 195-l98.

[6] Cheng-Shing L. y Shyh-Jye H., (2004), Dynamic behavior of an internal-loop airlift bioreactor for degradation of waste gas containing toluene, Chemical Engineering Science, **59**: 4517-4530.

[7] Chisti Y., (1989), Airlift reactors: current technology. En Airlift Bioreactors, Elsevier Science Publishers, New York.

[8] Chisti Y. Halard B. y Moo-yung M., (1988), Liquid circulation in airlift reactor, Chemical Engineering Science, **43:** 451-456

[9] Chisti Y. y Jáuregui-Haza U.J., (2002), Oxygen transfer and mixing in mechanically agitated airlift bioreactors, Biochemical Engineering Journal, **10**: 143-153.

[10] Clarke K.G., Williams P.C., Smit M.S. y Harrison S.T.L., (2006), Enhancement and repression of the volumetric oxygen transfer coefficient through hydrocarbon addition and its influence on oxygen transfer rate in stirred tank bioreactors, Biochemical Engineering Journal, **28:** 237-42.

[11] Daugulis A.J. y Janikowski T., (2002), Scale up performance for the degradation of polyaromatic hydrocarbons by *Sphyngomonas aromativorans*, Biotechnology letters, **24**: 591-594.

[12] Díaz-Ramírez I. J., Ramírez-Saad H., Gutiérrez-Rojas M. y Favela-Torres E., (2003), Biodegradation of Maya crude oil fractions by bacterial strains and a defined mixed culture isolated from Cyperus laxus rhizosphere soil in a contaminated site, Canadian Journal of Microbiology, **49** : 755-761.

[13] Doing S., Pickering S. C. R., Lye G.J. y Woodley J.M., (2002), The use of microscale processing technologies for quantification of biocatalytic Baeyer-Villiger oxidation kinetics, Biotechnology Bioengineering, **80:** 42-49.

[14] Dorobantu L. S., Yeung A. K. C., Foght J. M. y Gray M. R., (2004), Stabilization of oil-water emulsions by hydrophobic bacteria, Applied and environmental microbiology, **70**, 6333–6336.

[15] Fujio Y., Sambuichi M. y Ueda S., (1973), Numerical method of the determination of kLa and respiration rate in biological system, Journal of Fermentation Technology, **51:** 154-158.

[16] García-Ochoa F. y Gomez E., (2009), Bioreactor scale-up and oxygen transfer rate in microbial processes: An overview, Biotechnology Advances, **27:** 153-176.

[17] García-Salas S., Rosales-Peña M.E., Alfaro R. Porter M. y Thalasso F., (2008), Measurement of local specific interfacial area in bubble columns via a non-isokinetic withdrawal method coupled to electro-optical detector, Chemical Engineering Science, **63:** 1029 – 1038.

[18] Gargouri B., Karray F., Mhiri N., Alouia F. y Sayadi S., (2011), Application of a continuously stirred tank bioreactor (CSTR) for bioremediation of hydrocarbon-rich industrial wastewater effluents, Journal of Hazardous Materials, IN PRESS.

[19] Ghazali F.M., Abdul-Rahman R.N.Z., Salleh A.B. y Basri M., (2004), Biodegradation of hydrocarbons in soil by microbial consortium, International Biodeterioration & Biodegradation, **54**:61-67.

[20] González P., (2009), Efecto de la fracción arcillosa y de la vermicomposta en la biodegradación de hidrocarburos, Tesis de maestría, posgrado en Biotecnología UAM.

[21] Gumery F., Ein-Mozaffari F. y Dahman Y., (2009), Characteristics of local flow dynamics and macro-mixing in airlift column reactors for reliable design and scale-Up, International Journal of Chemical Reactor Engineering **7:** 1-45.

[22] Huang Q., Yang C., Yu g. y Mao Z., (2010), CFD simulation of hydrodynamics and mass transfer in an internal airlift loop reactor using a steady two-fluid model, Chemical Engineering Science, **65:** 5527-5536.

[23] Ichii T., Konno H., Ishida T., Sato H., Suzuki A. y Yamazumi K., (1993), Development of a new comercial-scale airlift fermentor for rapid growth of yeast, Journal of Fermentation Bioengineering, **75**: 375-379.

[24] Inakollu S., Hung H. y Shreve G.S., (2004), Biosurfactant enhancement of microbial degradation of various structural classes of hydrocarbon in mixed waste systems, Environmental Engineering Science, **21:** 463-469.

[25] Kantarci N., Borak F. y Klutlu O., (2005), Bubble column reactors, Process Biochemistry, **40:** 2263-2283.

[26] Kilonzo P.M., Margaritis A., Bergougnou M.A., Yu J.T. y Qin Y., (2006), Influence of the baffle clearance design on hydrodynamics of a two riser rectangular airlift reactor

with inverse internal loop and expanded gas-liquid separator, Chemical Engineering Journal, **121**: 17-26.

[27] Lemoine R. y Morsi B.I., (2005), Hydrodynamic and mass transfer parameters in agitated reactors Part II: Gas-holdup, Sauter mean bubble diameters, volumetric mass transfer coefficients, gas-liquid interfacial areas, and liquid-side mass transfer coefficients, International Journal of Chemical Reactor Engineering, **3:** 1-49.

[28] Lin T.J. y Chen P.C., (2005), Studies on hydrodynamics of an internal-loop airlift reactor in gas entrainment regime by particle image analyzer, Chemical Engineering Journal, **108:** 69-79.

[29] Liu T., Miura S., Yaguchi M., Arimura T., Park E.Y. y Okabe M., (2006), Scale up of L-Lactic acid production by mutant strain Rhizopus sp. MK-96-1196 from 0.003 m^3 to 5 m^3 in airlift bioreactors, Journal of Bioscience and Bioengineering, **101**(1): 9-12.

[30] Lizardi-Jiménez M. A., (2007), Evaluación del coeficiente de retención de la fase gaseosa como criterio para el escalamiento de un biorreactor de columna de burbujas, Tesis de maestría, posgrado en Biotecnología UAM.

[31] Lizardi-Jiménez M. A., Saucedo-Castañeda G. y Gutiérrez-Rojas M., (2007), Escalamiento de biorreactores para la producción de consorcios microbianos usando el coeficiente de retención de la fase gaseosa, *XII Congreso Nacional de Biotecnología y Bioingeniería*. Sociedad Mexicana de Biotecnología y Bioingeniería A.C. Morelia, Michoacán, México.

[32] Lizardi-Jiménez M. A., Bautista-Flores J. y Gutiérrez-Rojas M., (2009), Eficiencia degradadora de petróleo de un consorcio microbiano crecido con hexadecano en un biorreactor, *XIII Congreso Nacional de Biotecnología y Bioingeniería*. Sociedad Mexicana de Biotecnología y Bioingeniería A.C. Acapulco, Guerrero, México.

[33] Lizardi-Jiménez M.A., Saucedo-Castañeda G., Thalasso F. y Gutiérrez-Rojas M., (2011), Dynamic technique to determine hexadecane transfer rate from organic phase to aqueous phase in a three-phase bioreactor, International Journal of Chemical Reactor Engineering, **9:** S3.

[34] Lobo R., (1997), Modelos de transferencia de masa convectiva. En Principios de Transferencia de Masa, Universidad Autónoma Metropolitana. México.

[35] Lu M., Zhang Z., Sun S., Wang Q. y Zhong W., (2009), Enhanced degradation of bioremediation residues in petroleum-contaminated soil using a two-liquid-phase bioslurry reactor, Chemosphere, **77**: 161–168.

[36] Luo H.P. y Al-Dahhan H., (2011), Verification and validation of CFD simulations for local flow dynamics in a draft tube airlift bioreactor, Chemical Engineerig Science, **66:** 907-923.

[37] Martín M., Montes F.J. y Galán M.A., (2008), On the contribution of scales of mixing to the oxygen transfer in stirred tanks, Chemical Engineering Journal, **145:** 232-241.

[38] Medina-Moreno S. A., Huerta-Ochoa S. y Gutiérrez-Rojas M., (2005), Hydrocarbon biodegradation in oxygen limited sequential batch reactors by consortium from weathered oil-contaminated soil, Canadian Journal of Microbiology, **51**: 231-239.

[39] Medina-Moreno S.A., Huerta-Ochoa S., Lucho-Constantino C.A., Aguilera-Vázquez L., Jiménez-González A. y Gutiérrez-Rojas M., (2009), Biodegradation modeling of sludge bioreactors of total petroleum hydrocarbons weathering in soil and sediments, Revista Mexicana de Ingeniería Química, **8:** 245-258.

[40] Mehrnia M., Towfighi J., Bonakdarpour B. y Akbainejad M., (2005), Gas Hold-up and oxygen transfer in a draft-tube airlift bioreactor with petroleum based liquids, Biochemical Engineering Journal, **22**: 105-110.

[41] Mengxi L., Chunxi L., Mingxian S., Baoli G. y Jie H., (2007), Hydrodynamics and mass transfer in a modified three-phase airlift loop reactor, Petroleum Science, **4:** 91-96.

[42] Montoya-Ballesteros L.C., Gardea-Béjar A., Ayala-Chávez G.M., Martínez-Nuñez Y.Y. y Robles-Ozuna, L.E., (2010), Capsaicinoids and color in chilpetin (Capsicum annuum var. aviculare). Processing effect on sauces and pickles, Revista Mexicana de Ingeniería Química, **9:** 197-207.

[43] Nielsen J., Villadsen J. y Liden G., (2003), Mass transfer. En: Bioreactor Engineering Principles. Kuwler Academic/Plenum Publishers, New York.

[44] Olivieri G., Marzocchella A. y Salatino P., (2003), Hydrodynamics and mass transfer in a lab-scale three-phase internal loop airlift, Chemical Engineering Journal, **96:** 45-54.

[45] Orozco M., (2010), Selección de un ecotipo de Bouteloua curtipendula con potencial fitorremediador y su evaluación frente a diferentes mezclas de hidrocarburos, Tesis de especialidad, posgrado en Biotecnología UAM.

[46] Pemex, (2009), Informe de Responsabilidad Social , www.imp.gob.mx

[47] Pepi M., Cesàro A., Liut G y Baldi F., (2005), An antartic psychrotrophic bacterium *Halomonas sp*. ANT-3b, growing on n-hexadecane, produces a new emulsyfying glycolipid. FEMS, Microbiology Ecology, **53**: 157-166.

[48] Quijano G., (2006), Evaluación de los coeficientes de transferencia de masa y de reacción en un biorreactor de tres fases para la degradación de hexadecano, Tesis de Maestría en Biotecnología, Universidad Autónoma Metropolitana.

[49] Quijano G., Revah S., Gutiérrez-Rojas M., Flores-Cotera L. y Thalasso F., (2009), Oxygen transfer in three-phase airlift and stirred tank reactors using silicone oil as transfer vector, Process Biochemistry, **44:** 619–624.

[50] Quijano G., Huerta-Ochoa S. y Gutiérrez- Rojas M., (2010), Assessment of the limiting step of mass transfer in n- hexadecane biodegradation in a bubble column reactor, Water Science Technology, **62**: 906-914.

[51] Quintero R., (1990), Transferencia de oxígeno y diseño de fermentadores. En Ingeniería Bioquímica, Alambra, México.

[52] Ribeiro Jr C. P. y Lage P. L. C., (2004), Experimental study on bubble size distributions in a direct contact evaporator, Brazilian Journal of Chemical Engineering, **21**: 69-81.

[53] Sánchez-Mirón A., Cerón-García M.C, García-Camacho F., Molina-Grima E. y Chisti Y., (2004), Mixing in bubble column and airlift reactors. Transactions Institution of Chemical Engineers Part A. Chemical Engineering Research and Design, **82** (A10):1367-1374.

[54] Saravanan P., Pakshirajan K. y Saha P., (2009), Treatment of phenolics containing synthetic wastewater in an internal loop airlift bioreactor (ILALR) using indigenous mixed strain of *Pseudomonas* sp. under continuous mode of operation, Bioresource Technology, **100**: 4111-4116.

[55] Saval S., Bioremediation, Clean-up biotechnologies for soils and aquifers. En Environmental Biotechnology and Cleaner Bioprocesses, Taylor & Francis, Londres, 2000, pp. 155-166.

[56] Schmidt-Etkin D., (2010), Spill Occurrences: A World Overview. En Oil Spill Science and Technology. Editado por: Mervin Fingas, Gulf Professional Publising, Oxford.

[57] Shariati F.P., Bonakdarpour B. y Mehrnia M.R., (2007), Hydrodynamics and oxygen transfer behaviour of water in diesel microemulsions in a draft tube airlift bioreactor, Chemical Engineering and Processing, **46**: 334–342.

[58] Skladany G. J., y Metting F.B., (1993), Bioremediation of contaminated soil. En: Soil Microbial, Ecology, applications in agricultural and environmental management. Editado por: Metting F.B. Marcel Dekker, Inc. USA.

[59] Smith S.R.L., (1980), Single cell protein, Philosophical Transactions of the Royal Society, **290**: 341-354.

[60] Tang H., Wang D. y Ge X., (2004), Environmental nano-pollutants (ENP) and aquatic micro-interfacial processes, Water Science Technology, **50** (12):103-9.

[61] Torres-Martínez D., Melgarejo-Torres R., Gutiérrez-Rojas M., Aguilera-Vázquez L., Micheletti M., Lye G.J. y Huerta-Ochoa S., (2009), Hydrodynamic and oxygen mass transfer studies in a three-phase (air–water–ionic liquid) stirred tank bioreactor, Biochemical Engineering Journal, **45**:209-217.

[62] Tzintzun-Camacho O., Loera O., Ramiez-Saad H. C. y Gutierrez-Rojas M., (2011), Hexadecane degradation and mechanisms generated by changes on cell hydrophobicity of a bacterial consortium to produce biomass in three-phase bioreactors, Applied Microbiology and Biotechnology, ENVIADO**.**

[63] Röling W. F. M., Milner M. G., Jones D. M., Lee K., Daniel F., Swannell R. J. P. y Head I. M., (2002), Robust hydrocarbon degradation and dynamics of bacterial communities during nutrient-enhanced oil spill bioremediation, Applied and Environmental Microbiology, **68** (11): 5537-5548.

[64] Volke-Sepúlveda T. L., Gutiérrez-Rojas M. y Favela-Torres E., (2006), Biodegradation of high concentrations of hexadecane by *Aspergillus niger* in a solid-state system: Kinitec analysis, Bioresource Techology, **97:** 1583-1591.

[65] Wongsuchoto P. y Pavasant P., (2004), Internal liquid circulation in annulus sparged internal loop airlift contactors, Chemical Engineering Journal, **100***:* 1-9.

Anexo 1

Revista Mexicana de Ingeniería Química

Vol. 10, No. 1 (2011) 59-65

ASSESSMENT OF THE LOCAL HYDRODYNAMIC ZONES IN A THREE-PHASE AIRLIFT REACTOR: LOOKING FOR THE LOWEST LIQUID-PHASE Re

EVALUACIÓN DE LAS ZONAS HIDRODINÁMICAS LOCALES EN UN REACTOR AIRLIFT TRIFÁSICO: BUSCANDO EL Re DE FASE LÍQUIDA MÁS BAJO

M.A. Lizardi-Jiménez* and M. Gutiérrez-Rojas

Departamento de Biotecnología, Universidad Autónoma Metropolitana-Iztapalapa, Av. San Rafael Atlixco No. 186 Col. Vicentina, C.P. 09340, Ciudad de México, México.

Received 6 of October 2010; Accepted 2 of February 2011

Abstract

Hydrodynamic in main airlift reactor (ALR) zones (riser and downcomer) was evaluated in order to find the lowest Reynolds number (Re) in a three-phase ALR. In our study, three phases were identified: one gaseous (air) and two liquids (oil and aqueous). Two Re of the liquid species, one for each phase, were defined: Re_{aq} and Re_{oil} corresponding to the aqueous and oil phase, respectively. Since gas phase was considered by hold up (εg) in our work. In 10 L ALR, riser showed turbulent aqueous phase flow ($4000 < Re_{aq} < 9000$) whereas downcomer exhibited non-turbulent flow ($1250 < Re_{aq} < 4000$). Re_{oil} in riser ($5000 < Re_{oil} < 10000$) was higher than Re_{aq}; whereas in downcomer, Re_{oil} was lower than Re_{aq} ($200 < Re_{oil} < 2200$). The oil phase into the downcomer zone was demonstrated to be the most important hydrodynamic constraint and consequently limited mass transfer should be expected. The complexity of three-phase flow and the limited measurement technologies have generated few studies regarding the local hydrodynamics properties restricting three-phase reactors optimization and commercialization; our study is a contribution to identify such restrictions.

Keywords: airlift, hydrodynamics, riser, downcomer, three-phase, Re.

Resumen

Se evaluó la hidrodinámica en las principales zonas (ascenso y descenso) de un reactor airlift (ALR) trifásico para encontrar el numero de Reynolds (Re) más bajo. Las fases del estudio fueron: una gaseosa (aire) y dos líquidas (hidrocarburos y agua). Se definieron dos Re en las fases líquidas: Re_{aq} y Re_{oil} correspondientes a las fases acuosa y oleosa. La fase gaseosa fue considerada mediante el coeficiente de retención (εg). En el ALR (10 L) la zona de ascenso mostró flujo turbulento ($4000 < Re_{aq} < 9000$) mientras que en la zona de descenso no se observó flujo turbulento ($1250 < Re_{aq} < 4000$). El Re_{oil} en la zona de ascenso ($5000 < Re_{oil} < 10000$) fue mayor que el Re_{aq}; mientras que en la zona de descenso fue menor ($200 < Re_{oil} < 2200$). La fase oleosa en la zona de descenso fue la limitante hidrodinámica y consecuentemente se debería esperar una limitación en la transferencia de masa. La complejidad del flujo trifásico y las limitadas tecnologías para su medición han generado pocos estudios relacionados con las propiedades hidrodinámicas locales restringiendo la optimización y comercialización de los reactores trifásicos; nuestro estudio es una contribución a la identificación de este tipo de restricciones.

Palabras clave: airlift, hidrodinámica, ascenso, descenso, trifásico, Re.

* *Corresponding author. E-mail*: cbs204381858@xanum.uam.mx
Tel. + 52 (55) 5804 6505, Fax + 52 (55) 5804 6407

1 Introduction

Airlift reactor (ALR) is a pneumatic reactor agitated with a continuous gas phase provided in form of bubbles, breaking-up towards the liquid phase resulting in an isothermal expansion to keep homogeneity (Chisti, 1989). In case of ALR performance, attention has been focused on two fundamental phenomena: (i) agitation for well mixed liquid phases (Gumery *et al.*, 2009) and (ii) oxygen mass transfer considering geometrics in internal loop reactors (Cerri *et al.*, 2010) and CFD simulations (Huang *et al.*, 2010; Luo *et al.*, 2011). Agitation and mixing is often related to the Reynolds number (Re) as a global hydrodynamic parameter i.e., a bulk Re or a liquid phase Re (Wongsuchoto and Pavasant, 2004). Recent studies in ALR allow emphasizing the role of aqueous phase Re in two-phase ALR performance. Unfortunately, none of the works is oriented to study the different local hydrodynamic zones. For all types of ALR, it is possible to distinguish four different local hydrodynamic zones: riser, downcomer, top and bottom clearance (see Fig. 1). Although the hydrodynamic importance of zones in ALR performance is well documented (Sánchez-Mirón *et al.*, 2004; Kilonzo *et al.*, 2006) most of ALR studies neither take into account zones or non-soluble aqueous substrates (e.g. oil) in three-phase systems. Studying aqueous and oil phase hydrodynamics in main three-phase ALR zones is very important because hydrodynamic is strongly implicated in both, aqueous soluble and non-soluble substrates and mass transfer phenomena and the resulting ALR performance; for example, bioengineering and oil biodesulfuration purposes (Mehrnia *et al.*, 2005; Shariati *et al.*, 2007) or using silicone oil as an effective mass transfer vector (Quijano *et al.*, 2009). The aim of this work is to assess, in a trhee-phase ALR, the local hydrodynamic zone (riser or downcomer) with lower Re by measuring fluid velocities in the aqueous and oil phases.

2 Materials and methods

2.1 Reactor

A 10-L operation volume airlift reactor (ALR) was used. The ALR cylindrical vessel was built in Pyrex glass (0.005 m of wall thickness). Gas phase

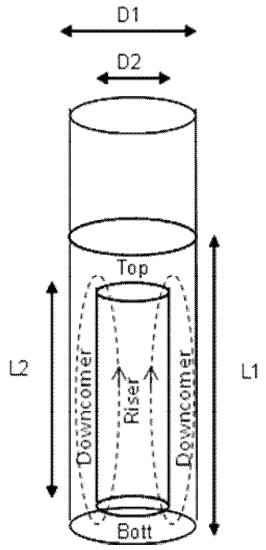

Fig. 1: Geometrical relations and flow pattern in our three-phase airlift reactor.

was introduced into the ALR draft tube. Draft tube was located 0.035 m above the bottom. Geometrical relations and the flow pattern are shown in Fig. 1, in brief: D1 and D2 are reactor (0.14 m) and draft tube (0.09 m) diameter, respectively; L1 and L2 represent reactor (0.70 m) and draft tube (0.54 m) height; riser, top clearance, downcomer and bottom clearance are identified. Geometrical relations: D2/D1 = 0.65, L2/L1 = 0.77 and L1/D1 = 5 were used.

2.2 Gas sparger

Air was sparged through the draft tube with an L-form perforated (7 orifices; 0.001 m of diameter and 0.004 m of separation) stainless steel tubing (0.006 m internal diameter) driving out air downwards.

2.3 Two-liquid phase model medium

In order to adjust surface tension (σ), a model medium was designed using reference values (50 - 65 dynes cm^{-1}) as suggested elsewhere (Bai *et al.*, 1997; Quijano *et al.*, 2010) by adding different Tween 20 (0-0.15 mL L^{-1}) concentrations and 13g L^{-1} of hexadecane (HXD). σ was measured with a Manual Fisher Surface Tensiometer Model 20 (Fisher Scientific International, Wisconsin, USA). Viscosity (μ) was determined by using a

viscometer Physica MCR Model 300 (Sttuttgart, Germany).

2.4 Hydrodynamic parameters

2.4.1 Gas hold up

Gas hold up (εg) was evaluated into riser and downcomer by photographic method (Ribeiro and Lage, 2004) using a digital camera (Pentax Optio 50) and image analysis software (Image Pro plus 4.1).

2.4.2 Aqueous and oil phase hydrodynamic

Three phases (air, aqueous and oil) were involved in ALR, the two slow-moving phases (aqueous and oil) velocities were experimentally evaluated. In order to clearly follow flow patterns thorough model medium, we used two substances simulating water (sodium polyacrylate hydrogel; ρ = 1.0 g cm^{-3}) and oil (oligosyloxane stained spheres; ρ = 0.77 g cm^{-3}). A digital videocamera (Sony HD) and on-line chronometer (StopWatch software) were used to monitoring velocities of single spheres as path length/elapsed time ratio in both ALR zones: riser and downcomer. In order to contrast sphere images, HXD was previously stained with red chillies (*Capsicum annuum*) oleoresin (Montoya-Ballesteros *et al.*, 2010), also known as rodophile (Bioquimex-Reka, México; 25.1 g of carotenoid kg^{-1}) (see Fig. 2). The resulting velocities were used to calculate two individual Reynolds numbers (Nielsen *et al.*, 2003) as follows:

$$\mathrm{Re}_{aq} = \frac{DV_{aq}\rho_{aq}}{\mu} \quad (1)$$

$$\mathrm{Re}_{oil} = \frac{DV_{oil}\rho_{oil}}{\mu} \quad (2)$$

Where: Re_{aq} and Re_{oil} are aqueous and oil phase Reynolds number, respectively. D = D2 for riser zone; and D = (D1-D2) for downcomer zone; D1 is the ALR diameter, cm; D2 draft tube diameter, cm; V_{aq} aqueous phase velocity, cm s^{-1}; V_{oil} oil phase velocity, cm s^{-1}; ρ_{aq} aqueous phase density, g cm^{-3}; ρ_{oil} oil phase density, g cm^{-3}; μ bulk viscosity (oil in water emulsion), g cm s^{-1}. In order to validate our method, the V_{aqd} values obtained were compared with acid pulse method (Sanchez- Miron *et al.*, 2004) . Chisti model (Chisti *et al.*, 1988; Abashar *et al.*, 1998) and the continuity criterion (Chisti, 1989) was used in order to predict superficial aqueous phase velocity (V_{aqd}) into downcomer using εg as follows:

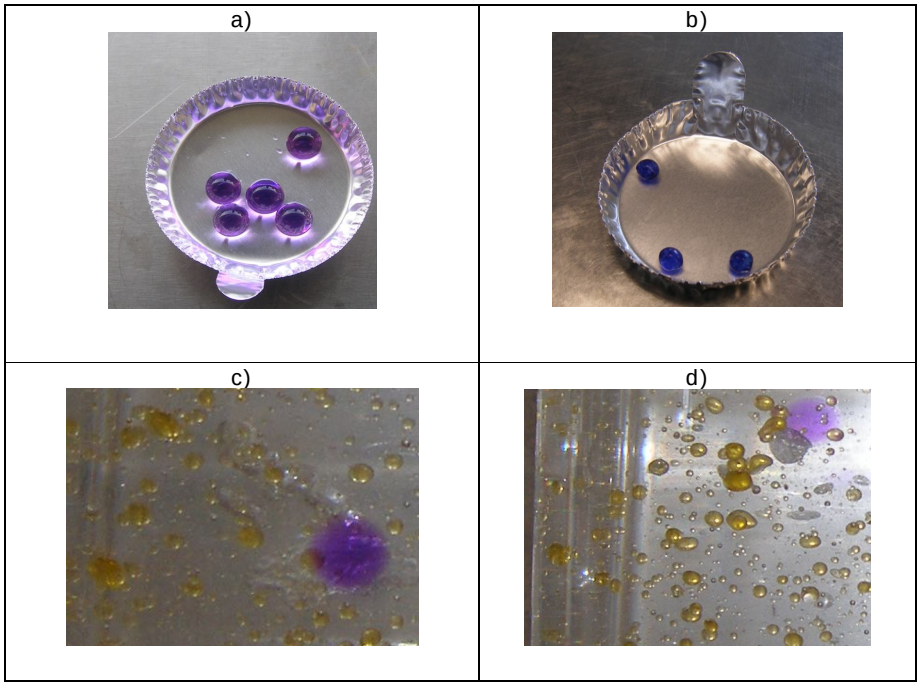

Fig. 2: Polyacrilate (a) and olygosyloxane (b) spheres. Polyacrilate sphere in downcomer (c) and riser (d) clearly distinguished from air bubbles and HXD yellow stained droplets.

$$V_{aqd} = \frac{A_r}{A_d}\left[\frac{2gL_D\left(\varepsilon g_r - \varepsilon g_d\right)}{K\left(\frac{1}{(1-\varepsilon g_r)^2} + \left(\frac{A_r}{A_d(1-\varepsilon g_d)}\right)^2\right)}\right] \quad (3)$$

Where: A_r and A_d are cross section area for riser and downcomer, m^2, respectively. εg_r and εg_d are gas hold up in riser and downcomer, dimensionless, respectively, K is the loss friction coefficient, dimensionless, g is the gravitational acceleration constat, m s^{-2} and L_D is the draft tube lenght, m.

The model assumes the following: (1) steady-state conditions, (2) isothermal conditions, (3) the energy losses terms due to the skin friction in the riser and the downcomer are negligible in comparison to the others dissipation terms, (4) the presure drop due to acceleration is negligible.

2.4.3 Statistical analyses

Data analyses were carried out by using NCSS-2000, version 2001 (Copyright 2001 by Jerry Hintze). Analysis of variance (ANOVA) was performed by comparing tests with $p < 0.05$.

3 Results and discussion

In order to evaluate hydrodynamic behavior in our three-phase ALR, εg, liquid phases velocities, Re_{aq} and Re_{oil} were measured using geometrical relations D2/D1 = 0.65 and L2/L1 = 0.77. The choice of this configuration is partially according to a similar hydrocarbon/liquid ALR (Gumery *et al.*, 2005) studying dynamics and macro-mixing for design and scale-up purposes. Fig. 3 shows εg as a function of Ug into riser and downcomer. The εg in the riser was slightly higher than in the downcomer. A potential model: $\varepsilon g = aUg^b$ (where a and b depend on local hydrodynamic) was used for both: riser ($a = 0.053$ and $b = 0.74$; $R^2 = 0.99$) and downcomer ($a = 0.045$ and $b = 0.72$; $R^2 = 0.98$). The differences between εg in riser and downcomer caused liquid phases circulation. The potential model data obtained from Fig. 3 were used in order to predict superficial aqueous phase velocities into downcomer (V_{aqd}) using the Chisti model, see Eq. 3. Fig. 4 shows experimental data of V_{aqd} as a function of Ug in addition to V_{aqd} values predicted by the Chisti model. A good fitting value for the loss friction coefficient (K) of 4, close to other work (1.8) with water and kerosene (Abashar *et al.*, 1998), was found.

Fig. 5 shows Re_{aq} as a function of Ug and σ, for the selected configuration in riser (3a) and downcomer (3b). As expected, in riser and downcomer, Re increased as Ug increased. On the other hand Re_{aq} slightly decreased as σ increased. A similar performance was also observed in other pneumatic reactors working with two-phase systems (Kantarci *et al.*, 2005). Riser shows turbulent flow ($Re_{aq} > 4000$; see red zone in Fig. 2a) when Ug was higher than 0.4 cm s^{-1}, whilst downcomer do not (red zone is absent in Fig. 3b). Re_{aq} increased as Ug probably due to differences in gas hold up between riser and downcomer, which produces differences in hydrostatic pressure at the ALR bottom, these differences in hydrostatic pressure produce the liquid phase being in continuos movement. The Re_{aq} decreasing as surface tension increased could be explained by reason of gas hold up decreased as a result of larger bubbles with lower residence time and the resultant decreasing in the differences in hydrostatic pressure. Moreover, lower Re_{aq} in downcomer (not turbulent) supposes a hydrodynamics limitation for mixing probably imposing mass transfer limitation (Nielsen *et al.*, 2003); this limitation is worst for oil phase as can be seen in figs. 3c and 3d. Figures show Re_{oil} as a function of Ug and surface tension. Re_{oil} in riser ($5000 < Re_{oil} < 10000$) (Fig. 3c) was higher than Re_{aq}; whereas in downcomer was lower ($200 < Re_{oil} < 2200$) (Fig. 3d). Re_{oil} in riser and downcomer were higher and lower than Re_{aq}, respectively, due to densities differences. Lower Re_{oil} values in downcomer involve an increasing in boundary layer between oil and aqueous phase, probably resulting in mass transfer constraints (Cerri *et al.*, 2010). Our results suggest that a carefully evaluation of the two Re species, involved in performance of three-phase ALR was needed since oil phase into the downcomer supposed a clear hydrodynamic and probably mass transfer limitation. Traditional two-phase model that considers only aqueous phase is not enough to explain oil in water reactors. For example, oil-degrading microorganism growth (Medina-Moreno *et al.*, 2009) should consider oil transfer constraints in the bulk. The complexity of three-phase flow and the limited

measurement technologies have generated few studies regarding the local hydrodynamics properties restricting three-phase reactors optimization and commercialization.

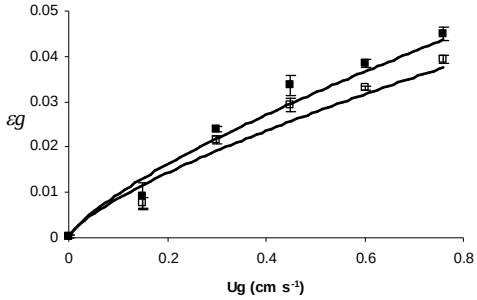

Fig. 3: Gas hold up (εg) as a function of superficial gas velocity (Ug): (■) riser and (□) downcomer. Continuos line represents potential model with R^2 higher than 0.98. Error bars represent the standard error for triplicate samples.

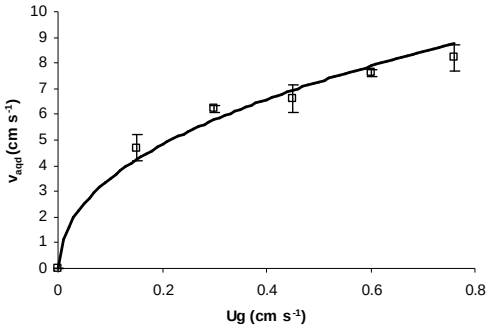

Fig. 4: Superficial aqueous phase velocity into the downcomer (V_{aqd}) as a function of superficial gas velocity (Ug). Continuous line represents Chisti model with R^2 higher than 0.96. Error bars represent the standard error for triplicate samples.

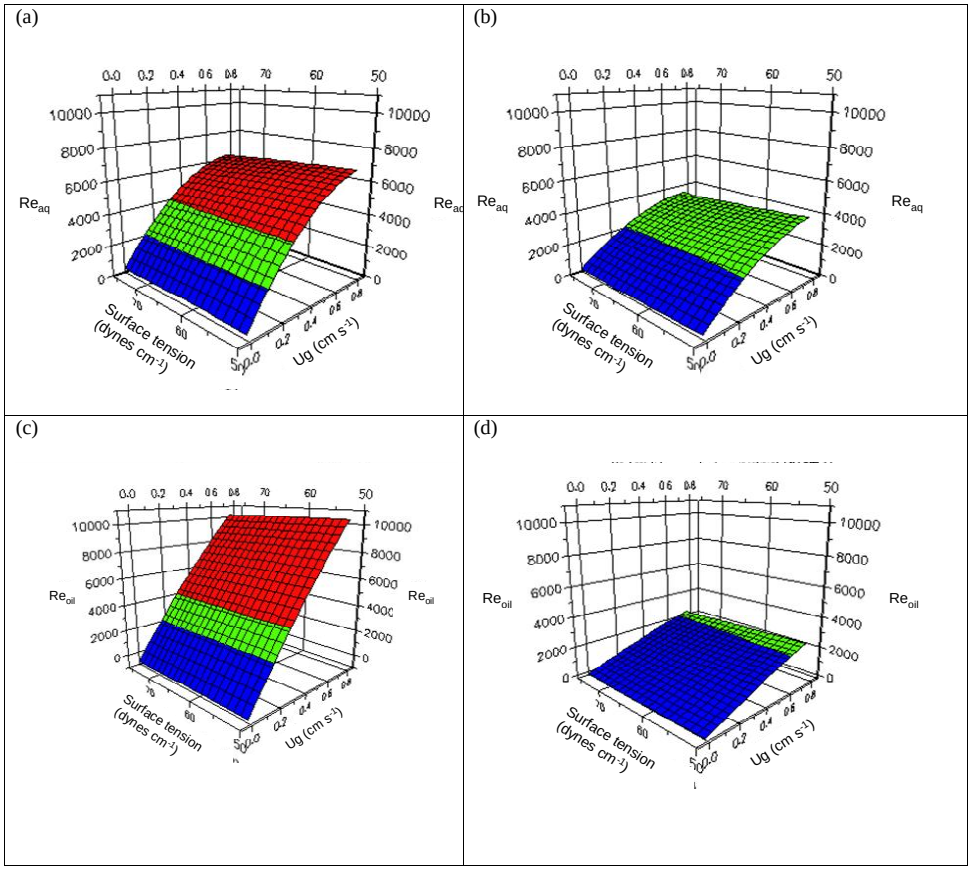

Fig. 5: Re_{aq} as function of superficial gas velocity (Ug) and surface tension (σ) in riser (a) and downcomer (b); Re_{oil} as function of Ug and σ in riser (c) and downcomer (d). Red zone: Re $\geq$ 4000; turbulent flow. Green zone: 4000 $\geq$ Re $\geq$ 2000; transient flow. Blue zone: Re $\leq$ 2000 ; laminar flow.

Conclusion

Aqueous and oil phase Re for main ALR local hydrodynamics zones, riser and downcomer, in a three-phase ALR were evaluated in this work. Riser shows turbulent aqueous phase flow: $4000 < \mathrm{Re}_{aq} < 9000$ for $0.15 < Ug < 0.76$ cm s^{-1} whereas downcomer shows non-turbulent aqueous phase flow: $1250 < \mathrm{Re}_{aq} < 4000$ at the same above mentioned Ug values. Oil phase Re in riser ($5000 < \mathrm{Re}_{oil} < 10000$) was higher than Re_{aq}; whereas in downcomer, Re_{oil} was lower than Re_{aq} ($200 < \mathrm{Re}_{oil} < 2200$). Re_{oil} into downcomer zone is supposed to be the most important hydrodynamic constraint allowing us to identify the downcomer as a relevant mass transfer limitation zone.

Acknowledgements

We acknowledge CONACYT (Consejo Nacional de Ciencia y Tecnología) by scholarship to M. A. Lizardi-Jimenez and PEMEX-Refinación for partial support. Thanks are due to Dr. J. Vernon in providing rhodophile pigment solution.

References

Abashar, M.E., Narssing, U., Rouilliard, A. E. (1998). Hydrodynamic Flow Regimes, Gas Holdup, and Liquid Circulation in Airlift Reactors. *Industrial and Engineering Chemistry Research 199*, 1251-1259

Bai, G., Brusseau, M.L. and Miller, R.M. (1997). Biosurfactant-enhaced removal of residual hydrocarbon from soil. *Journal of Contaminant Hydrology 25*, 157-170.

Cerri, M.O., Policarpo, L.M. and Badino, A. C. (2010). Gas Hold-Up and mass transfer in three geometrically similar internal loop airlift reactors using newtonian fluids. *International Journal of Chemical Reactor Engineering 8*, 1-14.

Chisti, Y. Halard, B., Moo-yung, M. (1988). Liquid circulation in airlift reactor. *Chemical Engineering Science 43*, 451-456

Chisti, Y. (1989). *Airlift Bioreactors*. Elsevier Science Publishers, New York.

Gumery, F., Ein-Mozaffari, F. and Dahman, Y. (2009). Characteristics of local flow dynamics and macro-mixing in airlift column reactors for reliable design and scale-Up. *International Journal of Chemical Reactor Engineering 7*, 1-45.

Huang, Q., Yang, C., Yu, g., Mao, Z. (2010). CFD simulation of hydrodynamics and mass transfer in an internal airlift loop reactor using a steady two-fluid model. *Chemical Engineering Science 65*, 5527-5536.

Kantarci, N., Borak, F. and Klutlu, O. (2005). Bubble column reactors. *Process Biochemistry 40*, 2263-2283.

Kilonzo, P.M., Margaritis, A., Bergougnou, M.A., Yu, J.T. and Qin, Y. (2006). Influence of the baffle clearance design on hydrodynamics of a two riser rectangular airlift reactor with inverse internal loop and expanded gas-liquid separator. *Chemical Engineering Journal 121*, 17-26.

Luo, H.P., Al-Dahhan, H. (2011). Verification and validation of CFD simulations for local flow dynamics in a draft tube airlift bioreactor. *Chemical Engineerig Science 66*, 907-923.

Medina-Moreno, S.A., Huerta-Ochoa, S., Lucho-Constantino, C.A., Aguilera-Vázquez, L., Jiménez-González, A. and Gutiérrez-Rojas, M. (2009). Biodegradation modeling of sludge bioreactors of total petroleum hydrocarbons weathering in soil and sediments. *Revista Mexicana de Ingeniería Química 8*, 245-258.

Mehrnia, M., Towfighi, J., Bonakdarpour, B. and Akbainejad, M. (2005). Gas hold-up and oxygen transfer in a draft-tube airlift bioreactor with petroleum based liquids. *Biochemical Engineering Journal 22*, 105-110.

Montoya-Ballesteros, L.C., Gardea-Béjar, A., Ayala-Chávez G.M., Martínez-Nuñez Y.Y. and Robles-Ozuna, L.E. (2010). Capsaicinoids and color in chilpetin (Capsicum annuum var. aviculare). Processing effect on sauces and pickles. *Revista Mexicana de Ingeniería Química 9*, 197-207.

Nielsen, J., Villadsen, J. and Liden, G. (2003). Mass transfer. In: *Bioreactor Engineering Principles*. Kuwler Academic/Plenum Publishers, New York.

Quijano, G., Revah, S., Gutiérrez-Rojas, M., Flores-Cotera, L. and Thalasso F. (2009). Oxygen transfer in three-phase airlift and stirred tank reactors using silicone oil as transfer vector. *Process Biochemistry 44*, 619-624.

Quijano, G., Huerta-Ochoa, S. and Gutiérrez-Rojas, M. (2010). Assessment of the limiting step of mass transfer in n-hexadecane biodegradation in a bubble column reactor. *Water Science and Technology 62*, 906-914.

Ribeiro, Jr C. P. and Lage, P. L. C. (2004). Experimental study on bubble size distributions in a direct contact evaporator. *Brazilian Journal of Chemical Engineering 21*, 69-81.

Sanchez-Mirón, A., Cerón-Garcia, M.C, Garcia-Camacho, F., Molina-Grima, E. and Chisti, Y. (2004). Mixing in bubble column and airlift reactors. *Transactions Institution of Chemical Engineers Part A. Chemical Engineering Research and design 82*, 1367-1374.

Shariati, F.P., Bonakdarpour, B. and Mehrnia, M.R. (2007). Hydrodynamics and oxygen transfer behaviour of water in diesel microemulsions in a draft tube airlift bioreactor. *Chemical Engineering and Processing 46*, 334-342.

Wongsuchoto, P. and Pavasant, P. (2004). Internal liquid circulation in annulus sparged internal loop airlift contactors. *Chemical Engineering Journal 100*, 1-9.

Anexo 2

INTERNATIONAL JOURNAL OF CHEMICAL REACTOR ENGINEERING

Volume 9 2011 *Note* S3

Dynamic Technique to Determine Hexadecane Transfer Rate from Organic Phase to Aqueous Phase in a Three-Phase Bioreactor

Manuel Alejandro Lizardi-Jiménez[*] Gerardo Saucedo-Castañeda[†]

Frederic Thalasso[‡] Mariano Gutiérrez-Rojas[**]

[*]Universidad Autónoma Metropolitana, cbs204381858@xanum.uam.mx

[†]Universidad Autónoma Metropolitana, saucedo@xanum.uam.mx

[‡]Cinvestav, thalasso@cinvestav.mx

[**]Universidad Autónoma Metropolitana, mgr@xanum.uam.mx

ISSN 1542-6580

Dynamic Technique to Determine Hexadecane Transfer Rate from Organic Phase to Aqueous Phase in a Three-Phase Bioreactor*

Manuel Alejandro Lizardi-Jiménez, Gerardo Saucedo-Castañeda, Frederic Thalasso, and Mariano Gutiérrez-Rojas

Abstract

Determination of mass transfer of non-water soluble substrates, as hexadecane (HXD), is an important constraint in three-phase airlift bioreactor. A new simple dynamic technique able to measure the hexadecane transfer rate (HTR) in a three-phase airlift bioreactor (ALB) was studied in this work. The image analyses technique allowed measuring the resulting specific mass transfer area (a_{HXD}). Gas chromatography was used to measure time-dependent transferred HXD and therefore the HXD transfer coefficient (k_{LHXD}). Finally, HTR was calculated by using the equation HTR = $k_L a_{HXD} \bullet (C_{HXD}^* - C_{HXD})$ where C_{HXD}^* and C_{HXD} are the saturation HXD-aqueous interphase and HXD aqueous phase concentration, respectively. As case study, we successfully applied to the measurement of HTR during a typical ALB microbial consortium culture; values from 0.010 to 0.042 mg HXD (L h)$^{-1}$ were found. This technique could be used to compare similar simultaneously occurring parameters to assess mass transfer constraints in three-phase systems.

KEYWORDS: airlift, three-phase system, mass transfer, technique, hexadecane

---

*We acknowledge CONACYT (Consejo Nacional de Ciencia y Tecnología), scholarship to M. A. Lizardi-Jimenez, and PEMEX-Refinación for partial support. Thanks are due to Dr. J. Vernon for providing HXD droplets pigment solution.

INTRODUCTION

Most of airlift bioreactor (ALB) studies, concerning three-phase systems, hydrocarbons in water emulsion included, usually consider only oxygen transfer and do not take into account water-insoluble liquid substrates (Medina-Moreno *et al.,* 2005; Mehrnia *et al*., 2005; Shariati *et al*., 2007). To determine volumetric oxygen transfer coefficient (k_La_{O2}) from the gas to the water phase and consequently oxygen transfer rate, dynamic and steady state methods can be used (Fujio *et al.,* 1973; Cerri *et al.,* 2010). In the dynamic method, the change of the dissolved oxygen concentration is monitored in time after a step-change of the concentration in the inlet gas. In the steady-state method, the concentration measurements are done at one moment after steady state has been reached (Cesario *et al.,* 1996). In order to use the dynamic method a quick and accurate measurement of the concentration is critical; for example in case of oxygen, where a continuous monitoring of the dissolved oxygen can be accomplished by using an oxygen probe. It is more difficult when an organic water-insoluble compound such as hexadecane (HXD) is used. Moreover, when HXD is the main substrate to be consumed as sole source of carbon and energy, the transport towards the aqueous phase is often the rate-limiting step in many microbial cultivation processes (Cesario *et al.,* 1996). Whilst the product k_La_{O2} is usually measured, such parameter characterizes the transport from gas to aqueous phase, the evaluation of oxygen transfer coefficient (k_{LO2}) and oxygen specific transfer area (a_{O2}) in pneumatic reactors has been recently studied (Cerri *et al.* 2010); unfortunately, there is no HXD probe available allowing any similar evaluation, it was necessary to measure both the HXD specific mass transfer area (a_{HXD}) and the HXD transfer coefficient (k_{LHXD}) separately. A new simple dynamic technique to determine the volumetric hexadecane transfer coefficient (k_La_{HXD}) and consecuently hexadecane transfer rate (HTR) is here proposed. The aim of this work was to propose an experimental technique able to determine HTR in a three-phase (air, aqueous, HXD) airlift bioreactor. The technique was applied to a HXD degrading bacterial consortium culture.

MATERIALS AND METHODS

Microbial consortium culture

A bacterial consortium (*Xanthomonas sp, Acinetobacter bouvetii, Shewanella sp* and *Defluvibacter lusatiae)* was cultured in a previously reported mineral medium (Medina-Moreno *et al*., 2005) added with 13 g L^{-1} of HXD (Sigma-Aldrich, 99.7 %).

Bioreactor

A 10-Liters airlift bioreactor (ALB) was used in this work. ALB cylindrical vessel was made of Pyrex glass (0.14 m diameter; 1.0 m height) provided with a draft tube (0.09 m diameter; 0.54 m height) located 0.035 m above the bottom; air was sparged through the draft tube with a L-shaped perforated (7 orifices; 1.0 mm diameter) stainless steel 1/4 inch internal diameter.

Abiotic medium

In order to adjust the bulk HXD concentration under saturation (C_{HXD}^{*}) up to 65 mg HXD L^{-1}, as published elsewhere (Bai *et al.,* 1997; Quijano *et al.,* 2010), an abiotic medium was designed by adding different Tween 20 (0-0.15 mL L^{-1}) concentrations and HXD (13g L^{-1}). Surface tension was measured in order to compare the chemical surfactant (Tween 20) to biosurfactant emulsification ability. The subsequent experiments were performed using the abiotic medium.

HXD specific area

The HXD specific mass transfer area (a_{HXD}) was calculated by Equation 1 (Torres-Martinez *et al.,* 2009).

$$a_{HXD} = \frac{6}{d_{32HXD}}\phi \qquad (1)$$

where d_{32HXD} is the Sauter mean diameter of HXD droplets (cm) and Ø is the HXD dispersed phase fraction (dimensionless); it was measured in the downcomer, located in annular zone in our ALB, through d_{32HXD} measurement with a digital camera and image analysis software (Image Pro Plus 4.1., Media Cybernetics, USA). In order to contrast droplet images, HXD was previously stained with red chillies (Capsicum *annuum)* oleoresin, also known as rodophile (Bioquimex-Reka, México; 25.1 g of carotenoid kg^{-1}). Assays were carried out by triplicate. d_{32HXD} was measured in triplicate. In each experiment, from 500 to 600 HXD droplets were measured. This number was always greater than 500 as recommended elsewhere (García-Salas *et.al,* 2008) for reliable results.

HXD transfer parameters

k_La_{HXD} was evaluated as follows: abiotic medium (10 L) was added to ALB. A stainless steel cylinder (1 cm diameter; 3.5 cm height) was filled with HXD and

introduced with the open side downward into the downcomer. The filled stainless steel cylinder was introduced into the medium before start aeration. Air supply was turned on and superficial gas velocity (Ug) was adjusted to any desired working value of 0.15 to 1.6 cm s^{-1}. Once aeration was steady, 5 mL samples were extracted each 60 min. Transferred HXD from organic to aqueous phase was recovered by three successive extractions with a sample to solvent ratio of 1:5 (*v/v*) using a hexane (J.T. Baker, 99.6%)/isotonic solution (1:3 *v/v*) as solvent. The organic phases containing transferred HXD were pooled and stored into vials (30 mL; 4°C) for further analysis. The HXD transfer coefficient (k_{LHXD}) was obtained from the stainless steel cylinder (cross section) mass transfer area as the one responsable for all HXD delivered to the medium. And we used, by analogy to oxygen transfer principles, the clasical dynamic method (Fujio *et.al*., 1973); whilst, k_La_{HXD} was obtained as the product of k_{LHXD} and specific mass transfer area of the HXD droplets (a_{HXD}). Finally, HXD transfer rate (HTR) was calculated with the equation $HTR = k_La_{HXD} (C_{HXD}^* - C_{HXD})$; where, C_{HXD} is the measured HXD concentration into the bulk.

RESULTS AND DISCUSSION

Abiotic medium

In order to find the Tween 20 concentration providing C_{HXD}^* up to 65 mg HXD L^{-1} assays at different concentrations were done. Surface tension was measured to compare with biotic medium characteristics (65-47 dynes cm^{-1}) (Quijano *et al.,* 2010). Figure 1 shows C_{HXD}^* (right-hand ordinate) and surface tension (left ordinate) profiles as a function of Tween 20 concentration. As we expected, surface tension values decreased as Tween 20 concentration was increased. In opposition, the increase in Tween 20 allowed increasing C_{HXD}^* up to 100 mg HXD L^{-1}. According to Figure 1, 0.08 mL of Tween 20 per liter of mineral medium are needed to reach 65 mg HXD L^{-1} and the resulting surface tension was 65 dynes cm^{-1}. Such surface tension values associated to C_{HXD}^* (65 mg HXD L^{-1}) were similar to those previously published (Quijano *et al.,* 2010) in bubble columns. The experimental abiotic medium was able to reproduce similar C_{HXD}^* values to those observed with biotic medium. The designed abiotic medium was used for HXD specific area and mass transfer parameters determination.

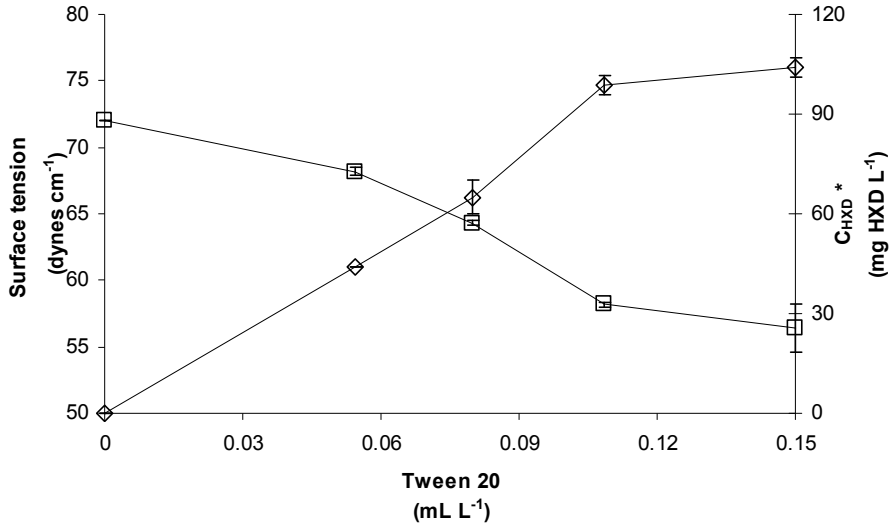

Figure 1. Surface tension (□) and C_{HXD}* (◊) as a function of Tween 20 concentration

HXD specific area

With the purpose of clearly distinguish between air bubbles and the HXD droplets, HXD was stained with rhodophile and image analyses were applied toward HXD. Figure 2 shows two kinds of HXD droplets: (a) non-stained and (b) stained. In Figure 2b all air bubbles were translucent and excluded during the image analysis. Droplets were easily contrasted when rhodophile pigment was used and d_{32HXD} was measured without doubt.

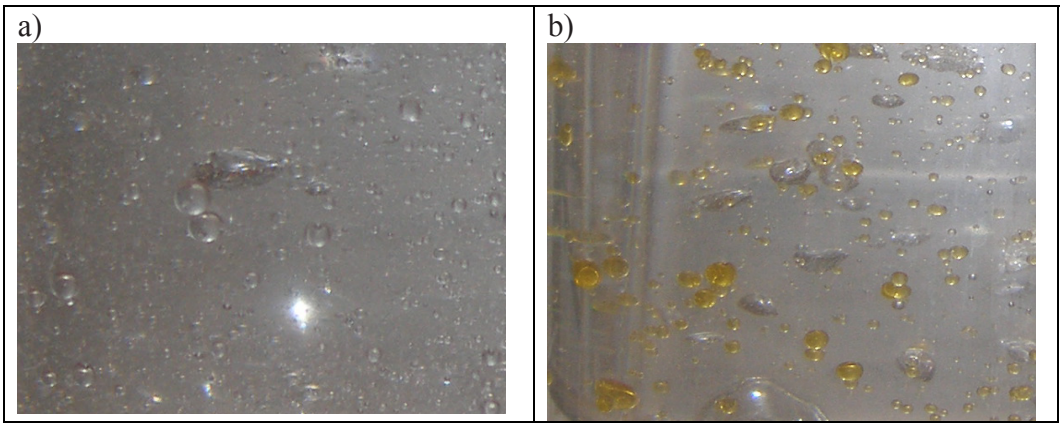

Figure 2. HXD droplets: (a) non-stained and, (b) rhodophile stained.

Table 1 shows d_{32HXD}, a_{HXD} and HXD transfer parameters as a function of Ug. a_{HXD} increased (0.35 – 0.87 cm^2 cm^{-3}) as Ug rose from 0.15 to 1.54 cm s^{-1} as can be seen in 3rd column. All a_{HXD} were used to calculate HXD transfer parameters.

HXD transfer parameters

HXD transfer coefficient (k_{LHXD}), HXD volumetric transfer coefficient (k_La_{HXD}) and HXD transfer rate (HTR) were evaluated as the main mass transfer parameters (Lemoine *et al.,* 2005). k_{LHXD} as a function of Ug is shown in Table 1. The increase in k_{LHXD} values could be due to rapid aqueous phase movement which diminished HXD-water boundary layer (Nielsen *et al.,* 2003). The product of k_{LHXD} by a_{HXD} was computed with the intention to obtain the mass transfer parameter k_La_{HXD}. k_La_{HXD} as a function of Ug is shown in Table 1. As expected, k_La_{HXD} increased (0.005 - 0.023 h^{-1}) with increasing Ug. Higher k_La_{HXD} values (0.8 - 1.3 h^{-1}) were estimated in a 1-Liter bubble column reactor working with constant Ug (1.0 cm s^{-1}) for different culture times involving HXD-water emulsions (Quijano *et al.,* 2010). Our data show at least two magnitude order lower; however, they did not evaluate a_{HXD} as a function of experimental d_{32HXD}. Finally, HTR from HXD droplets to the aqueous phase can be calculated by the product $k_La_{HXD} \cdot (C_{HXD}^* - C_{HXD})$; where C_{HXD}^* and C_{HXD} are the saturation HXD-aqueous interphase and HXD aqueous phase concentration, respectively. As an example, Table 1 shows maxima HTR (HTRmax; when $C_{HXD} = 0$) for all assayed Ug. HTRmax increased (0.32 – 1.52 mg HXD $(L\ h)^{-1}$) as Ug was increased. Higher HTRmax values (30 - 55 mg HXD $(L\ h)^{-1}$) were previously observed in bubble column (Quijano *et al.,* 2010). Our data show at least two magnitude order

lower. Since C_{HXD} is not zero during a typical culture, it was necessary to determine HTR by measuring C_{HXD} on the bulk.

Table 1. Sauter mean diameter (d_{32HXD}), HXD droplets specific area (a_{HXD}), HXD transfer coefficient (k_{LHXD}), HXD volumetric transfer coefficient (k_La_{HXD}) and maximum hexadecane transfer rate (HTRmax) as a function of Ug.

Ug (cm s^{-1})	d_{32HXD} (cm)	a_{HXD} (cm^2 cm^{-3})	k_{LHXD} (cm h^{-1})	k_La_{HXD} (h^{-1})	HTRmax[1] (mg HXD (L h)$^{-1}$)
0.15	0.32 ± 0.01	0.35 ± 0.02	0.014 ± 0.005	0.005 ± 0.0004	0.32 ± 0.03
0.46	0.25 ± 0.02	0.45 ± 0.02	0.016 ± 0.005	0.007 ± 0.001	0.46 ± 0.02
0.61	0.22 ± 0.03	0.51 ± 0.01	0.023 ± 0.003	0.011 ± 0.009	0.76 ± 0.04
0.76	0.18 ± 0.06	0.79 ± 0.06	0.026 ± 0.002	0.020 ± 0.003	1.33 ± 0.11
1.54	0.13 ± 0.04	0.87 ± 0.01	0.027 ± 0.005	0.023 ± 0.001	1.52 ± 0.13

[1] Values calculated for $C_{HXD} = 0$

Hexadecane transfer rate

As case study, HTR was determined in a 10 L ALB-bacterial culture. Figure 3 shows HTR and the C_{HXD} measured during a 10-day culture at constant Ug = 0.76 cm s^{-1}. At the beginning of culture C_{HXD} and HTR were 62.0 mg HXD L^{-1} and 0.042 mg HXD (L h)$^{-1}$, respectively; after day three C_{HXD} was close to 61.2 mg HXD L^{-1} keeping constant values (error bars did not allow us to observe differences) up to the end of culture. HTR decreased to 0.010 mg HXD (L h)$^{-1}$ up to the end of culture. HTR was around 33-fold lower than HTRmax. Our results suggested a possible dominant mass transfer constraint related to the HXD phase to be overcome.

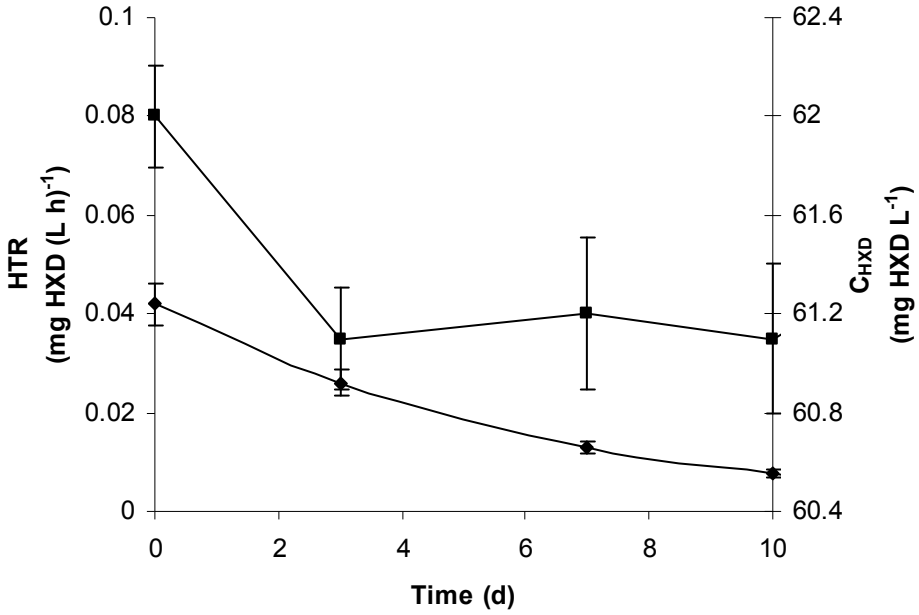

Figure 3.HTR (♦) and C_{HXD} (■) during a 10-day culture of a bacterial consortium at constant Ug = 0.76 cm s^{-1}.

CONCLUSIONS

In this work, a new simple dynamic technique that allows the accurate HTR determination in a three-phase (air, aqueous and HXD) airlift bioreactor was developed. The technique was successfully applied to the determination of HTR in a bacterial culture grown in an airlift bioreactor. Our results suggested a possible dominant mass transfer constraint related with HXD transfer to aqueous phase as the limiting step. HTR seems to be a good criterion for the control of processes where the biodegradation of HXD or other oils is involved.

REFERENCES

Medina-Moreno S.A., Huerta-Ochoa S. and Gutiérrez-Rojas M., "Hydrocarbon biodegradation in oxygen limited sequential batch reactors by consortium from weathered oil-contaminated soil", Canadian Journal of Microbiology, 2005, 51, 231-239.

Mehrnia M., Towfighi J., Bonakdarpour B. and Akbainejad M., "Gas hold-up and oxygen transfer in a draft-tube airlift bioreactor with petroleum based liquids", Biochemical Engineering Journal, 2005, 22, 105-110.

Shariati F.P., Bonakdarpour B. and Mehrnia M.R., "Hydrodynamics and oxygen transfer behaviour of water in diesel microemulsions in a draft tube airlift bioreactor", Chemical Engineering and Processing, 2007, 46, 334–342.

Fujio Y., Sambuichi M. and Ueda S., "Numerical method of the determination of kLa and respiration rate in biological system", Journal of Fermentation Technology, 1973, 51, 154-158.

Cerri M.O., Policarpo L.M. and Badino A. C., "Gas Hold-Up and mass transfer in three geometrically similar internal loop airlift reactors using newtonian fluids", International Journal of Chemical Reactor Engineering, 2010, 8, 1-14.

Cesario M.T., de Wit H. L., Tramoer J. and Beefiink H.H., "New technique for K_LA measurement between gas and water in aereated solvent-inwater dispersions", Biotechnology techniques, 1996, 10, 1 95-l 98.

Cerri M.O., Baldacin J.C., Cruz A.J.G., Hokka C.O. and Badino A.C., "Prediction of mean bubble size in pneumatic reactors", Biochemical engineering Journal, 2010, 53, 12-17.

Bai G., Brusseau M.L. and Miller R.M., "Biosurfactant-enhaced removal of residual hydrocarbon from soil", Journal of Contaminant Hydrology, 1997, 25, 157-170.

Quijano G., Huerta- Ochoa S. and Gutiérrez- Rojas M., "Assessment of the limiting step of mass transfer in n-hexadecane biodegradation in a bubble column reactor", Water Science and Technology, 2010, 62, 906-914.

Torres-Martínez D., Melgarejo-Torres R., Gutiérrez-Rojas M., Aguilera-Vázquez L., Micheletti M., Lye G.J. and Huerta-Ochoa S., "Hydrodynamic and oxygen mass transfer studies in a three-phase (air–water–ionic liquid) stirred tank bioreactor", Biochemical Engineering Journal, 2009, 45, 209-217.

García-Salas S., Rosales Peña M.E., Alfaro R. Porter M. and Thalasso F., "Measurement of local specific interfacial area in bubble columns via a non-isokinetic withdrawal method coupled to electro-optical detector", Chemical Engineering Science, 2008, 63, 1029 – 1038.

Lemoine R. and Morsi B.I., "Hydrodynamic and mass transfer parameters in agitated reactors Part II: Gas-holdup, Sauter mean bubble diameters, volumetric mass transfer coefficients, gas-liquid interfacial areas, and liquid-side mass transfer coefficients", International Journal of Chemical Reactor Engineering, 2005, 3, 1-49.

Nielsen J., Villadsen J. and Liden G., "Mass transfer", "Bioreactor Engineering Principles", 2003, Kuwler Academic/Plenum Publishers, New York.

Anexo 3

Elsevier Editorial System(tm) for Chemical Engineering Journal
Manuscript Draft

Manuscript Number:

Title: Simultaneous hexadecane and oxygen transfer rate on the production of an oil-degrading consortium in a three-phase airlift bioreactor

Article Type: Original Article

Section/Category: Environmental Chemical Engineering

Keywords: Oxygen, Hexadecane, Mass transfer, Oil-degrading consortium, Airlift bioreactor, bioremediation

Corresponding Author: Dr. Mariano Gutierrez-Rojas,

Corresponding Author's Institution:

First Author: Manuel Alejandro Lizardi-Jiménez

Order of Authors: Manuel Alejandro Lizardi-Jiménez ; Gerardo Saucedo-Castañeda ; Frederic Thalasso; Mariano Gutierrez-Rojas

Abstract: The hexadecane (HXD) transfer rate (HTR) and the oxygen transfer rate (OTR) were simultaneously evaluated as a single engineering criterion to enhance the production of an oil-degrading bacterial consortium. In order to accomplish the task, a 10-L three-phase airlift bioreactor (ALB) was used. Oxygen transfer volumetric coefficient (kLaO2) values of 25 - 49 h-1 were found for several superficial gas velocities (Ug 0.15 - 2.7 cm s-1). HXD transfer volumetric coefficient (kLaHXD) values of 0.005 - 0.041 h-1 were obtained for the same range of Ug values. OTR and HTR were calculated as the product of kLaO2 or kLaHXD and the respective concentration gradient. HXD transfer parameters were evaluated by using an early reported novel technique. During 14 days culture, using constant Ug values, the ratio of HTR to OTR (HTR/OTR) never reached the stoichiometric ratio (0.25 ± 0.05 g HXD (g O2)-1). However, the productivity at the higher assayed constant Ug (2.7 cm s-1) was as good as 1.02 ± 0.03 g SS (L d)-1. We propose a variable Ug strategy that consumes 33 % less energy than a higher constant Ug strategy to achieve the same yield and productivity. In this study, the oil-degrading consortium, able to remediate contaminated soils and water, productivity was successfully enhanced with simultaneous HXD and oxygen transfer considerations.

Opposed Reviewers: Mohammad Reza Mehrnia
College of Engineering, University of Tehran
mmehrnia@ut.ac.ir
Dr. Mehrnia is an expert in trhee-phase airlift reactors

Marcel Otavio Cerri
Department of Chemical Engineering, Federal University of S. Carlos, SP, Brazil
marcelcerri@gmail.com
Dr. Cerri is an expert regarding mass transfer in reactors

Hugo de Lasa
University of Western Ontario

hdelasa@eng.uwo.ca
Dr. de Lasa is a leader in chemical reactor enginerring

Cover Letter

May, 3rd 2011

Subject: First-draft manuscript to be published in the Chemical Engineering Journal

Dr. Marc Deshusses,

Editor,

Chemical Engineering Journal,
Dept. of Civil and Environmental Engineering,
Duke University,

Dear Dr. Deshusses:

According to the Instructions to Authors, enclosed you will find the first-draft of our manuscript entitled: “Simultaneous hexadecane and oxygen transfer rate on the production of an oil-degrading consortium in a three-phase airlift bioreactor”, authored by: *Lizardi-Jiménez M. A., Saucedo-Castañeda G., Thalasso F. and Gutiérrez-Rojas M.*; to be published in the **Chemical Engineering Journal.**

Recently, much effort is devoted to determine mass transfer parameters of non-water soluble substrates, like hexadecane, as an important constraint in airlift performance; in our work, an oil-degrading consortium, able to remediate contaminated soils and water was produced in airlift bioreactor. Airlift bioreactor performance was successfully enhanced with simultaneously HXD and oxygen transfer considerations.

Waiting for news, I remain truly yours,

Mariano Gutiérrez-Rojas

***List of Suggested Reviewers**

Reviewers

1) Mohammad Reza Mehrnia, School of Chemical Engineering, College of Engineering, University of Tehran, Tehran, Iran; mmehrnia@ut.ac.ir

2) Hugo de Lasa, Chemical Reactor Engineering Center, University of Western Ontario. Canada; hdelasa@eng.uwo.ca, hdelasa@fes.engga.uwo.ca

3) Marcel Otavio Cerri, Department of Chemical Engineering, Federal University of S. Carlos, S. Carlos, SP, Brazil; marcelcerri@gmail.com

***Highlights**

An oil-degrading consortium, able to remediate contaminated soils and water, was produced in airlift bioreactor.

Oil-degrading consortium productivity was enhanced with simultaneous hexadecane and oxygen transfer considerations.

The ratio of hexadecane to oxygen transfer rate never reached the stoichiometric.

Hexadecane transfer rate was found to be the mass transfer limitation.

Hexadecane transfer rate was evaluated by using a novel technique.

1. Introduction

An airlift bioreactor (ALB) is a pneumatic bioreactor agitated with a continuous gas phase in the form of bubbles that break towards the liquid phase, resulting in an isothermal expansion that maintains homogeneity within the reactor [1]. The main advantages of the ALB compared to conventional bioreactors (bubble column and stirred tank) are efficient mixing and higher aeration rates at lower energy consumption [2]. ALBs are used for the industrial production of lactic acid by fungi [3] and the degradation of phenol compounds by bacteria in axenic cultures [4]. However, very little information is available about microbial consortia grown in water-insoluble liquid substrates in ALBs for environmental purposes [5]. Water-insoluble contaminants in soil and water, oil in particular, are widely studied due to constant persistence, environmental impact and economical importance [6]. The alkanes are important oil constituents; hexadecane (HXD) is an alkane that is widely used as a model for oil degradation because it is easy to monitor and yields high biomass values [7]. Earlier studies [5] with pneumatic bioreactors were focused on the production of oil-degrading biomass; however, they found levels of productivity as low as 0.2 g L^{-1} d^{-1}. Biomass productivity is strongly related to bioreactor hydrodynamics and the resulting mass transfer phenomena [1, 8] and the resulting parameters (specific areas, coefficients and volumetric coefficients) [9]. The importance of oxygen transfer in ALB performance is well documented [2, 10, 11]. Numerous reports have used the volumetric oxygen transfer coefficient ($k_L a_{O2}$) as a practical single criterion to evaluate the oxygen transfer limitations; recent studies of the oxygen transfer rate (OTR) have been done to ensure an adequate delivery of oxygen from the gas stream to the culture broth [8]. However, most ALB studies concerning three-phase systems do not take water-insoluble liquid

substrates into account. When HXD is used as the only source of carbon and energy, HXD plays an important role because a new mass transfer limitation is added to that imposed by oxygen; HXD solubility is several-fold lower (~10^{-7} mg L^{-1}) than that of oxygen (~6.6 mg L^{-1}). Stirred tank reactors studies have focused on macromixing [12], hydrodynamics and oxygen mass transfer in three-phase reactors [13] or improving oxygen mass transfer by the addition of hydrocarbon [14]. However, there is little published work on oil-phase mass transfer phenomena; for instance, the hexadecane transfer rate (HTR), related to oxygen mass transfer and considering the stoichiometric consumptions of both. The aim of this study was to evaluate simultaneously hexadecane and oxygen transfer rates as a single criterion to enhance the productivity of an oil-degrading bacterial consortium in a three-phase ALB.

2. Materials and methods

2.1. Microbial consortium and culture medium

The indigenous oil-degrading bacterial consortium was isolated from the rhizosphere of *Cyperus laxus*, a native plant [15] growing in an oil-contaminated swamp in Mexico. The rhizospheric oil-degrading consortium was composed of four bacterial species: *Xanthomonas* sp., *Acinetobacter bouvetii*, *Shewanella* sp. and *Defluvibacter lusatiae*. The mineral medium was (g L^{-1}): 6.75, $NaNO_3$ (J.T. Baker, 99. 9%); 2.15, K_2HPO_4 (J.T. Baker, 99.3%); 1.13, KCl (J.T. Baker, 99.9%), 0.54, $MgSO_4.5H_2O$ (J.T. Baker, 100.1 %), the pH was adjusted to 6.5 with 1.0 M HCl. The consortium was cultivated in mineral medium containing 13 g L^{-1} HXD (Sigma-Aldrich, 99.7 %).

2.2. Inoculum preparation

The four bacterial species were cultivated separately in 250 mL flasks containing 50 mL of nutritive broth (Bioxon), which were incubated at 30 ^{o}C for 24 h with agitation at 200 rpm in a shaker (model I26, New Brunswick Scientific, USA). Then 2.5×10^5 colony-forming units mL^{-1}; i.e. 0.01 mL and 1.0 mL from each bacterial strain culture were used to inoculate 1 L of medium.

2.3. Bioreactor set-up and operation

The cylindrical vessel (0.14 m diameter, 1 m length) in the ALB was made of Pyrex glass. A draft tube (0.09 m diameter, 0.54 m length) was located 0.035 m above the bottom. The ALB (working volume 10 L) was air-sparged into the draft tube through a perforated L-shaped stainless steel pipe (0.006 m internal diameter) with seven perforations (0.001 m diameter, 0.004 m separation). The ALB was operated as a 14-day batch at 28 ^{o}C with HXD as the sole carbon and energy source. The first batch was inoculated as described in section 2.2. Subsequently, ALB batches were inoculated every 14 days with biomass (0.8 g L^{-1} dry weight) harvested from the preceding batch onto fresh culture medium where the initial culture conditions were restored. ALB was sampled (10 mL) at days 0, 3, 7, 10 and 14. The surface tension (σ) of the culture medium was measured with a surface tensiometer (SensaDyne, Chem-Dyne Research Corp., USA). Viscosity (μ) was measured with a viscometer (Physica MCR model 300, Germany).

2.4. Aqueous and HXD phase hydrodynamics

Three phases (air, aqueous and HXD) were involved in the ALB; the velocity of the two slow-moving phases (aqueous and HXD) was evaluated experimentally. We used sodium polyacrylate hydrogel (ρ_{aq} = 1.0 g cm^{-3}) and oligosyloxane-stained spheres

(ρ_{HXD} = 0.77 g cm^{-3}) simulating the aqueous and the HXD phase, respectively, in order to follow flow patterns through the mineral medium. A digital video camera (Sony HD) and an on-line chronometer (StopWatch software) were used to follow the velocity of single spheres as the ratio of path-length to elapsed time in both ALB zones: riser and downcomer. The resulting velocities were used to calculate two individual Reynolds numbers [16] and Re differences, as follows:

$$\mathrm{Re}_{aq} = \frac{DV_{aq}\rho_{aq}}{\mu} \quad (1)$$

$$\mathrm{Re}_{HXD} = \frac{DV_{HXD}\rho_{HXD}}{\mu} \quad (2)$$

$$\mathrm{Re}_{aq-HXD} = \frac{D}{\mu}\left|V_{aq}\rho_{aq} - V_{HXD}\rho_{HXD}\right| \quad (3)$$

where Re_{aq} and Re_{HXD} are the aqueous and HXD phase Reynolds number, respectively. D is for the riser zone is D_2; D for the downcomer zone is D_1–D_2; D_1 is the ALB diameter (m); D_2 is the draft tube diameter (m); V_{aq} is the aqueous phase velocity (cm s^{-1}); V_{HXD} is the HXD phase velocity (cm s^{-1}); ρ_{aq} is aqueous phase density (g cm^{-3}); ρ_{HXD} is the HXD phase density (g cm^{-3}); and μ is the bulk viscosity of HXD in a water emulsion (g cm s^{-1}). Absolute values were used because the HXD phase has greater velocity through the riser zone than that observed in the aqueous phase; simultaneously, the aqueous phase has greater velocity through the downcomer zone than that observed in the HXD phase. In order to simulate the physicochemical properties of the culture medium, an abiotic medium was designed using biotic values for σ (65 dynes cm^{-1}) and μ (1.05 cP) by adding Tween 20 and HXD to a final concentration of 0.081 mg L^{-1} and 13 g L^{-1}, respectively. The abiotic medium was used in the hydrodynamics and mass transfer experiments.

2.5. Oxygen transfer parameters

The dynamic numerical method [17] was used to determine k_La_{O2}. The concentration of dissolved oxygen (DO) was measured with a polarographic oxygen sensor (ADI dO_2, Applisens, The Netherlands) and a DO meter (model DO-40, New Brunswick Scientific, USA). OTR was calculated as the product of k_La_{O2} and the oxygen gradient concentration.

2.6. HXD transfer parameters and specific area

k_La_{HXD} was evaluated essentially by using an earlier reported novel technique [18] as follows: abiotic medium (10 L) was added to the ALB; a stainless steel cylinder (2.8 mL) was filled with HXD and introduced into the downcomer with the open side downward. Once aeration was in the steady state, 5 mL of ALB was withdrawn every 60 min. The HXD transferred to the aqueous phase was recovered by successive extractions with a sample to solvent ratio of 1:5 (v/v) using a hexane/isotonic solution (1:3, v/v) as solvent. The HXD transfer coefficient (k_{LHXD}) was obtained from the stainless steel cylinder mass transfer area and the relative liquid phase (aqueous and HXD) velocity. We set Ug level so that the difference in velocities, and the resulting $Re_{aq\text{-}HXD}$, between steel cylinder (static) and aqueous phase were the same to those values produced between HXD droplets and aqueous phase in the ALB. k_La_{HXD} was obtained as the product of k_{LHXD} and specific mass transfer area of the HXD droplets, a_{HXD}, was calculted by Equation 4 [13]

$$a_{HXD} = \frac{6}{d_{32HXD}}\phi \qquad (4)$$

where d_{32HXD} is the Sauter mean diameter of HXD droplets (cm) and ϕ is the HXD dispersed phase fraction (dimensionless), d_{32HXD} was measured with a digital camera

and image analysis software (Image Pro Plus 4.1., Media Cybernetics, USA) at three different height levels (0.02 m, 0.25 m and 0.50 m from the bottom) in the downcomer. In order to contrast droplet images, HXD was stained with red chilli (*Capsicum annuum*) oleoresin, also known as rodophile (Bioquimex-Reka, Mexico). We added 25.1 mg of rodophile per 1 g of HXD. The Sauter mean diameter (d_{32HXD}) was obtained as the average of two measurements for each droplet. The hexadecane transfer rate (HTR) was calculated as the product of the volumetric mass transfer coefficient ($k_L a_{HXD}$) and the HXD gradient concentration measured in the aqueous phase. We did not consider it to be pertinent to take into account the effect of bubble hydrodynamics because: (i) bubble hydrodynamics is quite important in the riser and more important than it is in the downcomer; (ii) our experimental method was implemented in the downcomer and we did not assay in the riser; and (iii) k_{LHXD} depends on $Re_{aq\text{-}HXD}$ in both zones (riser and downcomer).

2.7. Suspended solids

Samples (10 mL) from ALB were centrifuged (J2-HS, Beckman, USA) at 4000*g* for 30 min at 4 °C. Three phases were formed: HXD, aqueous and solid. The suspended solids (SS), including the rhizospheric oil-degrading consortium, were determined in the solid phase after heating in a low-pressure oven at 60 °C for 48 h (Duo Vac, Lab-line Inc. Instruments, USA). The SS fraction that remained trapped in the HXD phase was recovered by three successive extractions, as described above. The organic phases, including residual HXD, were pooled and stored at 4 °C in 30 mL vials.

2.8. Hexadecane

HXD in the pooled organic phases was measured by gas chromatography (Varian model 3900, USA) at 300 ^{o}C with a flame-ionization detector, a DB-Petro narrow-bore column

(30 m × 0.00025 m; J & W Scientific) and helium as the carrier gas. The injector and detector temperatures were constant at 290 °C and 300 °C, respectively. The temperature program was: 120 °C for 1 min; increase by 10 °C min^{-1} until 150 °C (2 min); then by 15 °C min^{-1} until 170 °C (1.5 min).

2.9. Statistical analysis

Data analysis was done with NCSS-2000, version 2001 (copyright 2001 by Jerry Hintze). One-way analysis of variance (ANOVA) was used with the level of statistical significance set at $p < 0.05$.

3. Results and discussion

3.1. HXD specific area and local Re differences

The HXD droplet Sauter mean diameter (d_{32HXD}) depends on surface tension (σ) and we measured the variation of σ with time in preliminary biotic ALB runs. For all Ug assayed, σ changed slightly from 72.6 ± 1.02 dynes cm^{-1} at day zero to 68 ± 1.30 dynes cm^{-1} at days 0, 3, 7, 10 and 14. When the abiotic medium was prepared using these two σ values, the diameters of the resulting droplets were not significantly different (d_{32HXD} = 0.157 ± 0.001 and 0.152 ± 0.01 cm for σ = 72.6 and 68 dynes cm^{-1}, respectively). By contrast, d_{32HXD} did change significantly with σ in bubble column reactors [11]. In this study, d_{32HXD} depends only on variations of Ug.

In order to evaluate the effect of Ug on d_{32HXD} and the resulting a_{HXD}, measured in the downcomer, six different Ug values were assayed using the abiotic medium described in section 2.4. d_{32HXD} of macroscopic droplets, number of droplets and a_{HXD} as a function

of Ug are given in Table 1. As expected, d_{32HXD} and Ug were negatively correlated and the number of droplets and Ug were positively correlated; therefore, for a given volume of HXD, a greater a_{HXD} is provided if HXD is dispersed into many small droplets rather than a few large drops. Finally, a_{HXD} increased with Ug and probably depends on local hydrodynamics (Table 1).

<Table 1>

Local Re differences between aqueous and hydrocarbon phase, according to equations (1), (2) and (3), in the riser and in the downcomer as a function of superficial gas velocity (Ug) are shown in Figure 1. Assays were done under abiotic conditions. $Re_{aq\text{-}HXD}$ follows the same increasing pattern for both zones except for Ug = 0.15 cm s^{-1}, where the HXD phase velocity is close to zero (HXD does not decrease). The results show also that $Re_{aq\text{-}HXD}$ was slightly higher in the riser than that in the downcomer in the range 0.46 – 0.76 cm s^{-1}, whereas $Re_{aq\text{-}HXD}$ between the riser and the downcomer were not significantly different for Ug >0.76 cm s^{-1}. Similar behavior in a bubble column has been reported [19]. Nevertheless, most of the studies that have been done using a three-phase ALB have examined only the aqueous and gas phase hydrodynamics [20, 21, 22]. Our results suggest (see Figure 1) that $Re_{aq\text{-}HXD}$ values were similar for the two zones (riser and downcomer), particularly at Ug > 0.76 cm s^{-1} there were no significant differences. Therefore, since d_{32HXD} depends on Ug (see Table 1) it is possible to conclude that d_{32HXD} were similar for the two studied zones at Ug > 0.76 cm s^{-1}; the resulting HXD-specific area measured in the downcomer can be recognized as the mass transfer-specific area (a_{HXD}) in the whole bulk, riser included. In this study, a_{HXD} was used to calculate the HXD mass transfer parameters.

<Figure 1>

3.2. Mass transfer parameters

Studies using three-phase pneumatic bioreactors [5,10] define the volumetric oxygen transfer coefficient (k_La_{O2}) as the only mass transfer parameter (as in a biphasic bioreactor). However, the hydrocarbon phase could be the limiting step in hydrocarbon-biodegrading processes. We studied k_La_{HXD} in order to consider both transfer phenomena.

3.2.1. Volumetric mass transfer coefficients

Owing to the difficulty of measuring the oxygen transfer coefficient (k_{LO2}) and the gas bubble-specific area (a_{O2}) separately, the product k_La_{O2} was measured, which is the parameter that characterizes transport from the gas phase to the aqueous phase. However, because there is no HXD probe available that would allow an evaluation similar to k_La_{O2}, it was necessary to measure a_{HXD} and k_{LHXD} separately; a_{HXD} was computed from experimental values of d_{32HXD} (Table 1). Table 2 shows the measured k_La_{O2} and k_La_{HXD} values and the ratio of hexadecane to oxygen volumetric mass transfer coefficient ((k_La_{HXD}) (k_La_{O2})$^{-1}$) as a function of Ug. Five different Ug values in the range 0.15 – 2.7 cm s^{-1} were investigated. As expected, both volumetric coefficients were correlated positively with Ug: k_La_{HXD} ranged from 0.005 – 0.041h^{-1} and k_La_{O2} ranged from 26 – 46 h^{-1} for all Ug values assayed. These k_La_{O2} values are higher than those reported for bubble column bioreactor using petroleum and paraffins [5] and similar to another ALB study with petroleum-based liquids [10]. The higher k_La_{O2} values in our ALB could be due to rapid circulation of the liquid phase, which would diminish the air

boundary layer; but not enough to produce higher $k_L a_{HXD}$ values, as can be seen in Table 2 where $(k_L a_{HXD})\ (k_L a_{O2})^{-1}$ was < 0.001 for all Ug values assayed, suggesting mass transfer limitation by HXD. $k_L a_{HXD}$ increased 8-fold, whereas $k_L a_{O2}$ did not achieve a 2-fold increase in the same increased range of Ug. However, studies regarding mass transfer rates are needed because oxygen and HXD consumption must be taken into account as described in the following section.

<Table 2>

3.2.2. Mass transfer rates

In two-phase ALB studies, the OTR is commonly considered to be the unique mass transfer limitation. However, the HXD transfer rate (HTR) must be simultaneously taken into account, in the three-phase ALB used in this study, and particular attention should be paid to the HTR/OTR ratio. In our work, HTR values were not computed as averages from the HXD transfer coefficient k_{LHXD} in ALB zones (riser and downcomer); instead we obtained k_{LHXD} from the downcomer by using steel cylinder and we used a generalized k_{LHXD} in the entire ALB due to $Re_{aq\text{-}HXD}$ was practically the same in both zones. The time profiles of the experimentally determined ratio for all constant Ug values are shown in Figure 2. For all Ug, the HTR/OTR value increased as Ug increased and all profiles decreased with time. In all cases, the maximum HTR/OTR value was obtained at the beginning of the culture and the minimum value was reached by day 7 and was constant to the end of culture, except for the Ug term of 2.7 cm s^{-1}; in this case, HXD was exhausted after day 6, so a_{HXD}, $k_L a_{HXD}$ and HTR were no longer applicable. The stoichiometric ratio between hydrocarbon and oxygen consumption values was obtained as:

$$CH_{2.125} + 0.06\ NO_3 + 1.56O_2 \rightarrow 0.35\ CH_{1.77}O_{0.55}N_{0.17} + 0.65CO_2 + 1.81H_2O$$

where the first left-hand term is 1 C-mol of HXD and the first right-hand term is 1 C-mol of biomass [16] and yields (biomass/HXD) were measured. Our stoichiometric approach shows that 0.25 g of HXD theoretically requires 1.0 g of oxygen. In Figure 2, all assayed Ug shows HTR/OTR at least ten times lower than 0.25 g HXD g of O_2^{-1} and three groups are distinguished; those at lower constant Ug (0.15 and 0.45 cm s^{-1}), middle Ug (0.61 and 1.54 cm s^{-1}) and higher Ug (2.7 cm s^{-1}). The three groups were selected on the basis of maximal slope computed for HTR/OTR versus time. The slope values were –0.002, –0.004 and –0.010 g HXD (g O_2)$^{-1}$ d^{-1} for the lower, middle and higher Ug group, respectively. These slopes represent the maximum rate at which the HTR/OTR ratio decreased. The maximum HTR/OTR at lower Ug was ~ 0.006 g HXD (g O_2)$^{-1}$; at middle Ug up to 0.012 g HXD (g O_2)$^{-1}$ and at higher Ug up to 0.025 g HXD (g O_2)$^{-1}$. Our results show that all HTR/OTR values lower than 0.25 g HXD (g O_2)$^{-1}$ are due to HXD transfer limitation. Such mass transfer limitation should impact both HXD biodegradation and the production of suspended solids (SS). The HTR/OTR ratio is applicable to real cultivation conditions because k_{LHXD} values were evaluated by considering the relative velocity differences between the aqueous and HXD phases. In addition, we did not assume constant $k_L a_{HXD}$ during the culture, although slow changes in surface tension did not affect d_{32HXD} (see section 3.1), because a_{HXD} diminished as culture proceed due to ϕ diminished too. The fact that HTR/OTR varies as a function of time was made clearer by examination of the HTR and OTR variations separately: (i) HTR is augmented with aeration owing to the decrease of droplet size with Ug; by contrast, culture time did not affect droplet size. (ii) OTR is augmented with aeration

but the increasing values were lower than those observed for HTR; however, OTR was affected by culture time because the dissolved oxygen aqueous phase concentrations measured in the bulk differed with time, –6.5 to 4.6 mg O_2 L^{-1} (30 % variation); whereas HXD was dispersed into droplets and reached aqueous phase concentration values of 65 – 61 mg of HXD L^{-1} (7 % variation).

<Figure 2>

3.3. HXD biodegradation and SS production

In order to enhance the productivity of SS, including the rhizospheric indigenous oil-degrading consortium, we studied total HXD (non-soluble and soluble into the aqueous phase) biodegradation following two different aeration strategies: constant Ug or variable Ug during the ALB culture.

3.3.1. HXD biodegradation and SS production using constant Ug

We measured SS production and HXD biodegradation at constant Ug in order to evaluate the effect of mass transfer limitations. Figure 3 shows total HXD biodegradation and SS production profiles as a function of culture time when five constant values of Ug (0.15, 0.45, 0.61, 1.54 and 2.7 cm s^{-1}) were used. Figure 3a shows that HXD was 98.47 ± 0.38 % degraded in only 6 days at higher constant values of Ug; HXD was practically exhausted within 14 days at middle constant values of Ug; whereas, 6 g L^{-1} of HXD remained at lower constant values of Ug. SS production (Figure 3b) increased as Ug increased; concentrations of SS were highest at the end of culture for middle and lower Ug and at day 6 for higher Ug. We considered it pertinent to compute batch culture productivity at higher Ug when the instant productivity,

defined as the derivative of SS (g L^{-1}) with respect to time, was zero (day 7). In the case of middle and lower Ug, the derivative never was strictly zero and productivity was computed at the end of the batch. SS yield and productivity were 0.46 ± 0.01 g SS (g HXD)$^{-1}$ and 0.25 ± 0.01 g SS (L d)$^{-1}$, respectively, at lower Ug; 0.58 ± 0.09 g SS (g HXD)$^{-1}$ and 0.51 ± 0.05 g SS (L d)$^{-1}$, respectively, at middle Ug; and 0.58 ± 0.02 g SS (g HXD)$^{-1}$ and 1.01± 0.03 g SS (L d)$^{-1}$, respectively, at higher Ug. Productivity was evaluated at day 14 for lower and middle Ug, whereas for higher Ug, productivity was evaluated when HXD was exhausted. Earlier studies [5] with sequential batch bubble column working at middle Ug (1 cm s^{-1}) gave similar SS yield values (0.45 g SS (g hydrocarbon)$^{-1}$) but lower productivity, 0.2 g SS (L d)$^{-1}$, as compared to our results at similar Ug. In our work, the oil-degrading consortium productivity was 2.5-fold enhanced. In those studies, it took nearly 21 days to degrade Maya crude oil and paraffins and those authors suggested oxygen transfer limitation. This study [5] relates SS yield to mass transfer phenomena, describing a low biomass formation under mass transfer limitation and explain this fact due to the high transformation of initial hydrocarbon in more soluble carbon forms and non-soluble metabolite production. However, we show here that, at all assayed Ug, HXD transfer limitation is predominant during the culture, then HXD transfer becomes the limiting phenomenon. Other work with fungi and HXD [23] showed the relationship between yield and HXD concentration. Our results showed that SS productivity was not affected by HXD limitation, although other explanation is: the given stoichiometry is probably not valid, similar result was obtained in other work [24] studying OTR in lactone formation. The highest SS productivity achieved, working at constant Ug, was obtained when higher Ug values were imposed; however, two operation problems emerged: (i) SS reached a maximum at 8.1 g L^{-1} but was decreased by up to 0.9 g L^{-1}, suggesting that autolysis of

suspended cells is probably due to the lack of energy and carbon source stimulated by the high aeration rate; and (ii) higher constant Ug values were associated with a higher energy consumption. Therefore, studies examining variable Ug strategies are needed in attempts to save energy and to avoid SS lysis.

<Figure 3>

3.3.2. HXD biodegradation and SS production using a variable Ug strategy

We propose a variable Ug strategy: to start using middle Ug (e.g. 0.61 cm s^{-1}; see Figure 2) up to day 3, then change to higher Ug (2.7 cm s^{-1}) until the end of culture. The effect of a selected variable Ug strategy on experimentally determined HTR/OTR is shown in Figure 4.

As we expected, initial HTR/OTR was close to 0.012 g HXD (g O_2)$^{-1}$, decreasing to 0.0015 g HXD (g O_2)$^{-1}$ by day 3. The increase in Ug (2.7 cm s^{-1}) allowed HTR/OTR to increase up to 0.0021 g HXD (g O_2)$^{-1}$. HXD was exhausted after day 10 and, to avoid cell lysis, we decided to stop the culture at day 10 where SS reached the highest production level. Figure 5 shows HXD and SS profiles when the variable Ug strategy was used. Although it is not possible to guarantee that the initial population composition will be the same in each batch owing to the complex population dynamics after subsequent cultures, our results show that it is possible to guarantee stable HXD degradation and SS production patterns for each tested Ug value (error bars in Figure 5 are for independent triplicate batches). This variable Ug strategy consumed 33 % less energy than higher Ug but reached the same yield and productivity.

<Figure 4>

<Figure 5>

4. Conclusions

$Re_{aq\text{-}HXD}$ in the riser and the downcomer were the same within the range 0.76 – 2.7 cm s^{-1}. The HXD mass transfer area (a_{HXD}) increased with increased Ug and decreased as culture proceeded. For all Ug values tested, $k_L a_{O2}$ values were higher (up to 10^3-fold) than the $k_L a_{HXD}$ values. The stoichiometric ratio (0.25 ± 0.05 g HXD (g O_2)$^{-1}$) was never reached. In our work, HTR and OTR were simultaneously evaluated on the production of an oil-degrading bacterial consortium in a three-phase ALB. Our results show that all HTR/OTR values were due to HXD transfer limitations. At constant Ug, the highest consortium biomass productivity was reached with the highest Ug (7 days). This value was 2.5-fold higher than those reported only considering oxygen transfer phenomena. In our three-phase airlift bioreactor, the constant and the variable strategies provided similar biomass productivity-enhanced values.

Acknowledgments

We acknowledge Consejo Nacional de Ciencia y Tecnología (CONACYT) for a scholarship to M. A. L-J.; and PEMEX-Refinación for partial support.

References.

[1] Y. Chisti, Airlift reactors: current technology, in: Y. Chisti (Ed.), Airlift Bioreactors, First ed, Elsevier, Essex, 1989. pp. 33-86.

[2] T.J. Lin, P.C. Chen, Studies on hydrodynamics of an internal-loop airlift reactor in gas entrainment regime by particle image analyzer, Chem. Eng. J. 108 (2005) 69-79.

[3] T. Liu, S. Miura, M. Yaguchi, T. Arimura, E.Y. Park, M. Okabe, Scale up of L-lactic acid production by mutant strain *Rhizopus* sp. MK-96-1196 from 0.003 m^3 to 5 m^3 in airlift bioreactors, J. Biosci. Bioeng. 101(2006) 9-12.

[4] P. Saravanan, K. Pakshirajan, P. Saha, Treatment of phenolics containing synthetic wastewater in an internal loop airlift bioreactor (ILALR) using indigenous mixed strain of *Pseudomonas* sp. under continuous mode of operation, Bioresour. Technol. 100 (2009) 4111-4116.

[5] S.A. Medina-Moreno, S. Huerta-Ochoa, M. Gutiérrez-Rojas, Hydrocarbon biodegradation in oxygen limited sequential batch reactors by consortium from weathered oil-contaminated soil, Can. J. Microbiol. 51 (2005) 231-239.

[6] S. Saval, Bioremediation, Clean-up biotechnologies for soils and aquifers, in: Olguin, G. Sanchez and E. Hernandez (Eds.), Environmental Biotechnology and Cleaner Bioprocesses, Taylor & Francis, London, 2000, pp. 155-166.

[7] S. Inakollu, H. Hung, G.S. Shreve, Biosurfactant enhancement of microbial degradation of various structural classes of hydrocarbon in mixed waste systems, Environ. Eng. Sci. 21 (2004) 463-469.

[8] F. Garcia-Ochoa, E. Gomez, Bioreactor scale-up and oxygen transfer rate in microbial processes: An overview, Biotechnol. Adv. 27 (2009) 153-176.

[9] R. Lemoine, B. I. Morsi, Hydrodynamic and mass transfer parameters in agitated reactors Part II: Gas-holdup, Sauter mean bubble diameters, volumetric mass transfer coefficients, gas-liquid interfacial areas, and liquid-side mass transfer coefficients, Int. J. Chem. React. Eng. 3 (2005) A20.

[10] M. Mehrnia, J. Towfighi, B. Bonakdarpour, M. Akbainejad, Gas hold-up and oxygen transfer in a draft-tube airlift bioreactor with petroleum based liquids, Biochem. Eng. J. 22 (2005) 105-110.

[11] G. Quijano, S. Revah, M. Gutiérrez- Rojas, L. B. Flores-Cotera, F. Thalasso, Oxygen transfer in three-phase airlift and stirred tank reactors using silicone oil as transfer vector, Process Biochem. 44 (2009) 619-624.

[12] M. Martín, F.J. Montes, M.A. Galán, On the contribution of scales of mixing to the oxygen transfer in stirred tanks, Chem. Eng. J. 145 (2008) 232-241.

[13] D. Torres-Martínez, R. Melgarejo-Torres, M. Gutiérrez-Rojas, L. Aguilera-Vázquez, M. Micheletti, G.J. Lye, S. Huerta-Ochoa, Hydrodynamic and oxygen mass transfer studies in a three-phase (air–water–ionic liquid) stirred tank bioreactor, Biochem. Eng. J. 45 (2009) 209-217.

[14] K.G. Clarke, P.C. Williams, M.S. Smit, S.T.L. Harrison, Enhancement and repression of the volumetric oxygen transfer coefficient through hydrocarbon addition and its influence on oxygen transfer rate in stirred tank bioreactors, Biochem. Eng. J. 28 (2006) 237-42.

[15] I. J. Díaz-Ramírez, H. Ramírez-Saad, M. Gutiérrez-Rojas, E. Favela-Torres, Biodegradation of Maya crude oil fractions by bacterial strains and a defined mixed culture isolated from *Cyperus laxus* rhizosphere soil in a contaminated site, Can. J. Microbiol. 49 (2003) 755-761.

[16] J. Nielsen, J. Villadsen, G. Liden, Mass transfer In Bioreactor Engineering Principles, Kuwler Academic/Plenum Publishers, New York, 2003.

[17] Y. Fujio, M. Sambuichi, S. Ueda, Numerical method of the determination of kLa and respiration rate in biological system, J. Ferment. Technol. 51 (1973) 154-158.

[18] M.A. Lizardi-Jiménez, G. Saucedo-Castañeda, F. Thalasso, M. Gutiérrez-Rojas, Dynamic technique to determine hexadecane transfer rate from organic phase to aqueous phase in a three-phase bioreactor, Int. J. Chem. React. Eng. 9 (2011) S3.

[19] N. Kantarci, F. Borak, O. Klutlu, Bubble column reactors, Process Biochem. 40 (2005) 2263-2283.

[20] F. P. Shariati, B. Bonakdarpour, M. R. Mehrnia, Hydrodynamics and oxygen transfer behaviour of water in diesel microemulsions in a draft tube airlift bioreactor, Chem. Eng. Process. 46 (2007) 334-342

[21] L. Mengxi, L. Chunxi, S. Mingxian, G. Baoli, H. Jie, Hydrodynamics and mass transfer in a modified three-phase airlift loop reactor, Pet. Sci. 4 (2007) 91-96.

[22] G. Olivieri, A. Marzocchella, P. Salatino, Hydrodynamics and mass transfer in a lab-scale three-phase internal loop airlift, Chem. Eng. J. 96 (2003) 45-54.

[23] T. L. Volke-Sepúlveda, M. Gutiérrez-Rojas, E. Favela-Torres, Biodegradation of high concentrations of hexadecane by *Aspergillus niger* in a solid-state system: Kinitec analysis, Biores. Tech. 97 (2006) 1583-1591.

[24] S. Doing, S. C. R. Pickering, G.J. Lye, J.M. Woodley, The use of microscale processing technologies for quantification of biocatalytic Baeyer-Villiger oxidation kinetics, Biotechnol. Bioeng. 80 (2002) 42-49.

Table(1)

Table 1. Sauter mean diameter (d_{32HXD}) of macroscopic droplets, total droplets number and a_{HXD} in downcomer, as a function of Ug.

Ug ($cm\ s^{-1}$)	d_{32HXD} (cm)	Total droplets number	a_{HXD} ($cm^2\ cm^{-3}$)
0.15	0.32 ± 0.01	11 080 ± 69	0.35 ± 0.002
0.46	0.25 ± 0.02	23 236 ± 23	0.45 ± 0.020
0.61	0.22 ± 0.03	34 096 ± 97	0.51 ± 0.017
1.00	0.15 ± 0.03	110 000 ± 100	0.79 ± 0.060
1.54	0.13 ± 0.04	165 251 ± 65	0.87 ± 0.010
2.70	0.09 ± 0.01	498 021 ± 122	1.30 ± 0.024

Table(2)

Table 2. Volumetric HXD transfer coefficient (k_La_{HXD}) and volumetric oxygen transfer coefficient (k_La_{O2}) at different Ug (day 0)

Ug ($cm\ s^{-1}$)	k_La_{HXD} (h^{-1})	k_La_{O2} (h^{-1})	$(k_La_{HXD})\ (k_La_{O2})^{-1}$
0.15	0.005 ± 0.00006	26.17 ± 2.62	0.0002
0.46	0.006 ± 0.00002	30.00 ± 2.00	0.0002
0.61	0.015 ± 0.00002	33.67 ± 3.37	0.0004
1.54	0.024 ± 0.00030	41.66 ± 3.10	0.0005
2.70	0.041 ± 0.00040	45.65 ± 2.09	0.0009

Figure(1)

Figure 1

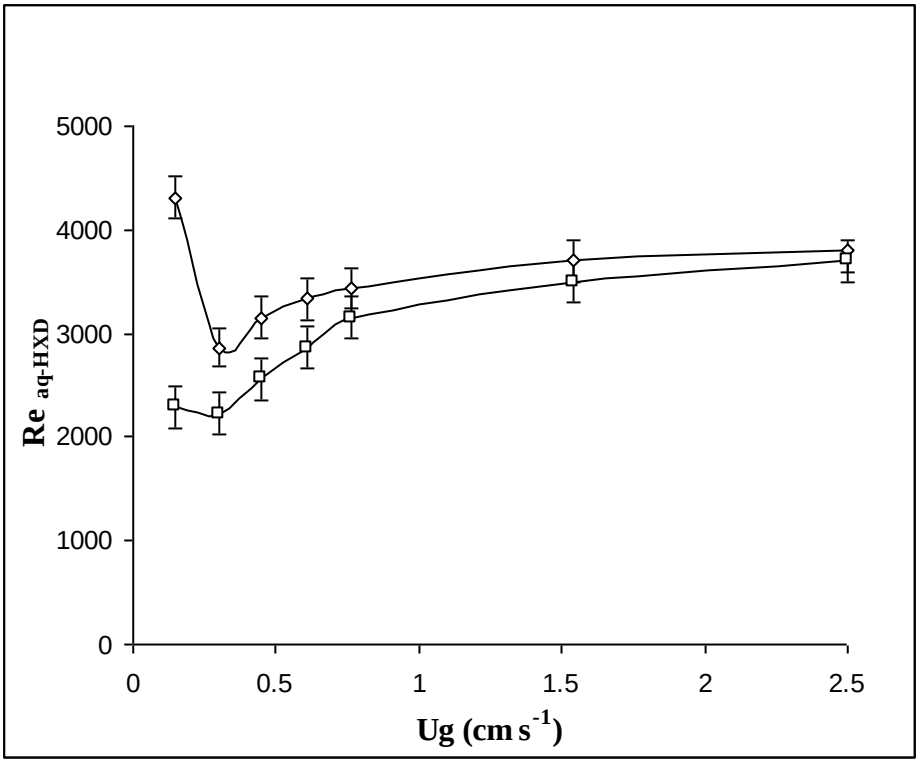

Figure(2)

Figure 2

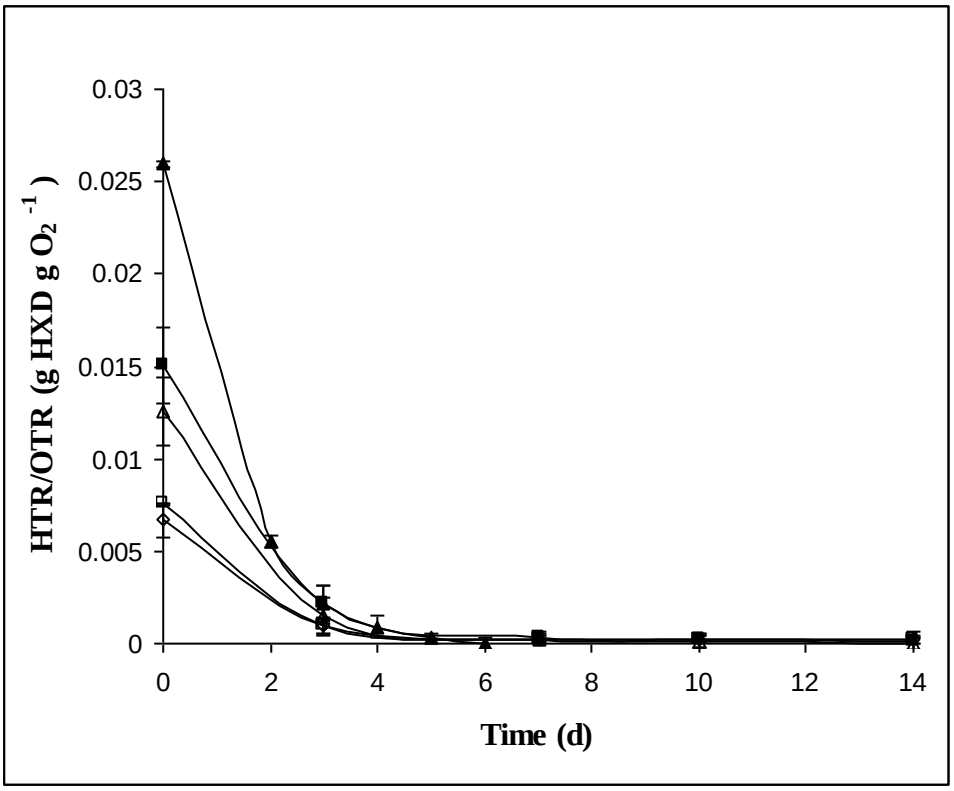

Figure(3)

Figure 3

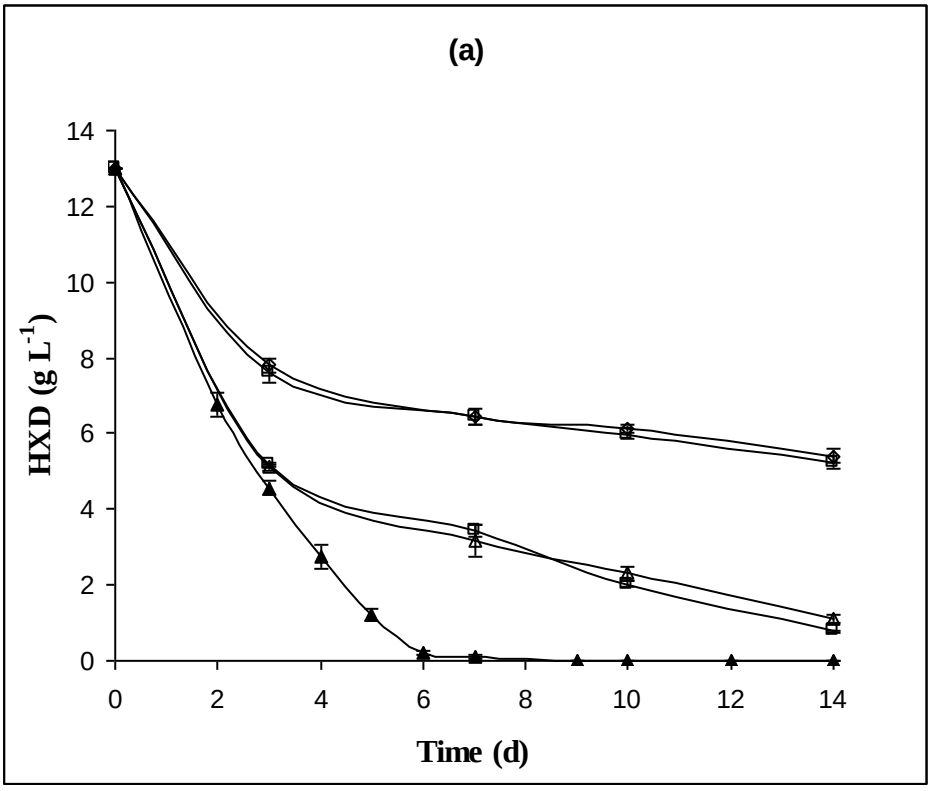

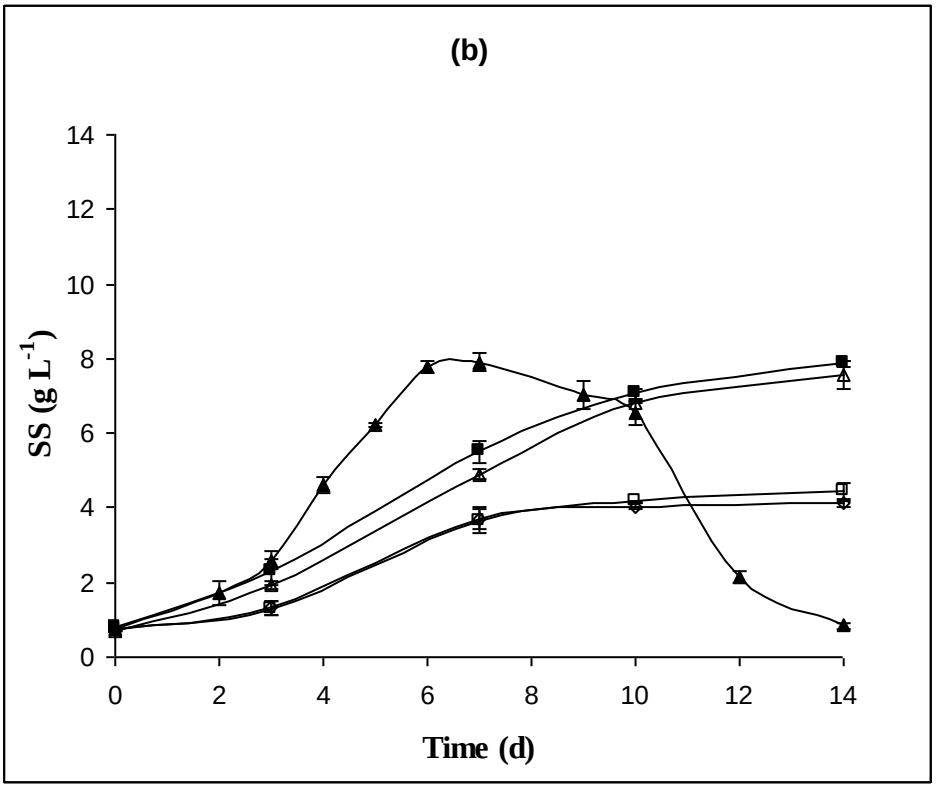

Figure(4)

Figure 4

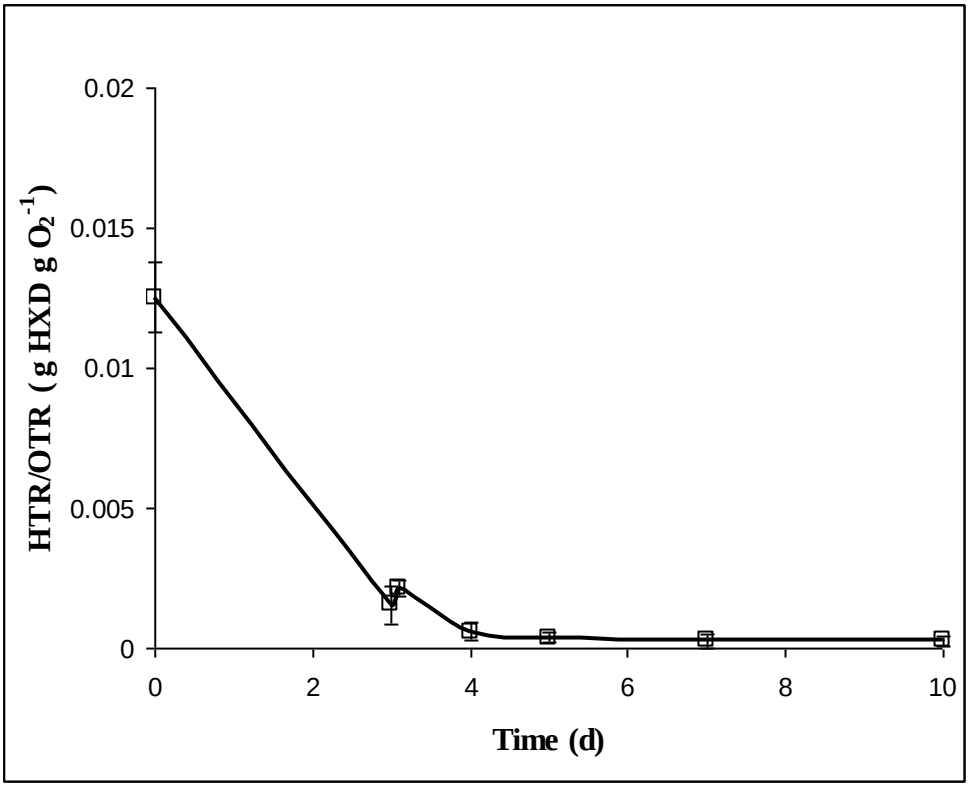

Figure(5)

Figure 5

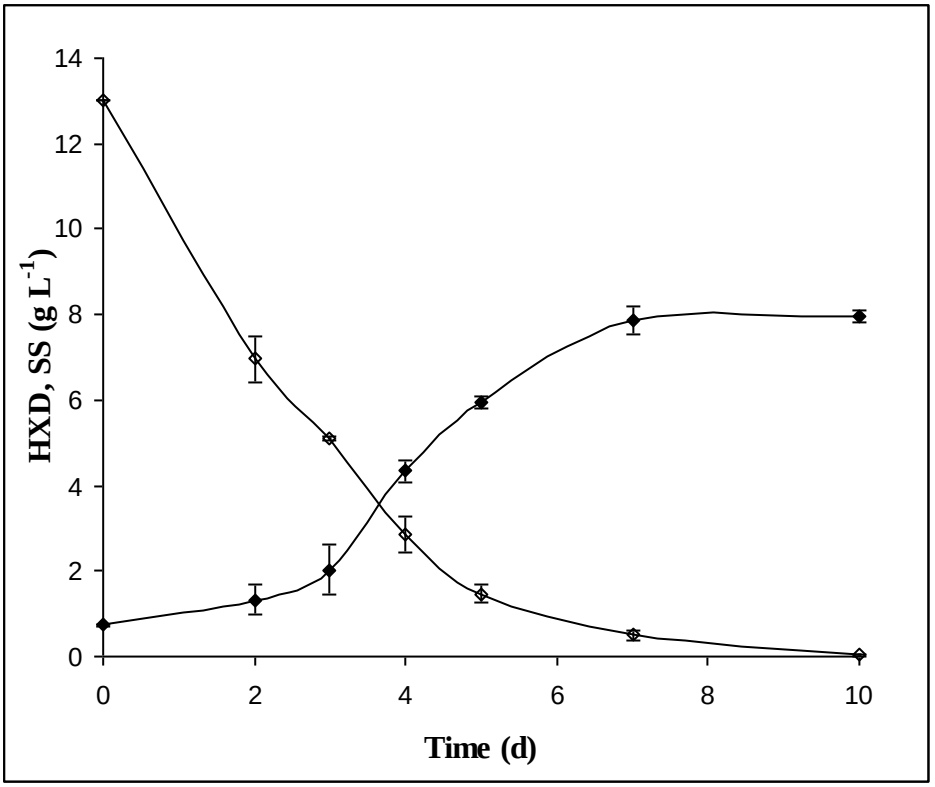

Figure captions

Figure 1. Local $Re_{aq\text{-}HXD}$ in riser (◊) and downcomer (□) as a function of Ug in 10 L airlift bioreactor.

Figure 2. Ratio of hexadecane to oxygen transfer rate, HTR/OTR, along culture time as a function of constant Ug (cm s^{-1}): (◊) 0.15, (□) 0.46, (Δ) 0.61, (■) 1.54 and (▲) 2.7.

Figure 3. HXD biodegradation (a) and SS production (b) time profiles for different Ug (cm s^{-1}) assayed: (◊) 0.15, (□) 0.46, (Δ) 0.61, (■) 1.54 and (▲) 2.7.

Figure 4. Ratio of hexadecane to oxygen transfer rate, HTR/OTR, along culture time with variable Ug strategy: Ug of 0.61 cm s^{-1} up to day 3; Ug of 2.7 cm s^{-1} up to the end of culture.

Figure 5. (◊) HXD or (♦) SS (g L^{-1}) with variable Ug strategy.